UNIVERSITA' VITA-SALUTE SAN RAFFAELE

CORSO DI DOTTORATO DI RICERCA

IN NEUROSCIENZE COGNITIVE

Early-determined differences in brain structure: a dissertation on sulcal patterns variability and sex differences in brain morphology

DoS: prof. Jubin Abutalebi

Tesi di DOTTORATO di RICERCA di Gianpaolo Del Mauro

matr. 015805

Ciclo di dottorato XXXV

SSD M-PSI/02

Anno Accademico 2019/2020

CONSULTAZIONE TESI DI DOTTORATO DI RICERCA

Il/la sottoscritto/*I*	Gianpaolo Del Mauro
Matricola / *registration number*	015805
nat_ a/ *born at*	Avellino (AV)
il/*on*	28/01/1994

autore della tesi di Dottorato di ricerca dal titolo / *author of the PhD Thesis titled*

Early-determined differences in brain structure: a dissertation on sulcal patterns variability and sex differences in brain morphology

✓ AUTORIZZA la Consultazione della tesi / AUTHORIZES *the public release of the thesis*

□ NON AUTORIZZA la Consultazione della tesi per …… mesi /DOES NOT AUTHORIZE *the public release of the thesis for …… months*

a partire dalla data di conseguimento del titolo e precisamente */ from the PhD thesis date, specifically*

Dal / *from* ……/……/…… Al / *to* ……/……/……

Poiché /*because*:

□ l'intera ricerca o parti di essa sono potenzialmente soggette a brevettabilità/ *The whole project or part of it might be subject to patentability;*

□ ci sono parti di tesi che sono già state sottoposte a un editore o sono in attesa di pubblicazione/ *Parts of the thesis have been or are being submitted to a publisher or are in press;*

□ la tesi è finanziata da enti esterni che vantano dei diritti su di esse e sulla loro pubblicazione/ *the thesis project is financed by external bodies that have rights over it and on its publication.*

Data /Date .14/11/22..... Firma /Signature ……

DECLARATION

This thesis has been:

- composed by myself and has not been used in any previous application for a degree. Throughout the text I use both 'I' and 'We' interchangeably.
- has been written according to the editing guidelines approved by the University.

Permission to use images and other material covered by copyright has been sought and obtained.

All the results presented here were obtained by myself, except for:

1) Neuroimaging and behavioral data in Experiment 2 and Experiment 3 were provided by the Human Connectome Project, WU-Minn Consortium (Principal Investigators: David Van Essen and Kamil Ugurbil; 1U54MH091657) funded by the 16 NIH Institutes and Centers that support the NIH Blueprint for Neuroscience Research; and by the McDonnell Center for Systems Neuroscience at Washington University.

2) Delta plots and neuroimaging analysis in Experiment 1 were performed in collaboration with dr. S. Sulpizio (Department of Psychology, Università degli Studi di Milano-Bicocca) and dr. D. Fedeli (Neuroradiology Department, Fondazione IRCCS Istituto Neurologico Carlo Besta)

Experiments 1, 2, and 3 have been previously published in peer-reviewed scientific journals, although with a marginally different wording and structure (Fedeli et al., 2022; Del Mauro et al., 2022; Del Mauro et al., 2022).
All sources of information are acknowledged by means of reference.

Acknowledgements

The present dissertation is the final product of the joint efforts and collaboration with my supervisor, prof. Jubin Abutalebi, my colleagues dr. N. Del Maschio, S. Sulpizio, D. Fedeli, C. Bellini and the other students of the Centre for Neurolinguistics and Psycholinguistics.

Dedication

Prof. Jubin Abutalebi: you are the coolest boss I could ever ask for. I will always carry with me our crazy “business trip” to Goa. Thank you for all the support, the help, and the opportunities you gave me over these years.

Nicola: I wouldn’t be here if it wasn’t for you and all the help and advice you gave me over the years. If you are at the CNPL, the new generation will be in good hands.

Giovanni, Valentina, and Lisa: thank you for all the unconditional support, patience, and undeserved help you gave me. You know nothing of this would literally have been possible without you. I will always be grateful for all you did and gave to me.

Ilaria, Davide Moschella, and Emma: each year you have been a safe haven to return to. I wouldn’t have enjoyed staying home so much if it wasn’t for you. There is a lot to say, but maybe it is enough to remember that I know you for half my life. I will treasure every walk, discussion, and drink at the “Bar Tony”, as well as the crazy week in Vieste three years ago (and many others with Davide). Thank you for your love and support, and all the laughs we shared together.

Calogero, Gianluca, Giovanni, and Andrea: I have always been the most emotional of the group, so let it be this last time too. I spent the greatest time since I’ve been living here with you. Every moment we’ve been through together is sculpted in my memory, from each sleepless night to the fights between Calogero and Gianluca. One should consider himself lucky to meet one or two persons like you in his entire life. I’ve met you all at once, and maybe this is even too much. I’m grateful to have met you, and however far our lives will bring us, I will always keep a night lamp ready for you.

Raina: thank you for your love and the beautiful time we spent together. I’m glad we have managed to be friends, despite the ocean and the six hours between us. Your continuous support has been precious during these years. I honestly thought we would never see each other again, but apparently, life is going to bring us unexpectedly close.

Giulia: the moments we've been through together are precious memories that I will always carry with me. I will treasure our walks and discussions in Cassinella, the night we watched together the new season of Twin Peaks, and the light of your room that was always on even in the middle of the night. When I first saw that light turned off and the window of your room opened, it broke my heart. From that moment, we haven't seen each other many times. But I know that sooner or later you will appear again, maybe bringing a pack of Oreo. When that happens, I will be there for you, and I am sure it will be like it's only been a day since the last time.

Davide: we worked together for four long years. You have been the best model I could ever have and taught me almost everything I know. We experienced together the extraordinary scientific revolution of 2020, when we passed from processing each participant individually to scripting almost everything we could. I will treasure our enthusiasm for each successfully functioning script, every lesson you taught me, all the cheap lunches, and the coffees, beers, and laughs we shared together.

Camilla Bellini, Marco, Camilla Venturini, and Gioia: thank you for having made this city a good place to live in again. I will remember everything of this last great year: each laugh, hangover, and dinner on the terrace. And Gioia and Camilla Bellini, how to forget our "business trip" in India? Especially when Indian taxi drivers tried to kidnap me. It's hard to leave, but it's equally hard to remain while the people we love go away. Please, keep having fun and taking care of each other and of the new generations as we always did here at the CNPL.

Cristina: All I can say, and I want everybody to know that, is that you are a thief. You stole from me a paper to present during the first year. At the time, I couldn't still remember your face, so I was constantly asking Giulia who was the girl that had stolen my paper. But except for this little incident, you are an extraordinary person. Thank you for all the support and the laughs over these years. I will always remember your frailty, your strength, and your childish enthusiasm.

Emanuela: you have been surprisingly supporting me for all these years, from the queue to retire our badges to today. I know I'm not an easy person and that our friendship has been through many ups and downs, but now we got here I like to think that the score is by far positive. I hope you feel the same. If I remember correctly, I have been one of the first persons you met in our classroom, just like you have been one of the first persons I met. Maybe it could have gone better for you, not for me.

Camilla: when we started our internship together, we barely knew each other, but from the moment we became friends I've never been alone not even for one second, no matter how far you were. During these years, you have been a safe haven that I have always been able to rely on. Your love, your patience and your friendship saved me more times than I can remember. If I was able to return you even half of what you did, then I have been a good friend.

Piergiorgio: the first time we talked we were in a disco. I was standing still in a corner, and you asked me "Don't you like dancing?" or something like that. This short conversation perfectly describes the two of us. I have a lot more to say, including the bottles of Lambrusco and every time we sang "Nuvole senza Messico" together, but if I was Chuck Palahniuk and this was a novel by Chuck Palahniuk, maybe I would start from that time we almost blew up our apartment. That night one of us (no one knows for sure who, but you know deep inside that it was you) left the gas on. We were saved by a bottle of peach flavored Estathé, which we exposed for some months in our library as *memento mori*. They say that, after the right amount of time, you can laugh about everything. For us, the right amount of time was the next morning, and I've never felt so alive like that day. Maybe almost dying with someone creates a special bond with that person. You will always be the person I almost died with.

To my family, thank you for all your love and support over the years.

Abstract

While the role of individual experience and environment in shaping human brain morphology is highly investigated and recognized, recent evidence suggests that some aspects of brain structure are determined during fetal development and remain largely unaffected by postnatal events. In recent years, the investigation of these early-determined differences in brain structure, as well as their potential influence on behavior and cognitive processes, has raised growing interest. This dissertation provides a systematic investigation on two main sources of early-determined differences in brain structure, namely the cortical folding process and biological sex. In particular, we aim at investigating whether and how the organization of cortical sulci influences cognitive processes, brain activity, and brain structure by means of multimodal neuroimaging techniques. Moreover, we investigate differences between males and females in brain structure by adopting multiple measures of cortical morphology, in order to provide a comprehensive picture of sex differences across the cerebral cortex.

Table of Contents

Acronyms and Abbreviations

ACC:	Anterior Cingulate Cortex
AC-PC:	Anterior commissure-Posterior commissure
ACT:	Anatomical Constrained Tractography
AD:	Alzheimer's Disease
AMAP:	Adaptive Maximum A Posterior
ANT:	Attention Network Task
ASD:	Autism Spectrum Disorders
ATH:	Axonal Tension Hypothesis
BOLD:	Blood Oxygen Level Dependent
CAT:	Computer Adaptive Testing
CAT12:	Computational Analysis Toolbox v.12
C.E.R.M.A.C:	Centro di Eccellenza Risonanza Magnetica ad Alto Campo
CM:	Connectivity Matrix
CS:	Cingulate Sulcus
CSF:	Cerebrospinal Fluid
CT:	Cortical Thickness
DMN:	Default Mode Network
DTI:	Diffusion Tensor Imaging
DW:	Diffusion-Weighted
EBM:	Extreme Male Brain
EFs:	Executive Functions
EPI:	Echo Planar Imaging

EQ:	Empathy Quotient
FA:	Fractional Anisotropy
FFA:	Face Fusiform Area
FD:	Fractal Dimension
FDR:	False-Discovery Rate
FG:	Fusiform Gyrus
FOV:	Field Of View
fMRI:	functional Magnetic Resonance Imaging
FOD:	Fiber Orientation Distribution
FSL:	FMRIB Software Library
FWE:	Family-Wise Error
FWHM:	Full-Width at Half Maximum
GLM:	General Linear Model
GM:	Gray Matter
GMV:	Gray Matter Volume
HCP:	Human Connectome Project
HRF:	Hemodynamic Response Function
IC(s):	Independent Component(s)
ICA:	Independent Component Analysis
iFOD2:	Second-order integration over Fiber Orientation Distribution
IFOF:	Inferior Fronto-Occipital Fasciculus
ILF:	Inferior Longitudinal Fasciculus
IPC(s):	Intermediate Progenitor Cell(s)

Iq:	Quality Index
ISI:	Inter-Stimulus Interval
ISVZ:	Inner Subventricular Zone
LAS:	Local Adaptive Segmentation
MANGO:	Multi-image Analysis GUI
MCC:	Middle Cingulate Cortex
MD:	Mean Diffusivity
MDD:	Major Depressive Disorder
MDL:	Minimum Description Length
MPRAGE:	Magnetization Prepared Rapid Gradient Echo
MRI:	Magnetic Resonance Imaging
MSMT-CSD:	Multi-Shell Multi-Tissue Constrained Spherical Deconvolution
NBS:	Network-Based Statistics
NECs:	Neuroepithelial cells
OFC:	Orbitofrontal Cortex
OSVZ:	Outer Subventricular Zone
OTS:	Occipitotemporal Sulcus
PBT:	Projection-Based Thickness
PCC:	Posterior Cingulate Cortex
PCS:	Paracingulate Sulcus
PE:	Phase Encoding Direction
PVE:	Partial Volume Estimation
RI:	Response Inhibition

ROI(s):	Region(s) Of Interest
RSC:	Restrosplenial Cingulate Cortex
RTs:	Reaction Times
SA:	Surface Area
SANLM:	Spatial Adaptive Non-Local Mean
SC:	Structural Connectivity
SD:	Sulcal Depth
SES:	Socioeconomic Status
SIFT2:	Spherical-deconvolution Informing Filtering of Tractograms
SLF:	Superior Longitudinal Fasciculus
SoBM:	Source-Based Morphometry
SQ:	Systemizing Quotient
SSAGA:	Semi-Structured Assessment for the Genetics of Alcoholism
St.Dev.:	Standard Deviation
STG:	Superior Temporal Gyrus
STS:	Superior Temporal Sulcus
SVZ:	Subventricular Zone
T1w:	T1-weighted image
TE:	Echo Time
TBV:	Total Brain Volume
TIV:	Total Intracranial Volume
TORRT:	Toolbox Oral Reading Recognition Test

TR:	Repetition Time
V1:	Primary Visual Cortex
VBM:	Voxel-Based Morphometry
vOTC:	ventral Occipitotemporal Cortex
vOF:	vertical Occipital Fasciculus
VWFA:	Visual Word Form Area
VZ:	Ventricular Zone
WM:	White Matter

List of Figure and Tables

1. Introduction

1.1 General overview

Despite sharing most of the macroscopic morphological features, brains exhibit large anatomical variability among individuals. It is only recently that the introduction of *in vivo* neuroimaging techniques led to the astonishing discovery that individual experience and external factors shape brain morphology on a large-scale level. Perhaps it is useful to think of the brain as the product of a cumulative natural selection process. Indeed, from an evolutionary perspective, the advantage of a brain that changes along with experience is evident: making predictions in a complex world is a risky business, and "*one way for genes to solve the problem of making predictions in rather unpredictable environments is to build in a capacity for learning. […] The advantage of this sort of programming is that it greatly cuts down the number of detailed rules that have to be built into the original program; and it is also capable of coping with changes in the environment that could not have been predicted in detail*" (Dawkins, 1989, p. 56).

Past research has mainly focused on investigating how environmental factors modulate the relationship between the brain and behavior. However, while each unique history of learning and experience significantly contributes to individual variability in brain structure, some aspects of brain morphology are determined by factors, such as genes and hormones, that operate prenatally. In recent years, the investigation of early-determined differences in brain structure, as well as their potential influence on behavior and cognitive processes, has raised growing interest. Following this line of research, this dissertation examines the interaction between brain, behavior, and environment from a different perspective. In particular, we will investigate two factors that influence neuroanatomical variability operating during fetal life, namely the cortical folding process and biological sex, and how they may possibly influence cognitive abilities. Exploring these factors may help to shed light on two key sources of interindividual variability in both brain morphology and cognitive abilities.

Evidence suggests that early-determined and longitudinally stable patterns of cortical morphology such as folding (or sulcal) patterns may reflect pre-natal events that influence the development of cognitive abilities in childhood and adult life among the

healthy population. In particular, recent studies have linked specific cortical folding patterns with advantages in cognitive abilities (e.g., better inhibitory control and reading ability). Similarly, abnormal distribution and morphology of brain sulci have been associated with symptoms and cognitive impairments of some psychiatric disorders such as schizophrenia. In this dissertation, we investigate whether and to what extent cortical folding patterns influence cognitive abilities, brain activity, and brain structure (both cortical morphology and structural connectivity) in the healthy population by means of multiple neuroimaging techniques. In addition to cortical folding, biological sex is another source of brain anatomical variability that operates during pre-natal life through the combined action of steroid hormones and sex-chromosome genes. A number of studies have shown that individual variability in cognitive abilities and in the phenotypical manifestation of many psychiatric and neurological disorders are influenced by sex. In this dissertation, we explore differences between males and females in brain structure by adopting multiple measures of cortical morphology that collectively provide a comprehensive picture of sex differences across the cerebral cortex. Such a picture may help to understand the neural correlates of the recurrently reported sex-related differences in cognitive abilities.

1.2 Executive summary

In Chapter 1, we first introduce the human brain cortex, its structure and development. In the following paragraphs, we focus on the most prominent features of the human brain cortex, that is brain gyri and sulci, and overview different models of cortical gyrification. Then, we examine folding patterns variability and describe two examples of sulcal patterns, namely the paracingulate sulcus and the left occipitotemporal sulcus, with a particular focus on previous evidence suggesting an association between the morphological organization of these sulci and cognitive abilities. In the second part of Chapter 1, we introduce sex differences in brain structure. In particular, we examine evidence from the theory of evolution and genetics that helps us to understand why and how males and females may have developed differences in brain morphology. The importance of examining sexual dimorphism in brain structure is emphasized by reviewing evidence of differences between males and females in cognitive abilities and the phenotypical manifestation of psychiatric and neurological disorders. Then, we describe previous evidence of sex differences in brain morphology. At the end of Chapter 1, we introduce three experiments that have been recently published on peer-reviewed journals. The first two experiments focus on the relationship between sulcal patterns variability and cognitive ability, while the third experiment examines sex differences in brain morphology. The main purpose of this dissertation is summarized in Chapter 2. In Chapter 3, we report the results of each experiment, which are later discussed in Chapter 4. Finally, Chapter 5 provides a detailed description of the materials and methods of each experiment.

1.3 The cerebral cortex and cortical folding

1.3.1 Cortical folding

The most prominent features of the human brain are the cerebral cortex and its folds, consisting in fissures (i.e., sulci) and ridges (i.e., gyri).

The cerebral cortex consists of a thin ribbon of gray matter (GM) surrounding the underlying white matter (WM). The GM contains approximately ∼20% of all brain neurons (Azevedo et al., 2009) supported by glial cells and blood vessels, whereas the WM consists of myelinated axons stemming from, or directed to, the overlying GM. The GM mantle extends approximately 2500 cm^2 with a thickness varying from 2.5 to 4 mm (Matelli & Umiltà, 2007).

The cerebral cortex is organized horizontally in six layers (i.e., laminar organization), which differ in the type of cell population and their distinctive connections with cortical and subcortical regions, and vertically into columns, consisting of cells synaptically interconnected across the horizontal layers (i.e., columnar organization) (Mountcastle, 1997).

In relation to the body size, the human brain is larger than that of most mammals, mainly due to the great expansion of the cerebral cortex, and in particular the prefrontal cortex (Toro et al., 2008; Van Essen et al., 2019). Comparative neuroimaging studies highlighted the exceptional expansion of the human prefrontal cortex compared to other primates (Glasser et al., 2014), and recent findings show that the human prefrontal cortex size deviates significantly from what we would expect if it was a simple scaled-up version of the monkey brain, suggesting that the development of the executive functions mediated by this cortical region may have played a crucial role in human evolution (Smaers et al., 2017)..

The size of the cerebral cortex is strictly related to its volume, i.e., the gray matter volume (GMV). However, the GMV is the product of two genetically and phenotypically distinct structural properties: the cortical surface area (SA) and the cortical thickness (CT) (Panizzon et al., 2009). The former refers to the area occupied by the surface of the cortex (Kaczkurkin et al., 2019), the latter refers to the thickness of the layers of the cerebral cortex, measured as the distance between the WM surface and the pial surface. Evidence suggests that the development of the SA and the CT is driven by two distinct processes, as specified by the Radial Unit Hypothesis (RUH) of

cortical expansion (Rakic, 1995), according to which the number of columns determines the SA, while the number of cells within each column determines the CT. Overall, the cortical development can be decomposed in two distinct processes: tangential expansion (i.e., an increase in the number of columns), which leads to increased SA; radial expansion (i.e., an increase in the number of cells within each column), which determines an increase in CT. Tangential expansion without a significant change in the number of neurons within each columnar unit would result in the expansion of the SA, whereas the opposite mechanism would lead to an increment in CT (Rakic, 1995). The remarkable size of the human cerebral cortex is determined by the disproportionate expansion of the cortical SA, which makes the human cerebral cortex profusely folded (Toro et al., 2008). This data is in line with evidence showing that the cortical volume is more closely related to SA than to CT (Winkler et al., 2010). While the mechanisms that regulate the growth of the cerebral cortex are well understood, the neural processes underpinning the development of sulci and gyri (i.e., the process of "cortical folding" or "gyrification") are still a topic of intense debate. In this section, we will summarize the neural developmental processes that ultimately lead to the arrangement of the cerebral cortex. Then, we will review the main hypothesis of cortical folding.

1.3.2 Brain development

In humans, the neural tube closes during the fifth week of gestation (Budday et al., 2015). In this phase, stem neuroepithelial cells (NECs) (i.e., founder progenitor cells) (Bayer & Altman, 1991) form a single layer at the center of the neural tube. Since the region of the neural tube where the NECs are located will become the ventricles, this region is usually referred to as ventricular zone (VZ). The proliferation of the NECs is determinant for the final number of neurons and is directly linked to the degree of folding. Between weeks 4th and 5th of gestation, NECs undergo to symmetrical division in two new progenitor cells, thus increasing exponentially their pool size (Budday et al., 2015; Miyata et al., 2010). Accordingly, already at the early stages of brain development, the abundance of NECs is much greater in human than in mouse embryo, reflecting human greater brain size and folds complexity (Fernández et al., 2016).

Around the 5th week, prior to the start of neurogenesis, NECs gradually shift from symmetrical to asymmetrical division. In particular, NECs divide in one new progenitor cell, plus a neuron or an intermediate progenitor cell (IPC) (Pontious et al., 2007). The new progenitor cell remains in the VZ, whereas the IPCs form the subventricular zone (SVZ), situated above the VZ (Haubensak et al., 2004), and start dividing in either two IPCs or two neurons. In species with a folded brain[1] the expansion of the SVZ is accompanied by its subdivision into an outer layer (OSVZ) and an inner layer (ISVZ) (Fernández et al., 2016).

Around weeks 6 and 7, neurons that have formed in the VZ and SVZ start migrating to the cortical surface along radial glial guide cells (i.e., radial migration; Rakic, 1972) (Budday et al., 2015). The migration follows an inside-out pattern: the earlier generation neurons form the deepest layers of the cortex, whereas later neurons form the more superficial layers. This process eventually leads to the development of the six-layered cerebral cortex (Stiles & Jernigan, 2010).

Gyrification of the human brain starts around 20 weeks of gestation and follows a specific hierarchical order (Dubois et al., 2019). The formation of the sulci starts at the central region of the brain (central sulcus), then spreads posteriorly towards temporo-parietal-occipital lobes and anteriorly towards the frontal lobes (Dubois et al., 2008).

The primary sulci (e.g., central sulcus, superior temporal sulcus) are the first to appear before 30 weeks of gestation (~ 20 weeks), whereas secondary sulci (e.g., orbital sulcus, olfactory sulcus) start to form after 30 weeks of gestation (~32 weeks), and tertiary sulci (e.g., tertiary sulci of the prefrontal cortex; see Voorhies et al., 2021) around term (~ 38 weeks) (Clouchoux et al., 2012; Dubois et al., 2019). Tertiary sulci are often the shallowest and smallest class of cortical folds, and their development continues after birth, further complicating the pattern of the cortical folds (Dubois et al., 2019). Of note, the primary sulci are highly hereditable and emerge in consistent locations and orientations across individuals, while secondary and tertiary sulci are characterized by a significant variability among individuals (Cachia et al., 2021; Ronan & Fletcher, 2015).

[1] Folded brains are referred to as gyrencephalic, in contrast to lissencephalic brains, which instead exhibit a smooth surface.

Cortical folding is mostly determined in utero. However, changes on the brain surface can be seen throughout the lifespan. Cao et al. (2017) have recently shown that the degree of folding of the human brain decreases non-linearly from the age of 4 to 83, and that this process can be modeled with a logarithmic function of age. It is however important to bear in mind that although measures of sulcal anatomy such as sulcal depth, width or length can change with age and experience, the inter-hemispheric distribution of cortical folds and the presence and location of a sulcal interruption have been proven to be stable over time (Cachia et al., 2016, 2021).

1.3.3 Models of cortical folding

Several models have been proposed to explain the development of cortical folds. These hypotheses tend to focus either on forces external to the developing cortex or on intrinsic forces. In this section, the main hypothesis of cortical folding will be examined.

The external constraint hypothesis

The external constraint hypothesis has been one of the first attempts to provide a biomechanical explanation of cortical folding. The main idea of this hypothesis is that, while cortical tissue grows, the skull offers resistance to its outward expansion, thus forcing the cortex to fold onto itself (Le Gros Clark, 1945).

However, evidence against this hypothesis showed that cortical folding in animal models occurs even without the constraints imposed by the skull (Welker, 1990). Furthermore, skull development seems to be influenced by brain expansion, rather than the opposite. For instance, in hydrocephaly, abnormal brain size determines an enlargement of the skull (Barkovich et al., 2012).

The axonal tension hypothesis

The axonal tension hypothesis (ATH) (Van Essen, 1997) proposed that tension exerted by cortico-cortical axons deforms the cortex, generating gyri and, for geometric necessity, sulci. In particular, brain regions more strongly connected by axons, which are subjected to greater pressure, would be drawn together to form gyri. In contrast, regions poorly connected would drift apart to form the opposite banks of the sulci (Figure 1a).

However, the ATH has been challenged by contrary evidence observed in animal models (Xu et al., 2010). In testing the ATH on the developing ferret brain, it has been observed that the primary forces exerted by axons are mostly located in the subcortical WM, which is too deep to generate the tension necessary for cortical folding (Xu et al., 2010). Furthermore, it has been shown that there is no significant axonal tension between the walls of developing gyri, as postulated by the ATH (Van Essen, 1997).
Overall, these results suggest that axonal tension is not sufficient to initiate, sustain, or maintain cortical folding. However, according to more recent models, cortico-cortical axons may still play a central role in the gyrification process. For instance, by exerting radial tension within gyri that would limit the expansion of the cortex (Toro & Burnod, 2005) or by influencing the maturation of neuronal populations (see next section; see also Ronan & Fletcher, 2015).

The differential tangential expansion hypothesis

In 1975, Richman proposed that cortical folding is driven by the greater radial growth of superficial layers (i.e., supra-granular layers) compared to deep layers (infra-granular layers) of the cerebral cortex, which would eventually forces the cortical surface to fold (Richman et al., 1975). In line with this model, named the "differential growth hypothesis" (Figure 1b), it has been shown that the abundance of progenitor cells in the SVZ (especially in the OSVZ) in gyrencephalic species is associated to increased surface expansion and degree of folding (Reillo et al., 2011). Crucially, the neurons that forms in the SVZ predominantly populate the upper layers of the cortex, thus suggesting that increased supra-granular compared to infra-granular expansion would be determinant for cortical folding (Poluch & Juliano, 2015; Reillo et al., 2011). However, this model has been challenged by several contrary evidence. For instance, the fact that disrupting the neurogenesis in the upper layers of the cortex does not affect cortical folding (Ronan & Fletcher, 2015).
More recently, a modified version of this hypothesis, named the "differential tangential expansion hypothesis", has been proposed. According to this hypothesis, tangential expansion of the cortex increases the tangential pressure, which has to be dissipated through the formation of gyri and sulci (Ronan et al., 2014; Toro & Burnod, 2005; Xu et al., 2010) (Figure 1c). This model is in line with the observation that neurons

migrating prior to gyrogenesis follow a conical trajectory that increases the tangential spread of neurons across the developing cortex (Borrell & Reillo, 2012).

However, this hypothesis has been criticized because it does not account for the high consistency of cortical folding across individuals (i.e., pattern specificity), as well as their correlation with cytoarchitecture and their heritability.

Trying to account for these limitations, a recent model by Ronan & Fletcher (2015) suggested that the pattern-specificity of cortical folds is determined by non-uniform (i.e., differential) cortical expansion, which in turn reflects non-uniform cytoarchitecture patterns across the cortex. In fact, surface expansion is ultimately driven by non-uniform regional cytoarchitecture (i.e., proliferation and growth of cells and their connections), meaning that if non-uniform patterns of regional cytoarchitecture are consistent across the individuals, surface expansion and consequently folding patterns will also be consistent (Ronan & Fletcher, 2015).

The differential tangential expansion hypothesis has recently gained consensus (e.g., Fernández et al., 2016; Kroenke & Bayly, 2018; Ronan & Fletcher, 2015), and is supported by evidence showing that the proliferation of cortical progenitor cells varies across the cortex, being more abundant in cortical regions that undergo to greater surface expansion (Reillo et al., 2011). Moreover, it has been shown that limiting neurogenesis in the upper layers of the parietal cortex, which is usually more extended and folded than the temporal cortex, reduces the extension and the degree of folding in the parietal (but not temporal) cortex (Poluch & Juliano, 2015). Another corroboration comes from early-enucleation studies (i.e., removal of the eyes in a developing fetus before the innervation of thalamo-cortical axons, thus influencing the cytoarchitecture of the visual cortex). In fact, early enucleation determines a significant reduction in extension and an increase in gyrification of the primary visual cortex (V1). This finding directly links cortical folding to cytoarchitecture, suggesting that an altered pattern of cytoarchitecture would be reflected in altered surface expansion and consequently gyrification (Dehay et al., 1991). Of note, despite contradicting the ATH in the specific mechanisms that underlie gyrification, this hypothesis suggests that cortico-cortical and thalamo-cortical axons may still play a central role in cortical folding, by influencing regional maturation of cortical regions (Kroenke & Bayly, 2018; Ronan & Fletcher, 2015).

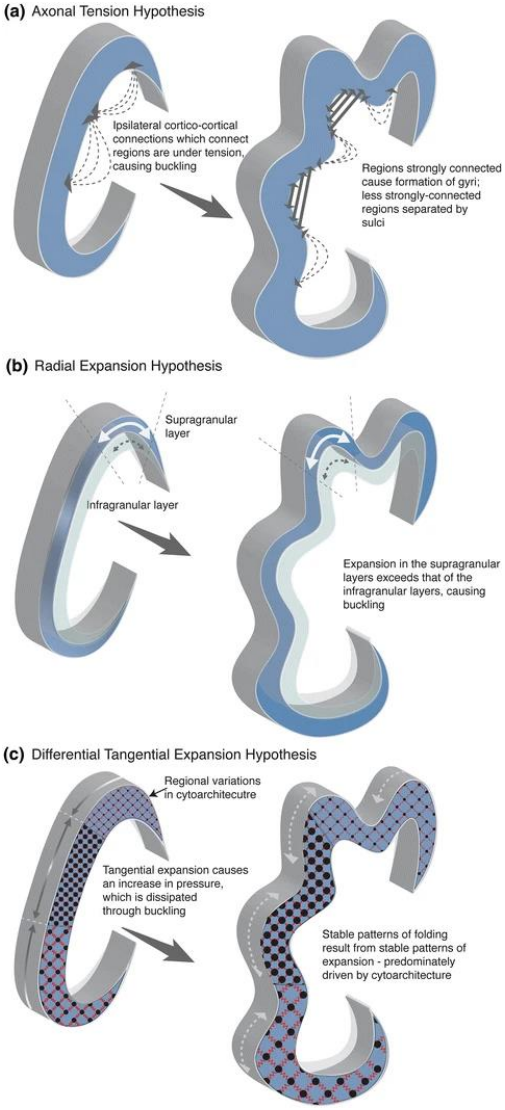

Figure 1. Models of cortical folding. *A) Axonal tension hypothesis: tension exerted by cortico-cortical axons pulls together strongly connected regions to form gyri. Regions poorly connected are drifted apart to form sulci (Van Essen, 1997); b) Radial expansion hypothesis: greater expansion of supra-granular relative to infra-granular layers forces the cortex to fold (Richman et al., 1975); c) Differential tangential expansion hypothesis: tangential expansion of the cortex generates tangential pressure, which is dissipated through buckling (Ronan & Fletcher, 2015). The figure is adapted with permission from Ronan & Fletcher (2015).*

1.3.4 Summary

Gyri and sulci are the most prominent features of the human brain cortex. The gyrification process starts in the later phases of the fetal development, around 20 weeks of gestation, and follows a hierarchical order. Primary sulci, which are highly hereditary and characterized by constant locations and orientations across individuals, are the first to appear. Then, the secondary and tertiary sulci develop, which are characterized by significant variability across individuals. Several models have been proposed to explain the development of cortical folds, including the external constraint hypothesis, the axonal tension hypothesis, and the differential tangential expansion hypothesis. In particular, the differential tangential expansion hypothesis claims that tangential expansion of the cortex generates tangential pressure, which is dissipated through the formation of gyri and sulci. Evidence that the inter-hemispheric distribution of cortical folds and the presence of sulcal interruptions are determined in utero and remain stable over time has prompted researchers to investigate the association between cortical folding patterns and cognitive abilities.

1.4 Folding pattern variability

It is now recognized that structural features of the cortical sheet are associated with inter-individual variability in cognitive abilities (Kanai & Rees, 2011; Schnack et al., 2015; Vuoksimaa et al., 2015) and psychiatric disorders (Birur et al., 2017; Giedd & Rapoport, 2010; Zhang et al., 2018).

However, growing evidence suggests that subtle variations in the intra-uterine environment that influence brain development are associated with postnatal cognitive abilities (Dawes et al., 2015; Raznahan et al., 2012) and later development of psychiatric disorders (Schork et al., 2019; Sey et al., 2020). Based on these findings, in recent years increasing interest has raised around brain structural features that could serve as an indirect marker of intra-uterine events that constrain, to some extent, later development of cognitive abilities (e.g., Cachia et al., 2017, 2018; Del Maschio et al., 2019). An excellent candidate for this purpose appears to be the folding (or sulcal) pattern of brain sulci.

While quantitative measures of cortical morphology (e.g., CT, gyrification index, sulcal depth) vary consistently with age (Cachia et al., 2016; Li et al., 2014; Li et al., 2011; Raznahan et al., 2011) and experience (Del Maschio, Fedeli, et al., 2019), the same is not true for cortical folding patterns. Indeed, the topology (e.g., interrupted vs continuous; Cachia et al., 2018) and the spatial organization (e.g., "power-button" shape; Mellerio et al., 2015) of brain sulci is determined in utero (Mangin et al., 2010) and has been proven to be stable over time (Cachia et al., 2016, 2021; Tissier et al., 2018). Some initial evidence suggests that folding patterns may represent an ideal proxy for prenatal events.

In this section, we will examine two cases of folding pattern variability that have been reported to be linked with differences in cognitive abilities, specifically the paracingulate sulcus and the left occipitotemporal sulcus.

1.4.1 Paracingulate sulcus

The cingulate cortex is located in the brain's medial wall of each hemisphere, above and adjacent to the corpus callosum. The cingulate cortex extends rostro-caudally from the rostrum to the splenium of the corpus callosum, and is delimited ventrally by the callosal sulcus, and dorsally by the cingulate sulcus (CS) (Heilbronner

& Hayden, 2016). Due to its functional and structural heterogeneity, the cingulate cortex is usually divided in distinct subregions. In particular, according to a widely accepted parcellation based on cytoarchitectural, histological, structural, and functional data, the cingulate cortex can be divided rostro-caudally into four subregions: anterior cingulate cortex (ACC), midcingulate cortex (MCC), posterior cingulate cortex (PCC), and restrosplenial cingulate cortex (RSC) (Vogt et al., 2005; Vogt & Gabriel, 1993). Since the sulcal variability of the cingulate cortex mainly affects the ACC and the MCC (Amiez et al., 2018), in this section we will focus on these two subregions.

Anterior cingulate cortex

The ACC is the most rostral region of cingulate cortex, extending below (subgenual ACC) and above (pregenual ACC) the genu of the corpus callosum (Palomero-Gallagher et al., 2009). In terms of structural connectivity, the ACC is extensively connected to brain regions involved in emotion regulation (e.g., amygdala), autonomic functions (e.g., hypothalamus), memory (e.g., hippocampus), and reward processing (e.g., orbitofrontal cortex, ventral striatum) (Stevens et al., 2011). These findings are supported by functional magnetic resonance imaging (fMRI) data, suggesting that the ACC may be greatly involved in affective processing (Stevens et al., 2011). In addition, the most ventral and rostral portion of the ACC, corresponding to the ventromedial prefrontal cortex, plays a crucial role in the default mode network (DMN). The DMN is a group of interconnected regions, including medial and lateral parietal, medial prefrontal, and medial and lateral temporal cortices, whose activation increases at resting state and decreases during goal-directed task performance (Raichle, 2015). For this reason, the DMN activity has been associated to spontaneous cognition (e.g., mind wandering, daydreaming, and stimulus-independent thoughts) (Raichle, 2015). Importantly, the functional integrity and connectivity of the DMN is correlated to normal cognitive functioning (e.g., Mak et al., 2017), as well as to the occurrence of psychiatric (e.g., major depressive disorder; Sheline et al., 2009) and neurological disorders (e.g., Alzheimer's disease; Jones et al., 2011).

Midcingulate cortex

The MCC extends caudally from the ACC until the marginal sulcus. It is structurally connected with the dorsal striatum (caudate and putamen), parietal cortex, premotor and primary motor cortices, precentral gyrus, and dorsal prefrontal cortex (Beckmann et al., 2009; Stevens et al., 2011). The connectivity pattern of the MCC unveils its functional specialization. Indeed, as confirmed by fMRI studies (Stevens et al., 2011), the MCC is extensively involved in motor and high-order executive functions (Efs) (also referred to as cognitive control; Diamond, 2013). Accordingly, the activation of the MCC has been associated to circumstances of conflict monitoring (Botvinick et al., 2004), which involve the presence of interfering information or multiple competing responses simultaneously activated. The MCC would then participate (in concert with other regions) in conflict detection and resolution, by focusing attentional resources on task-relevant output and by adapting the behavior to optimize the performance (Botvinick et al., 2004; Hung et al., 2018). In particular, the MCC has been functionally related to inhibitory control, a core component of EFs (Miyake & Friedman, 2012), which is the ability to stop unwanted thoughts or actions with or without intention (Hung et al., 2018; Zhang et al., 2017). In line with functional findings, the morphology (i.e., GMV, SA and CT) of the MCC has shown to be associated with cognitive performance in tasks that relies upon EFs, such as Flanker and Stroop tasks (Fjell et al., 2012; Takeuchi et al., 2012; Westlye et al., 2011).

Note that despite being two distinct regions in terms of cytoarchitecture (Vogt et al., 1995), structural connectivity (Beckmann et al., 2009) and functional properties (Stevens et al., 2011), the MCC and the ACC are not separated by a clear anatomical landmark. In fact, the term MCC was originally introduced to identify the dorsal portion of the ACC (Vogt & Gabriel, 1993). Moreover, the sulcal variability of the cingulate cortex impacts both the ACC and the MCC (Amiez et al., 2018), and the term “ACC” is still widely used to indicate both regions. For this reason, and to avoid any confusion about labeling, throughout this manuscript we will use the term “ACC” to indicate the ACC, the MCC, as well as the whole ACC-MCC complex.

Sulcal variability of the ACC

The ACC is dorsally delimited by the CS, a primary sulcus emerging early during fetal development (< 30 weeks of gestation) and present in all individuals with stable location and orientation (Amiez et al., 2018; Chi et al., 1977; Dubois et al., 2008).

However, a secondary sulcus running dorsal and parallel to the CS, named paracingulate sulcus (PCS) (Ono et al., 1990), has been observed in at least one hemisphere in 30-60% of individuals (Paus et al., 1996; Yücel et al., 2001), and recent findings suggest that it may be a recent evolutionary acquisition in primates (Amiez et al., 2019). The great variability of the PCS is due to the timing of its ontogenesis. Being a secondary sulcus, the PCS emerges later during fetal development (> 30 weeks of gestation), hence it is more likely to be subject to intra-uterine environmental factors (Amiez et al., 2018; Clouchoux et al., 2012). The PCS sulcal pattern and its inter-hemispheric distribution is presumably determined in utero (Mangin et al., 2010), and evidence suggests that its morphological organization is not affected by postnatal brain maturation (Cachia et al., 2016; Tissier et al., 2018).

The occurrence of the PCS is the primary anatomical landmark for identifying two distinct sulcal patterns of the ACC: a "single" pattern when only the CS is present, and a "double parallel" pattern when the PCS is present in addition to the CS (Ono et al., 1990). In addition, the variable inter-hemispheric incidence of the PCS determines four anatomical patterns, two symmetrical and two asymmetrical. The symmetrical patterns occur when the PCS is bilaterally absent (i.e., "double absence" pattern; Figure 2A) or present (i.e., "double presence" pattern; Figure 2B); the asymmetrical patterns occur when the PCS is present in only one hemisphere (i.e., "leftward asymmetry" when the PCS is present only in the left hemisphere, Figure 2C; "rightward asymmetry" when it is present only in the right hemisphere, Figure 2D). A number of studies showed that the leftward asymmetry is the most common pattern among the general population (Amiez et al., 2018; Leonard et al., 2009; Paus et al., 1996; Yücel et al., 2001). The greater occurrence of the left asymmetry is likely determined by weak genetic and stronger intra-uterine environmental factors, as demonstrated by Amiez et al. (2018). The importance of the prenatal environment is revealed by twin-studies, showing that the leftward asymmetry is more frequent in monozygotic and dizygotic twins (sharing 100% and 50% of their genotype, respectively), as compared to non-twin siblings (also

sharing 50% of their genotype, but developing in a different intra-uterine environment) (Amiez et al., 2018).

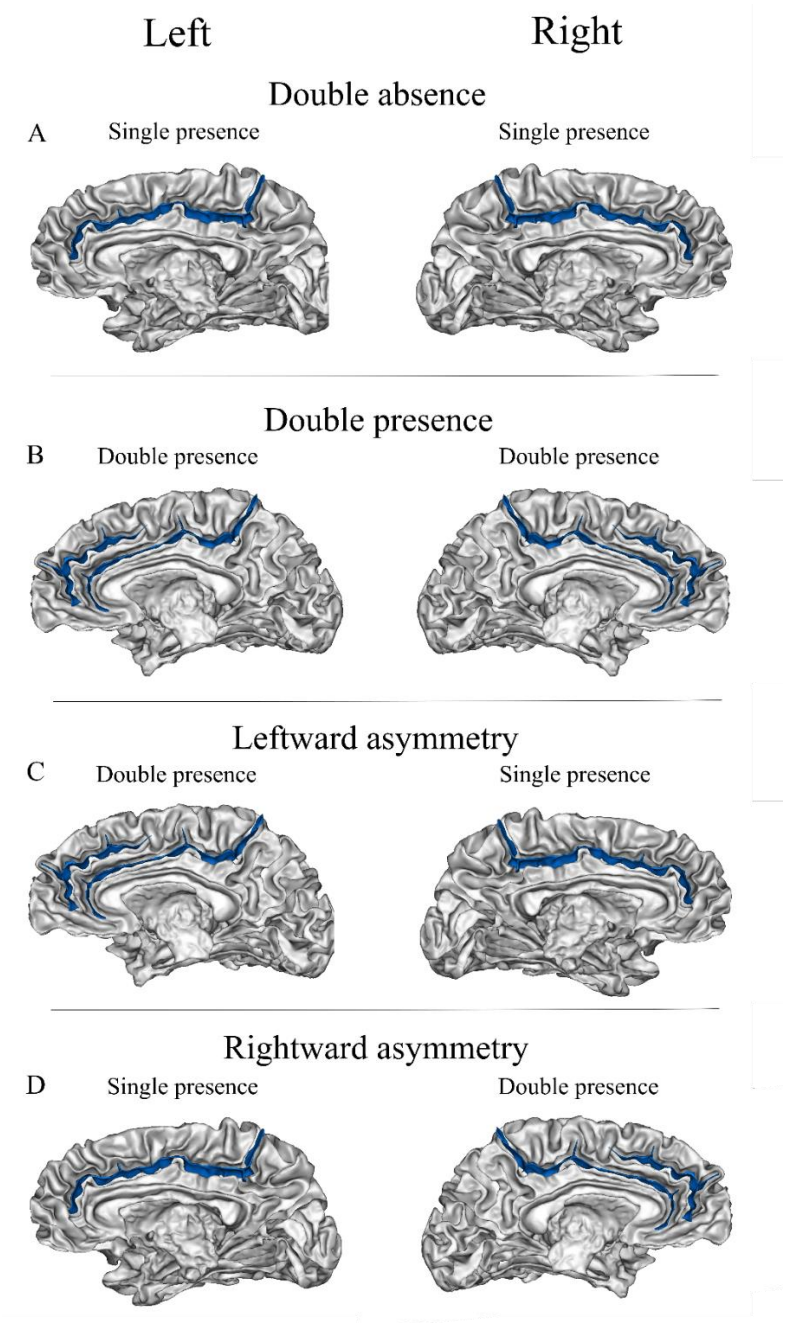

Figure 2. Anterior cingulate cortex (ACC) sulcal patterns*, based on the inter-hemispheric presence (Double presence) or absence (Single presence) of the paracingulate sulcus (PCS). A) Double absence pattern (the PCS is bilaterally absent); B) Double presence pattern (the PCS is bilaterally present); C) Leftward asymmetry pattern (the PCS is present in the left hemisphere and absent in the right hemisphere); D) Rightward asymmetry pattern (the PCS is absent in the left hemisphere and present in the right hemisphere).*

In recent years, a growing number of studies investigated whether the contribution of the ACC to EFs, with particular emphasis on inhibitory control, is modulated by its sulcal organization (Borst et al., 2014; Cachia et al., 2014, 2017; Del Maschio, Sulpizio, et al., 2019; Tissier et al., 2018). Collectively, these studies suggest that asymmetrical patterns – in particular the leftward asymmetrical pattern – are associated to greater cognitive efficiency as compared to symmetrical patterns. This effect has been reported in 5-years-old children performing the animal Stroop task (Cachia et al., 2014), as well as in 9-years-old children and young adults performing the color-word Stroop task (Borst et al., 2014; Tissier et al., 2018), and in adults engaged in the Flanker task (Cachia et al., 2017; Del Maschio, Sulpizio, et al., 2019). Overall, these findings suggest that PCS asymmetry may confer an advantage in tasks requiring to suppress interfering information and prepotent but inappropriate responses. However, these results should not be interpreted as a cue for a deterministic relationship between sulcal organization and cognitive abilities. In fact, PCS asymmetry has been found to explain only 14-27% of variability in behavioral interference scores in the animal and color-word Stroop tasks (Borst et al., 2014; Cachia et al., 2014; Tissier et al., 2018). Furthermore, the putative advantage of PCS asymmetry is modulated by environmental factors such as the bilingual background. In particular, bilingual and monolingual speakers showed reversed patterns of structure-function relationship during a Flanker task: asymmetrical compared to symmetrical sulcal patterns were associated with a performance advantage in monolinguals and a performance disadvantage to bilinguals and vice versa (Cachia et al., 2017; Del Maschio, Sulpizio, et al., 2019). The relevance of the PCS sulcal pattern on cognitive processes has also been reported in the clinical population. For instance, abnormal morphology and reduced leftward asymmetry of the PCS have been linked to EFs impairment (Fornito et al., 2006; Yücel et al., 2002), as well as to the presence of specific symptoms (e.g., hallucinations; Garrison et al., 2015, 2019) in patients with schizophrenia. Similarly, anomalies in PCS patterns have also been observed in the obsessive-compulsive disorder (Shim et al., 2009) and bipolar disorder (Fornito et al., 2007).

From a functional perspective, a few studies examined whether the sulcal organization of the ACC modulates the topology of task-related neurofunctional activity. In a verbal

fluency task, Crosson and colleagues (1999) showed that when the PCS was present, cingulate activation was centered on the PCS. On the other hand, when the PCS was absent, clusters of cingulate activation were centered on the CS. The same result has been reported by Amiez et al. (2013) for the feedback-related activity of the ACC during a trial-and-error learning task. Further studies showed that the ACC sulcal pattern impacts local brain activity during saccadic and tongue movements (Amiez & Petrides, 2014) and pain processing (Jahn et al., 2016). Furthermore, a recent resting-state functional connectivity study showed that the occurrence of the PCS, in concert with age, modulates the functional connectivity pattern of the ACC (Fedeli et al., 2020).

The relationship between PCS morphological variability and cognitive processes may reflect structural changes in the ACC on a micro-structural level (i.e., cytoarchitecture; Vogt et al., 1995) that take place early during fetal development. For instance, it is possible that the sulcal organization of the ACC may influence the extension and the connectivity pattern of the entire region by altering mechanisms of axonal tension (Van Essen, 1997) or tangential surface expansion (Ronan & Fletcher, 2015).

1.4.2 Left Occipitotemporal sulcus

The visual word form area

Reading ability relies on an extended left-lateralized network of brain regions in both children and adults, including the inferior frontal gyrus (extending into the middle and precentral gyri), which is involved in several language processes (e.g., speech planning and production); the temporoparietal cortex, that plays a key role in mapping orthographic into phonological representations and serves as an interface between multimodal sensory and motor regions; the ventral occipitotemporal cortex (vOTC), which is linked to the prelexical processing of orthographic representations within visual words (Houdé et al., 2010; Martin et al., 2015).

In particular, reading has been associated to a specific region within the left lateral occipitotemporal sulcus (OTS), a secondary sulcus running antero-posteriorly on the inferior surface of the temporal lobe, separating the inferior temporal gyrus laterally from the fusiform gyrus medially. This region, termed the “visual word form area” (VWFA) (Cohen & Dehaene, 2004), shows a selective activation to visually presented words compared to other categories of stimuli (Dehaene & Cohen, 2011; Lerma-

Usabiaga et al., 2018). It has been shown that the functional specialization of the VWFA emerges progressively with reading acquisition (Brem et al., 2010; Dehaene-Lambertz et al., 2018; Dehaene et al., 2010) and across different cultures and script types (Bolger et al., 2005).

It has been proposed that the VWFA may rise by coaptation of pre-existing cortical tissue involved in visual objects recognition characterized by a combination of structural properties that makes this site optimal for the analysis of visual letter patterns (Dehaene & Cohen, 2011). In particular, the VWFA may have a privileged position in communicating orthographic visual information from the visual cortex (e.g., V1) to language regions. This hypothesis has been supported by an fMRI study showing that the left lateral OTS is functionally segregated in two subregions with distinct cytoarchitecture: a posterior region associated with low-level visual information processing (i.e., bottom-up processing), and an anterior region related to lexical information processing (i.e., top-down processing), representing the gateway between the visual and language systems (Lerma-Usabiaga et al., 2018).

Note that in many studies the term "VWFA" refers indifferently to the left lateral OTS and to the left fusiform gyrus (FG). This ambiguity is related to the topology of the lateral OTS, which is adjacent to the inferior temporal gyrus laterally and to the fusiform gyrus medially, such that in fMRI studies reading-related activation clusters may encompass both the left lateral OTS and the FG. Throughout this manuscript we will use the labels "VWFA", "lateral OTS" and "OTS" interchangeably, and we will refer separately to the FG. This choice is in line with the original definition of VWFA (Cohen & Dehaene, 2004; Dehaene et al., 2010), with structural connectivity studies in which the left lateral OTS is used as an anatomical proxy of the VWFA (Bouhali et al., 2014; Lerma-Usabiaga et al., 2018), and with recent studies on folding pattern variability in which the VWFA is identified within the left lateral OTS (Cachia et al., 2021).

The relationship between reading ability and cortical morphology

When it comes to examining the relationship between reading ability and cortical morphology, it must be noted that no study has specifically focused on the left OTS. In addition, there is still debate on whether there is a linear relationship between reading ability and structural properties of the left vOTC. For instance, Pernet et al.

(2009) reported a positive correlation between GMV in the left FG and reading skills in typically reading adults, while Johns et al. (2018) did not replicate this result. Moreover, Torre & Eden (2019) observed a significant correlation between reading ability and GMV in the same region, although this effect was present only in female participants. For what concerns other indices of GM morphology, such as CT and SA, findings are also inconsistent. While Torre et al. (2020) observed a positive association between reading ability and CT in the left FG, other studies did not replicate this result, reporting no association between reading ability and local CT (Frye et al., 2010; Goldman & Manis, 2013), a significant association with other reading-related brain regions (e.g., superior temporal cortices, angular gyri) (Blackmon et al., 2010; Johns et al., 2018), or even a negative correlation between reading ability and CT in the left FG (Blackmon et al., 2010). Similarly, no association (Torre et al., 2020) or a negative association (Frye et al., 2010) have been reported between reading ability and SA in the left FG.

In addition to "classic" structural indices such as CT and SA, Kristanto et al., (2020) recently showed that individual differences in reading ability can also be predicted by a measure of sulcal morphology such as sulcal depth (SD). No significant association was reported between reading ability and SD in the left OTS. However, a more pronounced SD in auditory areas was found to be related to better reading ability, while the SD of the right motor cortex was negatively correlated with reading performance (Kristanto et al., 2020).

The relationship between reading ability and structural connectivity

Connectivity studies revealed a consistent and reproducible structural connectivity pattern within the VWFA. Overall, the VWFA is posteriorly connected to visual regions (e.g., left occipital pole, calcarine fissure, and contralateral occipital lobe) (Bouhali et al., 2014), and anteriorly to left brain regions related to language processing. Specifically, the VWFA communicates with perisylvian regions (e.g., inferior frontal gyrus and superior temporal gyrus) through the superior longitudinal fasciculus (SLF); orbitofrontal cortex through the inferior fronto-occipital fasciculus (IFOF); lateral occipital and inferior parietal lobes, including the angular gyrus, through the ventral occipital fasciculus (vOF); anterior, inferior and medial temporal regions through the inferior longitudinal fasciculus (ILF) (Bouhali et al., 2014; Chen

et al., 2019; Yeatman et al., 2013, 2014). Of note, connections between VWFA and left superior temporal regions through the SLF seem to be particularly relevant for reading. Indeed, the developmental rate of this pathway was significantly modulated by reading skills in a longitudinal study conducted on a sample of children aged 7-12 (Yeatman et al., 2012). Moreover, structural connectivity between the VWFA and the left superior temporal sulcus (STS) uniquely predicted reading ability in a sample of adult participants (Chen et al., 2019). Another longitudinal study examined VWFA functional activation and structural connectivity pattern in children at age 5, before they learned to read, and again at age 8, after they learned to read (Saygin et al., 2016). This study revealed that the specific pattern of structural connectivity (but not the functional specialization) of the VWFA could be already observed in 5 years old children. Notably, after the follow-up the VWFA developed functionally and its location in a particular child at age 8 could be predicted from that child's connectivity fingerprints at age 5 (Saygin et al., 2016).

Sulcal variability of the left OTS

Being a secondary sulcus, the lateral OTS starts developing after 30 weeks of gestation (Nishikuni & Ribas, 2013) and is characterized by large individual morphological variability. In particular, the lateral OTS can be present with two distinct sulcal patterns, "continuous" or "interrupted", with a higher rate of the interrupted with respect to the continuous pattern (60% and 52% interruption rate for the left and right OTS, respectively) (Ono et al., 1990).

In line with findings showing a relationship between PCS asymmetry and Efs (Cachia et al., 2021), and with evidence suggesting that the presence of early-developed patterns of structural connectivity biases the subsequent localization of functional activation (Saygin et al., 2016), in recent years some studies investigated whether the sulcal organization of the left OTS constrains subsequent development of reading ability.

The potential relationship between left OTS sulcal pattern and reading ability has been examined in 10-years-old children (Borst et al., 2016). In this first experiment, participants with an interrupted left (but not right) OTS had significantly better reading abilities than participants with a continuous left OTS (Borst et al., 2016) (Figure 3).

This result was later replicated in a sample of adult participants (Cachia et al. 2018). In particular, the effect was specific to the posterior portion of the left OTS, that is, better reading skills were associated to a posterior, but not anterior, interruption of the left OTS. Crucially, the posterior part of left OTS hosts the VWFA. Moreover, the age of reading acquisition significantly modulated the effect of the left OTS sulcal organization. Indeed, the relationship between posterior interruption and reading ability was found in literate, but not ex-illiterate, participants. Of note, the effect of left OTS sulcal pattern accounted for a significant but small portion of the variability in reading ability (4.25%), while most of the variance was explained by environmental factors (e.g., socioeconomic status) (60.25%). It has been proposed that the sulcal pattern of the left OTS may be an indirect marker of increased cortical tissue or connectivity within the VWFA (Ronan & Fletcher, 2015). Recently, however, Roell et al. (2021) failed to replicate these findings, reporting no significant association between the left OTS sulcal pattern and reading ability in a large sample of children.

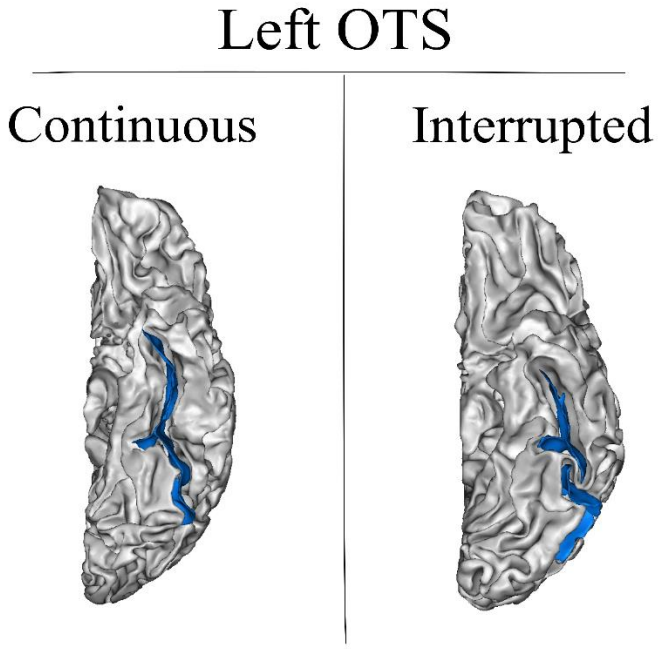

Figure 3. Left occipitotemporal sulcus (OTS) folding patterns*. Continuous left OTS (left panel); Interrupted left OTS (right panel). The same pattern can be observed in the right OTS (not represented).*

1.4.3 Summary

Folding patterns are supposed to reflect pre-natal processes that constrain and influence the development of cognitive abilities. An example of folding patterns variability is represented by the PCS, a secondary sulcus that runs dorsal and parallel to the CS on the medial surface of at least one hemisphere. The variable occurrence and inter-hemispheric distribution of the PCS are determined in utero and are largely unaffected by brain maturation and environmental influences. Moreover, the occurrence of the PCS is partially influenced by hereditary factors and recent evidence suggests that this sulcus represents a recent evolutionary acquisition in the human species. The inter-hemispheric distribution of the PCS determines symmetric (i.e., PCS present or absent in both hemispheres) or asymmetric patterns (i.e., PCS present in one hemisphere and absent in the other). PCS asymmetry has been related with an advantage in response inhibition assessed by means of tasks that require EFs, such as the Stroop and the Flanker tasks. In addition, altered morphology and distribution of the PCS have been linked with cognitive impairments in some psychiatric disorders, such as the schizophrenia. From a functional perspective, distinct PCS patterns have been associated with differences in neurofunctional activity during verbal production, trial-end-error learning, pain processing, saccadic and tongue movements.

More recently, the sulcal organization of the left OTS, which can be continuous or interrupted, has been linked to reading ability. The posterior part of the left OTS contains the VWFA, a brain region whose activity has been specifically associated with the recognition of words and letters during reading tasks. The presence of a left OTS interruption, and in particular a posterior interruption, has been related with better reading ability in childhood and adult life. An increasing number of evidence suggests that early-determined and longitudinally stable morphological features of brain sulci influence cognitive abilities. However, there is another source of brain anatomical variability that operates prenatally before the cortical folding process. This is biological sex, whose influence is determined by genetic and hormonal mechanisms that have been set up during the entire evolution of the human species.

1.5 Sex differences in brain structure

Sex represents an important factor of inter-individual variability in cognitive abilities and in the phenotypical manifestation of many psychiatric and neurological disorders. Therefore, a full comprehension of sex differences in brain structure might significantly contribute to shed light on a key source of variability in both the healthy and diseased brain. In this dissertation, we will use the term "sex" in its biological meaning, indicating an individual's combined sex-chromosome complement (XX in females, XY in males) and gonadal phenotype, and we will distinguish biological sex from gender, a cultural concept that incorporates the self-perception of one's sex. In the present section, we describe the mechanisms that presumably cause sex differences in the brain structure. Then, we focus on the main sex differences in cognitive abilities and psychiatric and neurological disorders. Finally, we provide an overview of the extant evidence of sex differences in brain structure.

1.5.1 Evolution and sexual selection

Although the theory of evolution is beyond the scope of this work, it's worth mentioning what Charles Darwin and modern evolutionary biologists say about differences between sexes, as it could provide useful insights to explain why sex differences in brain structure have developed.

Sex differences have been a topic of interest in biological disciplines since Darwin's second book *The Descent of Man, and Selection in Relation to Sex* (Darwin, 1871), where he presented for the first time the idea of sexual selection. Darwin stated that evolution proceeds following two mechanisms: natural selection and sexual selection. The former is based on an organism's ability to survive and consents diffusion of traits that confer ecological advantages; the latter is based on an organism's reproductive success and consents the diffusion of traits whose advantages are restricted to the mating context (e.g., anatomical ornaments) (Darwin, 1871). In particular, the sexual selection theory was originally introduced to explain the evolution of anatomical or behavioral traits that were apparently useless or harmful for survival, but which nevertheless increased reproductive success (for instance, the male peacock's tail). In general, the spread of sexually dimorphic traits that enhance same-sex (e.g., male-

male) competition or cross-sex (e.g., male-female) attractiveness can be explained by sexual selection.

The basic idea of this theory is that males and females are confronted with similar ecological problems, but they are subject to quite different selection pressures in the mating context (Andersson, 1994; Darwin, 1871; Fisher, 1930). In this section, we will take mammals, the group humans belong to, as main example. In mammals, females make a greater physiological commitment to rearing the offspring compared to males. Therefore, after successfully mating, females take no advantage of additional copulations, and their reproductive success is rather determined by resource availability and acquisition (Clutton-Brock & Huchard, 2013). On the other hand, males could increase their offspring by additional copulations, hence their reproductive success is limited only by access to mates and number of mating opportunities (Andersson, 1994). Accordingly, in order to maximize their reproductive success, males and females developed different reproductive strategies, on which selection acted in sex-specific ways. Of note, according to this model, sex differences are not a consequence of "maleness" or "femaleness", but rather depend on sex-specific reproductive problems and selection pressures in mating (Gaulin, 1995).

While the evolution of conspicuous sexually dimorphic traits, like ornaments and weapons, is easily explained by sexual selection, the mechanisms that drove the development of less visible sexual dimorphisms, including sex differences in brain structure, are less intuitive. Nonetheless, just as any other organ or anatomical structure, the brain can be a potential target of sexual selection. Hence, we should expect to observe sex differences in brain structure whenever males and females were subject to sex-specific adaptive problems and selection pressures throughout the history of the species.

Sexual selection is able to provide an effective explanation of several sex differences in mammals' behavior, including aggressive behavior and spatial ability. For example, greater aggressive behavior in males could have been selected as a consequence of male-male competition for mating opportunities (Lindenfors & Tullberg, 2011). On the other hand, the mechanisms that led to the evolution of sex differences in spatial ability are more complex. It has been proposed that greater spatial ability has specifically evolved in the sex with a higher reproductive rate (i.e., males) since it

would benefit more from the ability to navigate in the environment and locate members of the opposite sex (Gaulin, 1995). Another theory states that sex differences in spatial ability developed as a consequence of labor division, especially after the start of agriculture (i.e., the "hunter-gatherer" theory): female gatherers had to orient in stable and circumscribed food sites, while male hunters had to move across long distances (Silverman et al., 2007).

Obviously, if sexual selection shaped human behavior, this must have been achieved at some neural and metabolic costs, hence influencing brain development in sex-specific ways.

1.5.2 Genes, hormones, and environment

Evolution and sexual selection theories provide a useful framework for explaining why sex differences in brain structure could have been developed, but genetic and hormonal mechanisms can explain how these differences emerge during ontogenesis.

The first event determining the sexual differentiation of the embryo is generally considered the expression of the *Sry* gene encoded in the mammalian Y chromosome, which initiates testicular differentiation (the absence of the *Sry* gene determines the differentiation of the ovaries). Gonads differentiation is of remarkable importance as it determines sex differences in the concentration of and exposure to steroid hormones (e.g., androgens and estrogens), which play a crucial role in determining embryo biological sex through the differentiation of the organism's tissues.

The current view of how steroid hormones affect brain structure has been largely influenced by the organizational-activational hypothesis (McCarthy & Arnold, 2011). Early organizational effects take place during sensitive, usually prenatal, periods and are responsible for permanent and irreversible masculinization or femininization of the brain. The main role in this process is played by androgens, which are the main responsible for the masculinization of the brain, since the development of the female brain represents the default state (McCarthy et al., 2017; McCarthy & Arnold, 2011). An additional wave of organizational effects also occurs during the puberty. Activational effects of steroid hormones determine the expression of sex-specific behaviors in adulthood, by affecting the neural substrate shaped and organized in the earlier sensitive periods.

Steroid hormones play a crucial role in determining sex differences in the human brain, as demonstrated by experimental evidence showing that steroid hormone level variations during fetal development (Lombardo et al., 2012) and puberty (Liao et al., 2021; Peper et al., 2011) are associated to modifications in brain morphology. Similarly, it has been shown that ovarian hormones fluctuation during females' menstrual cycle (Dubol et al., 2021) and gender-affirming hormonal therapies (Kranz et al., 2020) modulates the structure of brain regions.

However, not all sex differences in brain structure are orchestrated by steroid hormones. Indeed, in recent years growing interest has surrounded the specific effects of sex-chromosome genes, which can directly influence brain morphology without the intermediation of steroid hormones (Arnold, 2012; McCarthy & Arnold, 2011; Raznahan & Disteche, 2021).

Indeed, sex-chromosome complement modulates brain structure in different ways, such as male-specific expression of Y-chromosome genes; sex-specific expression of X-linked genes, due to X-chromosome inactivation in females[2]; different parental origin of X-chromosome genes in males (only maternal) and females (either maternal or paternal) (Raznahan & Disteche, 2021). Evidence of direct effects of sex-chromosomes on brain structure comes from genetic disorders characterized by an altered sex-chromosome count (i.e., sex chromosome aneuploidy syndromes). In particular, it has been shown that X-chromosome supernumerary (i.e., excessive number of the X-chromosomes) is associated with reduced structural features of brain structure (e.g., total brain volume, total cortical volume), whereas Y-chromosome supernumerary (i.e., excessive number of Y-chromosomes) is associated with increased structural features of the brain (Raznahan et al., 2016). This trend is consistent with findings in the healthy population, where males usually exhibit larger brain size than females (see section 1.4.5; but also Ruigrok et al., 2014). In addition, alteration of X- or Y-chromosome dosage modulates the GMV in cortical and subcortical regions (Lenroot et al., 2014; Raznahan et al., 2016; Skakkebæk et al., 2014). Interestingly, recent studies observed that X- and Y-chromosome dosage

[2] X-chromosome inactivation is the silencing of one X-chromosome in female mammalian cells in order to equalize the dosage of X-chromosome genes between XX females and XY males (Panning, 2008). However, a relatively large number of X-linked genes escapes silencing, so that a larger proportion of X-linked genes is expressed in females compared to males (Fernández et al., 2016).

alterations have both convergent and divergent (i.e., sex-specific) effects (for a comprehensive review, see Raznahan & Disteche, 2021). Brain structures where X- and Y-chromosome alterations exhibit convergent affects correspond to regions associated with socio-communicative and socio-emotional processing (Raznahan et al., 2016), while specific effects have been found in structures that usually exhibit differences between males and females in the healthy population (Raznahan & Disteche, 2021).

In addition to genetic and hormonal effects, environmental factors also play a crucial role in determining sex differences in brain morphology. Indeed, males and females have different experience throughout the lifespan that affect brain organization (Decasien et al., 2022; McCarthy & Arnold, 2011). For instance, pregnancy experience has been related to an overall reduction in GMV (Cárdenas et al., 2020), especially in brain regions associated to social processing, presumably due to a further specialization of social cognition networks through mechanisms of synaptic pruning (Hoekzema et al., 2017). Sex differences can be found in many sociodemographic domains, including education and occupation, which presumably interact with genes through epigenetic mechanisms, which makes it particularly difficult to disentangle their specific effects on brain structure (Decasien et al., 2022; McCarthy & Arnold, 2011).

1.5.3 Sex matters: sex differences in cognitive abilities and psychiatric and neurological disorders

Sex differences in cognitive abilities

Sex differences in cognitive domains have been extensively documented in the general population (e.g., see Gur & Gur, 2017). Overall, males perform better than females in visuospatial (De Frias et al., 2006; McCarrey et al., 2016; Moreno-Briseño et al., 2010) and motor abilities (Shah et al., 2013), and in mathematical reasoning (Ball et al., 2014). On the other hand, females outperform males in verbal abilities (Jack et al., 2015; McCarrey et al., 2016) and social cognition tasks, such as emotion identification (De Frias et al., 2006; Gur et al., 2012). Accordingly, females also exhibit higher levels of empathy than males from infancy to adulthood, suggesting that

this difference may be the product of some evolutionary process, rather than the result of postnatal events (Christov-Moore et al., 2014).

However, these differences should not be interpreted as deterministic, as they are presumably influenced by environmental factors, such as educational differences between males and females. For instance, it has been shown that reducing the educational gap between males and females also decreases sex-specific advantage in some cognitive abilities (e.g., male advantage in mathematical reasoning) (Weber et al., 2014).

Sex differences in psychiatric and neurological disorders

In the clinical population, many psychiatric (e.g., schizophrenia, major depressive disorder), neurodevelopmental (e.g., autism spectrum disorders, dyslexia, attention deficit hyperactivity disorder), and neurodegenerative (e.g., Alzheimer's disease) disorders are characterized by sex differences in prevalence, age at onset, symptomatology, and response to treatment (e.g., see Kaczkurkin et al., 2019; McCarthy et al., 2017). In what follows, we provide a description of the most consistent sex differences observed in the clinical population.

Schizophrenia

Males compared to females with schizophrenia typically show an earlier age at onset, more severe negative symptoms and cognitive impairments, and worse treatment response (Gobinath et al., 2017; Li et al., 2016). Sex differences in the phenotypical manifestation of schizophrenia may involve sex-chromosomes and steroid hormones. For instance, some evidence suggests that estrogens may play a neuroprotective role against schizophrenia in females, in line with females' second incidence peak during menopause, which is characterized by a decrease of estrogen levels (Li et al., 2016). Moreover, sex-specific alterations in brain structure have been found in schizophrenia patients. For example, male compared to female patients exhibit a greater reduction in total intracranial volume (TIV) (Bora et al., 2011) and local GMV in several brain regions, including bilateral insula, left inferior and medial frontal cortices, and thalamus (Haijma et al., 2013).

Autism Spectrum Disorders

Males show a higher prevalence in neurodevelopmental disorders, in particular the Austim Sprectrum Disorders (ASD) (Ferri et al., 2018). Evidence regarding the influence of sex-chromosomes and steroid hormones is promising but still inconclusive and warrants more study (Ferri et al., 2018). One of the most promising theories that accounts for sex differences in ASD is the "extreme male brain" (EMB) theory, which attributes the male preponderance in ASD to a hyper-masculinized version of the male brain, possibly due to alterations in fetal testosterone levels (Baron-Cohen et al., 2011). Interestingly, this hypothesis is grounded on evidence suggesting that females score higher in empathy and social cognition tasks (Empathy Quotient; EQ), while males are more adept at tasks requiring to analyze a system in terms of the rules that govern it, in order to predict the behavior of the system itself (Systemizing Quotient; SQ) (Baron-Cohen et al., 2005). According to the EMB theory, people with ASD would be characterized by an extreme male profile, i.e., extremely low EQ scores and extremely high SQ scores (Baron-Cohen et al., 2011; Ferri et al., 2018). While this hypothesis refers to a psychological level, supporting evidence has been found in some aspects of neuroanatomy and brain functional connectivity. Indeed, the typical neuroanatomical sex differences observed in the general population seem to be attenuated or absent between males and females with ASD (Beacher et al., 2012). For instance, while healthy males compared to females usually show larger brain size during infancy (Gilmore et al., 2007; Lenroot et al., 2007), this difference is absent in ASD patients, with males and females both showing an equal overgrowth of brain size during the same time period (Courchesne et al., 2011). Another study observed that the functional connectivity within the DMN is equally reduced in males and females with autism compared to controls, whereas in the healthy population females usually show higher DMN intra-connectivity than males (Ypma et al., 2016).

Major depressive disorder

Among affective and anxiety disorders, the most consistent sex difference is the higher prevalence in females, compared to males, in the major depressive disorder (MDD) (Rubinow & Schmidt, 2019). Moreover, females exhibit more internalizing symptoms and attempts of suicide, whereas males show higher risk of substance abuse, aggressive

behavior and completed suicide due to the use of more lethal suicidal methods (Rubinow & Schmidt, 2019).

Magnetic resonance imaging (MRI) studies investigating the neural underpinnings of sex differences in MDD observed sex-specific alterations in local GMV. For instance, GMV of limbic regions was selectively reduced in females with MDD, whereas GMV of striatal regions was reduced only in males with MDD, compared with sex-matched healthy controls (Kong et al., 2013). More recently, Yang et al. (2017) reported smaller GMV in bilateral middle temporal gyrus and left ventromedial prefrontal cortex in males with MDD, while female patients exhibited smaller GMV in the left lingual gyrus and dorsomedial prefrontal cortex, compared with sex-matched healthy controls. Similarly, in another study females with MDD had significantly lower SA and GMV in bilateral prefrontal regions than female controls, while males with MDD had significantly higher SA and GMV in the same regions than male controls (Hu et al., 2022).

Again, steroid hormones are likely to play a crucial role in sex-specific manifestations of MDD. Evidence pointing in this direction comes from sex-specific mood disorders (e.g., postpartum depression and premenstrual dysphoric disorder), which are presumably triggered by changes in ovarian hormone levels (Schmidt et al., 1998). Moreover, steroid hormones influence brain networks development and regulation, such that environmental events are differentially processed (e.g., females experience emotional stimuli as more arousing than males; Andreano & Cahill, 2009) (Rubinow & Schmidt, 2019). On a genetic level, findings suggest that some genes are differentially expressed in males and females with MDD (Labonté et al., 2017). Finally, genes and hormones create a neural substrate that interacts with environment, resulting in susceptibility of resilience to stressful stimuli (Rubinow & Schmidt, 2019).

Alzheimer's disease

Females show higher prevalence in Alzheimer's disease (AD), as well as faster cognitive decline after diagnosis and higher rates of brain atrophy (Ferretti et al., 2018). Experimental evidence concerning sex difference in the levels of AD biomarkers (e.g., accumulation of amyloid-β and tau proteins) is overall inconsistent (Ferretti et al., 2018; Mielke, 2020). However, a recent longitudinal study observed a significant interaction between sex and AD biomarkers, such that for a given level of

amyloid-β concentration, females showed greater hippocampal atrophy and cognitive decline (e.g., memory and EFs) than males (Koran et al., 2017). This result is in line with other findings suggesting that the link between AD neuropathology and its clinical expression could be stronger in females than males. In particular, a seminal paper by Barnes et al. (2005) showed that for each additional unit of AD neuropathology females were more likely to express dementia than males (Barnes et al., 2005). In the same study, females also showed more global AD neuropathology than males (Barnes et al., 2005). This result has been recently replicated in an autopsy study, where females compared to males had an overall higher increase of AD neuropathology with age, especially in the hippocampus (Liesinger et al., 2018).

Of note, prevalence and effects of AD risk factors (e.g., cerebro- and cardiovascular disease, depression, sleep disorders, and low socio-economic status) vary between females and males, with some evidence suggesting the presence of female-specific risk factors (e.g., pregnancy, menopause) (Ferretti et al., 2018). Moreover, sex differences in AD presumably result from interaction between biological and environmental factors (e.g., education and occupational level) (Malpetti et al., 2017). The potential influence of the environment is supported by the cognitive reserve theory, which was originally introduced to account for the discrepancy between the pathology and the clinical outcome in AD patients (Stern, 2002, 2012).

1.5.4 Sex differences in global brain structure

Sex differences in overall brain size are highly consistent across studies. Males show larger total brain volume (TBV) at birth (Knickmeyer et al., 2017), in line with male-bias in fetal head circumference (Broere-Brown et al., 2016). This difference holds throughout childhood, adolescence, and adulthood (Brain Development Cooperative group, 2012; Ritchie et al., 2018; Ruigrok et al., 2014; Sowell et al., 2007). Notably, it has been proposed that sex difference in TBV would be explained by larger body size in males (e.g., height) (Eliot et al., 2021). However, recent studies showed that brain size is disproportionally greater in males compared to females above and beyond sex differences in height (Ritchie et al., 2018; Williams et al., 2021b).

Sex differences in TBV hold when examining GM and WM separately (Ritchie et al., 2018; Ruigrok et al., 2014), despite these two tissue classes follow generally opposing trajectories of volume change with increasing age. In particular, cortical and

subcortical GMV follows an inverted U-shaped trajectory, reaching their peak during puberty, then decreasing and stabilizing during adulthood (Giedd et al., 2015; Mills et al., 2016; Narvacan et al., 2017; Peper et al., 2020) (although subcortical compared to cortical structures show reduced loss of volume with age; see Tamnes et al., 2013). On the other hand, WM volume continues to grow throughout adolescence up until 30 years of age, then it stabilizes and begins to decline during late adulthood (Giedd et al., 2015; Lenroot et al., 2007; Mills et al., 2016; Peper et al., 2020). Studies investigating sex differences in developmental trajectory reported overall inconsistent results (Peper et al., 2020), with some studies suggesting later age-at-peak volumes in males (Giedd et al., 2015; Lenroot et al., 2014; Raznahan et al., 2011, 2014), and others reporting no sex difference (Giedd et al., 2015; Narvacan et al., 2017; Wierenga et al., 2014).

1.5.5 Sex differences in regional gray matter

Gray matter volume

The investigation of sex differences in regional GMV has raised many problems, due to the overall larger body and brain size in males compared to females (Eliot et al., 2021). When regional GMV values are not adjusted to account for these differences, males usually show larger volume in all brain regions, whereas these differences are significantly reduced once that an appropriate correction is applied (Sanchis-Segura et al., 2019). In addition, regional differences observed comparing males and females are significantly influenced by the method used to correct for the brain size (Sanchis-Segura et al., 2019, 2020). A recent review by Eliot et al. (2021) stated that, when accounting for sex-dimorphism in brain size, differences between males and females in the volume of cortical and subcortical regions are null or negligible (Eliot et al., 2021).

However, these results have been disconfirmed by recent findings showing that, when applying a proper correction to account for variations in brain size, sex differences in cortical and subcortical volumes are still consistently and systematically observed (Williams et al., 2021a, 2021b). Recent studies that used large samples and state-of-the-art statistical approaches, revealed highly reproducible sex differences in regional GMV. In particular, Williams et al. (2021a) examined volumetric sex differences in a sample of ~ 40,000 from the UK Biobank Dataset (Miller et al., 2016). In this study,

they observed that 42% (62/148) of cortical brain regions were larger in males (largest difference in the right occipital pole), while 24% (35/148) were larger in females (largest difference in the right postcentral gyrus). Overall, these results are in line with previous large cohort studies (Lotze et al., 2019; Ritchie et al., 2018; Ruigrok et al., 2014) and reveal a pattern of sex differences where females have larger volume in fronto-parietal regions, and males in occipito-temporal regions (Lotze et al., 2019). For what concerns subcortical structures, males usually show greater putamen, amygdala and pallidum (Liu et al., 2020; Ritchie et al., 2018; Williams et al., 2021a), while more mixed results have been found for other subcortical regions. For instance, some studies reported greater thalamus in females (Ruigrok et al., 2014) and others in males (Williams et al., 2021a). Similarly, inconsistent findings have been reported for the hippocampus (males > females: Liu et al., 2020; Lotze et al., 2019; females > males: Williams et al., 2021a). Finally, some studies observed greater caudate (Liu et al., 2020) and accumbens (Ritchie et al., 2018; Williams et al., 2021a) in females, while most studies did not report sex differences in these regions (e.g., see Lotze et al., 2019; Ruigrok et al., 2014).

A recent conjunction analysis performed on the results from three large cohort studies (Figure 4A-4C) revealed a consistent pattern of sex differences, indicating that putamen, amygdala, hippocampus, and temporal pole are larger in males, while cingulate, superior parietal, and lateral prefrontal cortices are larger in females (Figure 4D). In addition, only small clusters showed opposing directions between studies (Decasien et al., 2022) (Figure 4E). A pioneering structural MRI study in neonates showed that sex differences in local GMV can be already observed at birth, and that some of these differences are in line with those detected in adulthood (Knickmeyer et al., 2017). For instance male neonates had larger GMV in left medial temporal cortex and anterior inferior temporal gyrus, while females had larger GMV in posterior middle temporal gyri and parietal cortex (Knickmeyer et al., 2017).

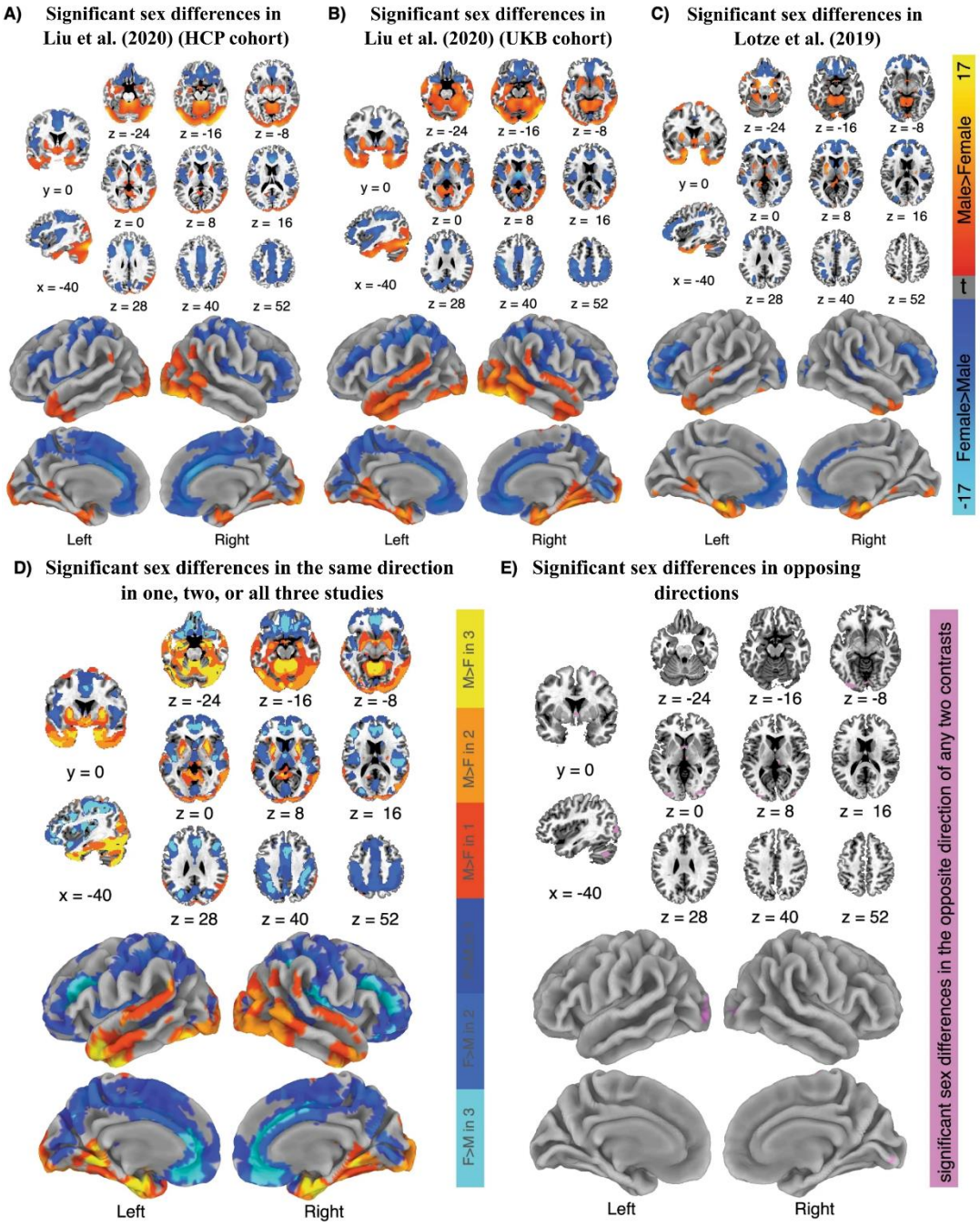

Figure 4. Sex differences in regional gray matter volume across three independent cohorts. *A) Results from the Human Connectome Project (HCP) cohort in Liu et al. (2020) (N = 976); B) Results from the UK Biobank (UKB) cohort in Liu et al. (2020) (N = 1176); C) Results from the Study of Health in Pomerania (SHIP) cohort in Lotze et al. (2019) (N = 2838). D) Conjunction analysis showing overlapping sex differences among the three cohorts. Color indicates whether overlapping results have been found in 1, 2, or 3 of these cohorts (cool colors = F > M; warm colors = M > F). E) Regions that showed inconsistent sex differences across these cohorts. The figure is adapted with permission from Decasien et al. (2022) according to the Creative Commons license (http://creativecommons.org/licenses/by/4.0/).*

Surface area and cortical thickness

On average, males exhibit higher total SA than females, and vice versa females have higher mean CT than males (Williams et al., 2021a). In terms of brain regions, sex differences in SA and CT do not display a consistent and reproducible pattern as observed for the GMV. Overall, males compared to females have greater SA in several brain regions even after adjusting for the total SA, although the effect sizes and the spatial location of the differences vary across studies. For instance, Ritchie et al. (2018) found that 18 regions had higher SA in males, while only 9 regions showed higher SA in females. Similarly, Williams et al. (2021a) observed greater SA in males in 50 regions, whereas females had higher SA in 34 regions. Findings from CT studies are more mixed. Indeed, some studies reported that sex differences in CT were balanced in both directions (i.e., M > F and F > M) (Ritchie et al., 2018; Williams et al., 2021a). On the other hand, other studies observed thicker cortex in males compared to females in most brain regions (Duerden et al., 2020; Escorial et al., 2015), or found only minimal differences, suggesting that males and females may be more similar in CT than in other indices of cortical structure (Wierenga et al., 2014).

1.5.6 Sex differences in white matter and structural connectivity

Microstructural changes in WM bundles are usually addressed by fitting a model to diffusion-weighted (DW) imaging data. The most used model is the diffusion tensor (diffusion tensor imaging; DTI), consisting of an ellipsoid that indicates the direction and the rate of diffusion of water molecules in the brain. Two commonly reported parameters of diffusion tensor imaging are fractional anisotropy (FA) and mean diffusivity (MD). MD reflects the overall diffusion, while FA describes the degree of anisotropy or the direction of the diffusion of water molecules (i.e., how much water molecules are constrained in one direction) and is linked to axon diameter, fiber density, and myelination (Jones et al., 2013; Soares et al., 2013). When investigating sex differences in microstructural properties of WM, males usually show higher FA and lower MD in several WM bundles (e.g., cortico-spinal tract, cingulum, superior longitudinal fasciculus) in adulthood (Lebel et al., 2012; Ritchie et al., 2018) and childhood (Herting et al., 2012; Lebel et al., 2010). However, some studies reported higher FA in females (Bava et al., 2011) or even no sex difference (Krogsrud et al., 2016).

Rather than investigating individual WM bundles, some studies analyzed the whole structural connectome as a complex network. Using this approach, it has been shown that females compared to males have overall higher connectivity within the cerebral cortex, as well as increased efficiency in information processing both locally and across remote cortical regions (Gong et al., 2009; C. Yan et al., 2011). Moreover, males showed greater within-hemispheric connectivity in all supratentorial regions, whereas between-hemispheric connectivity was greater in females. On the other hand, cerebellar connections, which exert their influence on ipsilateral motor behavior communicating with contralateral supratentorial areas, exhibited the reversed pattern (i.e., greater between-hemispheric connectivity in males) (Ingalhalikar et al., 2014). These results suggest that higher within-hemispheric supratentorial connectivity and between-hemispheric cerebellar connectivity in males may facilitate linking between perception and coordinated action. In contrast, higher between-hemispheric supratentorial connectivity in females may facilitate the communication between analytical processing of the left hemisphere and intuitive processing of the right hemisphere (Ingalhalikar et al., 2014).

1.5.7 Greater male variability in brain structure

Robust evidence suggests that males show greater variability than females at both upper and lower extremes of the distribution, meaning that male brains vary more than female brains. This finding has been consistently reported for cortical and subcortical GMV, SA and WM organization across the lifespan (Ritchie et al., 2018; Wierenga et al., 2018, 2020; Williams et al., 2021a). In contrast, contradictory findings have been reported for the CT, with some studies suggesting greater variance in males (Wierenga et al., 2020), others greater variance in females (Williams et al., 2021a), and still others no difference between males and females (Ritchie et al., 2018; Wierenga et al., 2018). It has been proposed that the higher representation of male brains at both extremities of the distribution, rather than mean differences in brain structures, may explain the higher prevalence of several developmental disorders in males compared to females. Furthermore, the greater male variability in brain structure has been linked to the presence of only one X-chromosome in males and to the mosaic of X-chromosome inactivation in females, which would cause the X-linked genes

relating to brain morphology to be expressed in 100% of male cells and 50% only of female cells (Peper et al., 2020).

1.5.8 Summary

Biological sex represents a source of brain anatomical variability the operates mostly during prenatal life. The theory of sexual selection and the modern genetics help us to understand why and how sex differences in brain morphology have developed. On the one hand, the theory of sexual selection states that males and females were subject to sex-specific adaptive problems and selection pressures throughout the history of the species leading to the evolution of sexually dimorphic traits, which include the brain. On the other hand, the genetics demonstrated that steroid hormones play a crucial role in determining sex differences in the human brain during fetal life. Additionally, specific effects of sex-chromosome genes can directly influence brain morphology. The investigation of sex differences in brain morphology assumes importance when we consider evidence showing that males and females in the healthy population differ with respect to cognitive abilities. In particular, females outperform males in verbal abilities, social cognition and empathy, whereas males perform better in visuospatial and motor tasks, as well as in mathematical reasoning. In the clinical population, males and females differ in the prevalence, age at onset, symptomatology and response to treatment of many psychiatric and neurological disorders (e.g., schizophrenia, autism spectrum disorders, major depression, Alzheimer's disease). Sexual dimorphism in brain structure presumably underpins these repeatedly reported sex differences in cognitive abilities and psychiatric/neurological disorders. Robust evidence from neuroimaging studies indicates that males have larger brain size than females. When investigating sex differences in the GMV of brain regions, a consistent and reproducible pattern emerges after accounting for greater male brain size. Specifically, females have larger volume in fronto-parietal regions, and males in temporo-occipital cortices, as well as some subcortical areas (e.g., putamen). However, the GMV is a composite measure resulting from the product between SA and CT. When examining these two components separately, a more mixed pattern of results has been reported.

1.6 Experiment 1 (Introduction): "Cingulate cortex morphology impacts on neurofunctional activity and behavioral performance in interference tasks"

Previous in this dissertation (see section 1.3.1), we overviewed experimental evidence concerning the relationship between the PCS sulcal pattern and cognitive processes, with particular emphasis on inhibitory control. A core dimension of inhibitory control is response inhibition (RI), defined as the ability to withhold and override inappropriate responses that compete for limited cognitive resources (Hung et al., 2018; Zhang et al., 2017). Several studies suggest that PCS asymmetry versus symmetry increases efficiency in RI, as revealed by tasks that involve RI such as the Stroop and the Flanker tasks. Specifically, a PCS asymmetry advantage has been observed in 5-years-old children using the animal Stroop task (Cachia et al., 2014), as well as in 9-years-old children and adults using the color-word Stroop task (Cachia et al., 2014; Tissier et al., 2018). Similarly, advantage in RI associated with asymmetric PCS was also reported for the Flanker task (Cachia et al., 2017; Del Maschio, Sulpizio, et al., 2019).

Functional neuroimaging studies showed that the variable occurrence of the PCS modulates brain functional connectivity at rest (Fedeli et al., 2020), along with the topology of neurofunctional activity during word generation (Crosson et al., 1999), decision-making (Amiez et al., 2013), saccadic and tongue movements (Amiez & Petrides, 2014), and pain processing (Jahn et al., 2016). However, despite the central role played by the ACC in inhibitory control (Hung et al., 2018; Zhang et al., 2017) and the advantage in RI associated with asymmetric PCS distribution, no study has so far investigated whether the ACC folding pattern modulates the neurofunctional activity associated with this crucial component of the EFs.

Therefore, the main goal of Experiment 1 is to investigate whether the repeatedly reported PCS asymmetry advantage in RI is associated with difference in neurofunctional activity during tasks that involve EFs, and specifically inhibitory control. We adopted the Attention Network Task (ANT) (Eriksen & Eriksen, 1974; Fan et al., 2002, 2005) and the Numerical Stroop task (Bush et al., 1998; Windes, 1968) to investigate, respectively, the Flanker effect and the Numerical Stroop task during an fMRI scanning session. Importantly, these two tasks have been related to

distinct dimensions of inhibitory control, namely the "Attention Constraining" and the "Attention Restraining" (Unsworth et al., 2009; Unsworth & Spillers, 2010). The ANT requires participants to indicate the direction of a central horizontal arrow, surrounded on both sides by arrows flanked in the opposite or in the same direction. In this task, participants must constrain their attention on the target stimulus presented among distractors and suppress the interfering information, hence resorting to Attention Constraining. On the other hand, in the Numerical Stroop participants are required to identify the number of digits or alphabetical characters within a sequence of items, while suppressing automatic responses based on the value of the numbers. In this task, participants are instructed to refrain from an automatic (but inappropriate) response (i.e., the number values) in favor of a novel, goal-directed, response (i.e., the number of the items), thereby resorting to Attention Restraining (Unsworth et al., 2009; Unsworth & Spillers, 2010).

In the present study, we classified the ACC sulcal patterns of 42 participants as either symmetric or asymmetric. Then, we compared the reaction times (RTs) and the neurofunctional activity of individuals with symmetric and asymmetric PCS profile. Based on previous findings, we expect that individuals with an asymmetric (vs symmetric) PCS profile would exhibit a marked advantage in RI in terms of response speed (i.e., RTs). Furthermore, we would expect to observe a similar advantage associated with PCS asymmetry when examining the temporal dynamic of inhibitory control by means of delta plots. In terms of functional activity, we expect to observe greater activation in medial frontal regions, including the ACC and PCS, in individuals with symmetric PCS. Indeed, greater cognitive load and task difficulty are typically associated with increased activation of these regions. Finally, we correlated brain neurofunctional activity and RTs to test the relationship between ACC functional activity and behavioral responses.

1.7 Experiment 2 (Introduction): "The relationship between reading abilities and the left occipitotemporal sulcus: a dual perspective study"

As mentioned in the section 1.3.2, reading engages a network of left-lateralized brain regions, including the inferior frontal gyrus, the temporoparietal cortex, and the vOTC (Houdé et al., 2010; Martin et al., 2015). In particular, reading has been associated to a region within the left OTS, namely the VWFA, which exhibits a selective activation to visually presented words compared to other categories of stimuli (Cohen & Dehaene, 2004; Dehaene et al., 2010).

A number of experiments investigated whether reading ability is associated to morphological features (e.g., GMV, SA and CT) and structural connectivity of reading-related brain regions, with particular focus on the left vOTC. However, findings concerning a linear relationship between reading ability and cortical morphology in the left vOTC are overall inconsistent (e.g., see Torre et al., 2020; Torre & Eden, 2019). In addition to "classic" structural indices such as CT and SA, evidence regarding a relationship between reading ability and measures of sulcal morphology such as SD are lacking, and the availably results did not suggest a significant relationship in the left vOTC (Kristanto et al., 2020). Of note, no study has specifically addressed the relationship between cortical morphology and reading ability in the left OTS.

On the other hand, connectivity studies focusing on the left OTS consistently found that this area is extensively connected to language-related brain regions, including left perisylvian regions (e.g., inferior frontal and superior temporal gyri) (Bouhali et al., 2014; Yeatman et al., 2013). In particular, connections between the left OTS and superior temporal regions, which are presumably involved in mapping the orthographic into phonological representations, seem to be associated to reading ability (Chen et al., 2019; Yeatman et al., 2012).

Recent studies proposed that early-determined and life-stable folding patterns of the left OTS may influence later development of reading ability. In particular, it has been proposed that interruption – particularly a posterior interruption – of the left OTS may be associated to better reading ability in children (Borst et al., 2016) and adults (Cachia et al., 2018). Significantly, it has been shown that sulcal pattern variability in specific brain regions may affect cortical morphology. For example, variability of the PCS is

associated to variations in GMV, SA and CT of the adjacent cingulate cortex (Fornito et al., 2008).

To summarize, studies investigating the relationship between reading ability and brain structure have so far examined two distinct research questions: how reading ability is related to brain morphology (Torre et al., 2020; Torre & Eden, 2019) and structural connectivity (e.g., Yeatman et al., 2012), and whether prenatal and life-stable individual differences in the folding pattern of the left OTS, hosting the VWFA, are related to (and may possibly modulate) reading ability (Cachia et al., 2018; Roell et al., 2021).

Currently, no study has examined the relationship between reading ability and cortical morphology by focusing on the left OTS and simultaneously examining the two research questions above described. The goal of Experiment 2 is to adopt a twofold approach to investigate the relationship between the left OTS and reading ability in a sample of 86 healthy adult participants drawn from the Wu-Minn Human Connectome Project (HCP) dataset (Van Essen et al., 2013). First, we tested whether reading skills predict the GM morphology (as indexed by GMV, CT, SA, and SD) and the structural connectivity of the left OTS. Based on previous mixed findings, we expect that cortical morphology may either be associated or not with reading ability. On the contrary, we hypothesize that reading ability would modulate the structural connectivity of the left OTS, in particular with left-lateralized brain regions involved in language and reading processing. Then, we examined whether the sulcal organization of the left OTS modulates reading skills in the adult life. In accordance with previous findings, we expect that the posterior interruption of the left OTS would be associated with better reading ability. Related to this second goal, and based on the evidence suggesting a relationship between folding patterns and brain structure (Fornito et al., 2008), we investigated whether the folding pattern of the left OTS correlates with the morphometric properties and the structural connectivity of this region. We hypothesize that the sulcation pattern of the left OTS would be associated with differences in the cortical morphology and the structural connectivity of the sulcus.

1.8 Experiment 3 (Introduction): "Investigating sexual dimorphism in human brain structure by combining multiple indexes of brain morphology and source-based morphometry"

Sex differences in cognitive abilities (Gur & Gur, 2017) and in neurological/psychiatric disorders (e.g., Rubinow & Schmidt, 2019) arguably reflect differences in brain structure between males and females. Evolutionary biology and genetics suggest that these differences developed as a consequence of sex-specific selective pressures that took place during the evolution of the human species. Moreover, these differences are likely to emerge during the ontogenesis as a result of genetic and hormonal mechanisms, that epigenetically interact with environmental factors throughout life (Decasien et al., 2022; Raznahan & Disteche, 2021).

Neuroimaging studies repeatedly reported highly consistent and reproducible patterns of sex differences in volume. In particular, males usually exhibit greater brain size and greater GMV in occipito-temporal and subcortical regions (e.g., putamen), whereas females show greater volume in fronto-parietal regions (e.g., Decasien et al., 2022). When examining the two determinants of GMV (i.e., SA and CT), males usually show overall higher SA in most cortical regions (Williams et al., 2021a), while studies on CT reported more mixed findings (Ritchie et al., 2018; Wierenga et al., 2014)

In Experiment 3, we aimed at investigating sex differences in a sample of 829 participants drawn from the Wu-Minn HCP dataset (Van Essen et al., 2013). In order to characterize different and complementary aspects of brain morphology, we investigated sexual dimorphism in GM structure by combining distinct facets of cortical morphology, namely GMV, SA, and CT.

In addition, we provide supplemental information on cortex morphology by measuring the cortical complexity, which was quantified using the fractal dimension (FD), a parameter employed to describe the geometry of complex natural systems (Mandelbrot, 1967). In particular, the FD represents an estimate of shape complexity that summarizes in a single numeric value the roughness and the irregularity of a natural object, so that the more irregular an object is, the higher its FD value. In light of evidence that the brain has fractal properties (e.g., self-similarity) at the microscopic and macroscopic levels (Di Ieva et al., 2014, 2015) the use of the FD has increasingly been prompted as a measure of cortical folding complexity. According to previous

studies, the FD is associated with cognitive abilities (Im et al., 2006; Mustafa et al., 2012). Furthermore, the FD differs significantly between clinical (e.g., schizophrenia and Alzheimer's disease) and non-clinical populations (Yotter et al., 2011; King et al., 2009, 2010), and varies across the lifespan in healthy individuals (Kalmanti & Maris, 2007; Madan & Kensinger, 2016).

In addition, we used the source-based morphometry (SoBM) (Xu et al., 2009) to address sex differences in GMV. This technique represents a multivariate extension of the voxel-based morphometry (VBM), and uses the independent component analysis (ICA) (Xu et al., 2009) to identify brain regions with similar patterns of variance. Then, these regions are grouped into independent components (ICs) of GM covariance that are supposed to correspond, to some extent, to resting-state ICs (Segall et al., 2012). To determine whether there is a group difference in an IC, statistical analyses are performed on the loading coefficients, i.e. scalar values representing how an individual component is expressed in each participant (Gupta et al., 2019). So far, no study has used the SoBM to address sex differences in GMV.

Overall, SoBM offers several advantages with respect to VBM. For instance, because it takes into account covariation between voxels and provides information from a network perspective, GM structures within the same IC are supposed to reflect shared morphological features (Kašpárek et al., 2010). Moreover, it also acts as a spatial filter in order to identify and remove artifacts from real brain signals (Xu et al., 2009).

Based on previous findings (see Chen et al., 2007; Ruigrok et al., 2014; Williams et al., 2021a), we predict that both males and females will show regional differences in GMV, with a greater number of regions showing increased GMV in males compared to females, rather than vice versa.

Moreover, we expect that the SoBM will provide more detailed information about sex differences in GMV. Specifically, in line with prior findings, we expect females to show larger volume in fronto-parietal regions, and males to exhibit larger volume in occipito-temporal and subcortical regions.

With regard to SA, we expect to observe greater SA throughout the cerebral cortex for males. Moreover, we expect differences in CT to be balanced in both directions.

Finally, the only study (Luders et al., 2004) that used the FD to characterize sex differences in cortical complexity found higher FD in females in the superior frontal

and parietal lobes bilaterally and in the right inferior frontal lobe (Luders et al., 2004). Our results might corroborate and further expand these previous findings.

In conclusion, we expect that using different techniques and multiple measures, which can capture different and complementary aspects of brain morphology, would provide the best multidimensional and realistic picture of sex differences in GM structure.

2. Aim of the work

It is now unanimously recognized that the brain can reorganize itself at both structural and functional levels as a response to environmental factors (e.g., learning and experience), and this phenomenon greatly contributes to individual differences in brain structure and functional activity. However, some aspects of brain structure are determined by factors, such as genes and hormones, that operate during fetal development and are partly responsible for the individual variability in brain morphology. These early-determined features of the brain may constrain the postnatal development of cognitive abilities providing a differentiated neural substrate on which the environment can operate in specific ways. In this dissertation, we examine the dynamic interplay between the brain, behavior and environment by exploring two main sources of individual neuroanatomical variability that are operate during prenatal life, namely the cortical folding process and biological sex, and how they may possibly be related to interindividual differences in cognitive abilities.

Inter-subject differences in longitudinally stable gyro-sulcal patterns, such as the PCS and left OTS, have been recently linked to differences in functional activity, brain structure, and cognitive performance (e.g., inhibitory control and reading ability). Moreover, biological sex is a factor that shapes the human body from fetal development onwards. This includes conspicuous as well as less visible characteristics of the organism such as the brain. Evolution theory and genetics are informative about why and how sex differences in brain structure have developed during phylo- and ontogenesis. Crucially, a number of evidence suggests that males and females differ in some cognitive abilities, and that the mechanisms underlying some of these differences can be found in brain structure.

In Experiment 1, we used fMRI to investigate whether the ACC sulcal morphology is associated to different patterns of brain activity while performing tasks that rely upon EFs. In Experiment 2, we investigated the dynamic interplay between reading ability and the structure (morphology and structural connectivity) of the left OTS, hosting the VWFA, and examined the putative association between the sulcal morphology of the left OTS and reading ability. In Experiment 3, we explored sex differences in cortical morphology by adopting different neuroimaging techniques that provide distinct and complementary information about brain structure.

3. Results

3.1 Experiment 1 (Results)

In this section, we present the results of the Experiment 1, which investigated the association between ACC sulcal pattern and inhibitory control, addressed by using the ANT and the Numerical Stroop task. First, we describe the ACC sulcal patterns distribution among the study sample. Then, we report, for each task, the clusters of neurofunctional activation detected by comparing tasks conditions (i.e., incongruent, congruent, neutral) and individuals with different PCS profiles (i.e., PCS asymmetry and PCS symmetry). For this purpose, we adopted a state-of-the-art approach to fMRI analysis, the surface-based fMRI, which is supposed to provide a more precise anatomical localization of the clusters of neurofunctional activity compared to the standard volumetric approach (Brodoehl et al., 2020). In terms of behavioral performance, we outline for each task the effects of Condition and ACC sulcal pattern on RTs. Additionally, we report the results of delta plotting, which enables to describe the temporal dynamics of cognitive processes by plotting task effects as a function of response speed (De Jong et al., 1994; Ridderinkhof, 2002; Ridderinkhof et al., 2004). Then, we report results of brain-behavior correlations. At the end of the paragraph, we provide a short summary of the results. Detailed statistical procedures are reported in Section 5.1.

ACC sulcal patterns classification

PCS asymmetry was observed in 20 participants (47.62%), while PCS symmetry was present in 22 participants (52.38%). Among participants with asymmetric sulcal patterns, leftward asymmetry was reported for 12 participants (28.57%), and rightward asymmetry for 8 (19.05%). With regards to symmetric patterns, a double PCS presence was observed in 8 participants (19.05%), and a double PCS absence in 14 participants (33.33%). Sulcal patterns were equally distributed with respect to symmetry and asymmetry ($\chi^2(1) = 0.09$, $p = 0.76$). Moreover, participants with symmetric and asymmetric profiles did not differ in age, gender, handedness, education, socioeconomic status (SES), fluid intelligence quotient, and visuo-spatial working memory (all χ^2 s < 1; all ps > 0.3; all ts < 1).

Neuroimaging analyses

ANT. Irrespective of ACC sulcal pattern, the incongruent vs congruent contrast revealed significant activation in fronto-occipital regions, including the right paracingulate gyrus and orbitofrontal cortex, the bilateral precentral gyrus, the left ventral inferior temporal gyrus, and the right lateral occipital cortex. The incongruent vs neutral contrast resulted in a similar pattern, including the bilateral paracingulate gyrus, superior frontal gyrus, orbitofrontal cortex, and fusiform gyrus. The congruent vs neutral contrast showed increased activation of bilateral occipital regions and the left superior parietal lobule. No significant effect of ACC sulcal patterns was observed. Results are reported in Experiment 1; Figure 1 and Experiment 1; Table 1.

Numerical Stroop. Irrespective of ACC sulcal pattern, the incongruent vs congruent contrast showed the activation of frontal, insular, parietal, and occipital regions, including the left paracingulate gyrus, the right superior frontal gyrus, the bilateral anterior cingulate, orbitofrontal and insular cortices. The incongruent vs neutral contrast resulted in the increased activation of frontal, parietal, and occipital regions, including the bilateral pre- and postcentral gyri, the right paracingulate gyrus and orbitofrontal cortex. The congruent vs neutral contrast did not reveal significant results. When examining the effect of ACC sulcal patterns in the incongruent vs neutral contrast, PCS symmetry compared to PCS asymmetry revealed increased activation of the right paracingulate gyrus and the left superior frontal gyrus. Results are reported in Experiment 1; Figure 2 and Experiment 1; Table 2.

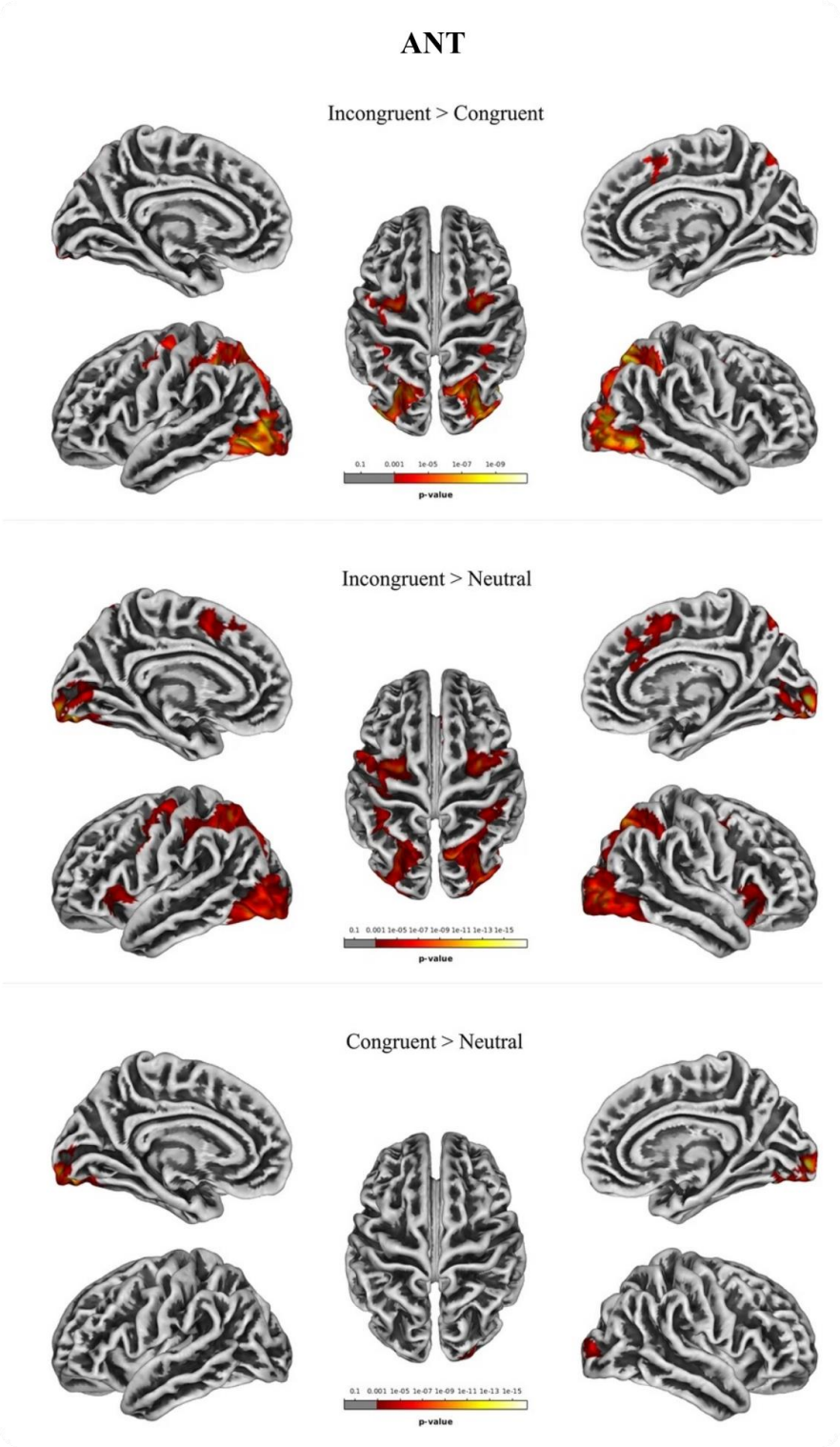

Experiment 1; Figure 1. Significant clusters of neurofunctional activity during the Attention Network Task (ANT). *Results at the cluster level are corrected for multiple comparisons using the Family-Wise Error (FWE) correction. Thresholds: p-FWE < 0.05 at the cluster level, and p < 0.001 uncorrected at the vertex level. The figure is adapted with permission from Fedeli et al. (2022) according to the Creative Commons license (http://creativecommons.org/licenses/by/4.0/).*

ANT										
Contrast	Hemisphere	Region (Harvard–Oxford)	Cluster p -FWE	K (mm^3)	T value	Z score	Peak p-unc	x	y	z
Incongruent > Congruent	R	Lateral Occipital Cortex, inferior division	< 0.001	2151	8.3	6.32	< 0.001	52	− 68	− 8
	L	Inferior Temporal Gyrus, temporooccipital part	< 0.001	2006	8.26	6.3	< 0.001	− 42	− 62	− 3
	R	Precentral Gyrus	< 0.001	233	6.89	5.58	< 0.001	32	− 4	46
	L	Precentral Gyrus	< 0.001	279	5.55	4.76	< 0.001	− 24	− 5	49
	L	Postcentral Gyrus	0.004	39	5.27	4.58	< 0.001	− 46	− 28	35
	L	Precentral Gyrus	0.019	31	4.67	4.16	< 0.001	− 57	6	32
	R	Paracingulate Gyrus	< 0.001	82	4.27	3.86	< 0.001	6	23	47
	R	Frontal Orbital Cortex	0.008	35	4.24	3.84	< 0.001	31	25	− 7
	R	Precentral Gyrus	0.002	43	4.03	3.67	< 0.001	46	8	35
Incongruent > Neutral	R	Occipital Pole	< 0.001	238	13.03	Inf	< 0.001	11	− 96	− 5
	L	Occipital Fusiform Gyrus	< 0.001	3019	12.41	Inf	< 0.001	− 21	− 82	− 18
	R	Occipital Fusiform Gyrus	< 0.001	2762	9.74	6.97	< 0.001	24	− 78	− 14
	R	Middle Frontal Gyrus	< 0.001	400	8.76	6.54	< 0.001	33	− 2	50
	L	Superior Frontal Gyrus	< 0.001	849	8.3	6.32	< 0.001	− 22	− 4	49
	L	Frontal Orbital Cortex	< 0.001	249	6.75	5.51	< 0.001	− 31	26	− 6
	R	Paracingulate Gyrus	< 0.001	359	6.47	5.34	< 0.001	5	17	43
	R	Frontal Orbital Cortex	< 0.001	534	6.24	5.2	< 0.001	26	14	− 19
	L	Paracingulate Gyrus	0.048	27	6.07	5.1	< 0.001	− 10	45	12
	L	Juxtapositional Lobule Cortex	< 0.001	163	5.7	4.86	< 0.001	− 5	5	45
	R	Precentral Gyrus	< 0.001	107	5.44	4.69	< 0.001	47	9	29
	L	Juxtapositional Lobule Cortex	< 0.001	50	5.14	4.49	< 0.001	− 6	− 7	49
	R	Superior Frontal Gyrus	0.012	34	4.49	4.03	< 0.001	13	10	66
	R	Intracalcarine Cortex	0.01	35	4.32	3.9	< 0.001	15	− 61	6
Congruent > Neutral	L	Occipital Fusiform Gyrus	< 0.001	439	12.26	Inf	< 0.001	− 19	− 83	− 13
	R	Occipital Fusiform Gyrus	< 0.001	279	11.7	7.71	< 0.001	23	− 79	− 12
	R	Occipital Pole	< 0.001	94	11.62	7.68	< 0.001	11	− 96	− 7
	R	Occipital Pole	< 0.001	90	5.63	4.81	< 0.001	30	− 93	8
	L	Superior Parietal Lobule	0.025	30	4.84	4.28	< 0.001	− 27	− 54	46
	R	Intracalcarine Cortex	0.15	21	4.57	4.09	< 0.001	15	− 78	11
	L	Lateral Occipital Cortex	0.013	33	4.55	4.07	< 0.001	− 26	− 83	17
	L	Intracalcarine Cortex	< 0.001	50	4.16	3.78	< 0.001	− 6	− 87	3

Experiment 1; Table 1. Significant clusters of neurofunctional activity during the Attention Network Task (ANT). *Significance threshold is set at p-uncorrected < 0.001 at the vertex level, and p-FWE < 0.05 at the cluster level. For each cluster, only the local maximum is reported. Coordinates are based on MNI standard template. L = Left hemisphere; R = Right hemisphere.*

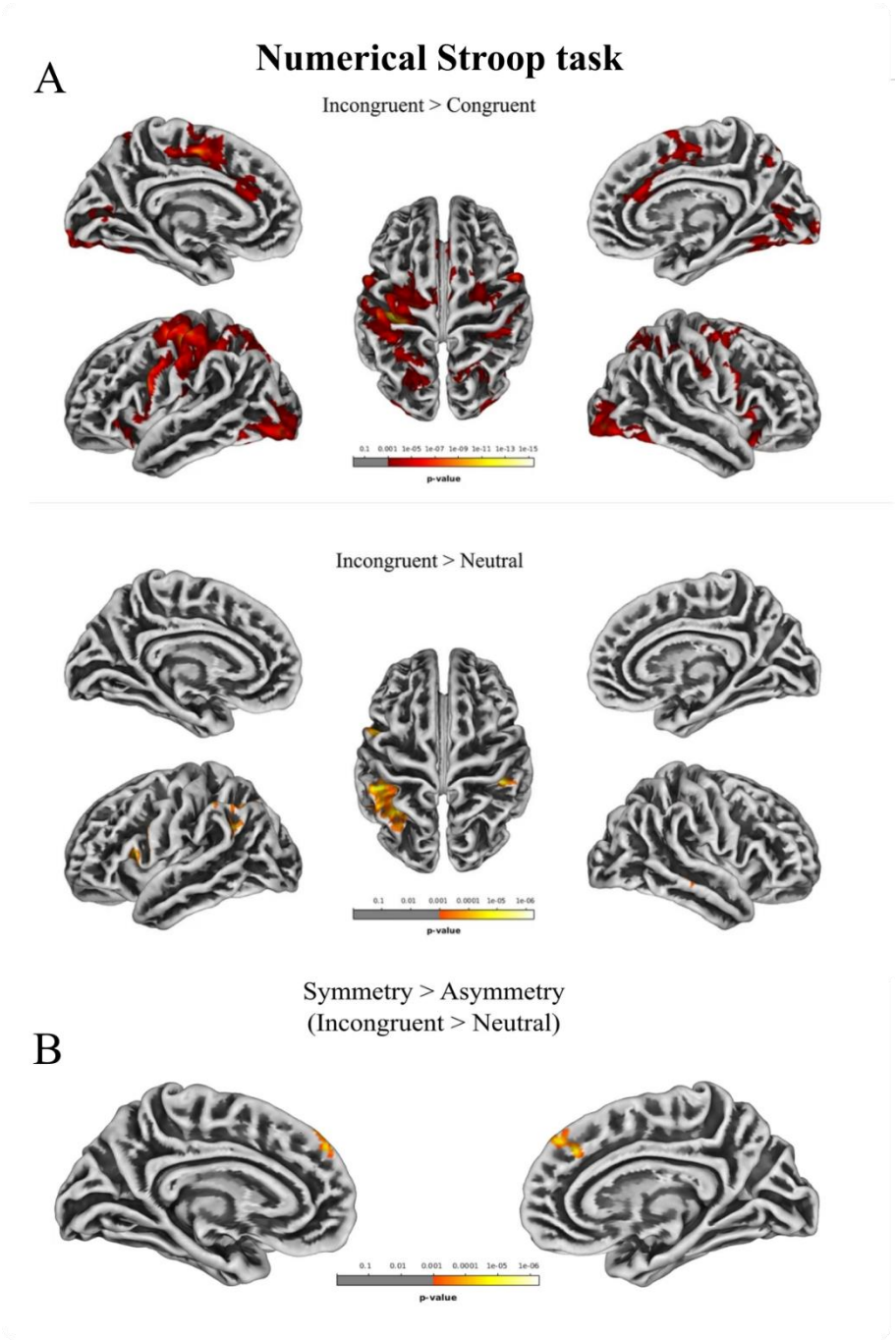

Experiment 1; Figure 2. Significant clusters of neurofunctional activity during the Numerical Stroop task. *A) Significant activations resulting from comparing task conditions. B) Significant activations resulting from the contrast PCS symmetry vs PCS asymmetry. Results at the cluster level are corrected for multiple comparisons using Family-Wise Error (FWE) correction. Thresholds: p-FWE < 0.05 at the cluster level, and p < 0.001 uncorrected at the vertex level. The figure is adapted with permission from Fedeli et al. (2022) according to the Creative Commons license (http://creativecommons.org/licenses/by/4.0/).*

Emotional Stroop Task

Contrast	Hemisphere	Region (Harvard–Oxford)	Cluster p-FWE	K (mm^3)	T value	Z score	Peak p-unc	x	y	z
Incongruent > Congruent	L	Precentral Gyrus	< 0.001	2902	11.6	7.68	< 0.001	− 34	− 23	46
	L	Occipital Fusiform Gyrus	< 0.001	796	7.2	5.76	< 0.001	− 28	− 79	− 14
	L	Precentral Gyrus	< 0.001	313	7.18	5.74	< 0.001	− 56	9	23
	R	Lateral Occipital Cortex, inferior division	< 0.001	732	7.14	5.72	< 0.001	38	− 86	− 9
	R	Precentral Gyrus	< 0.001	122	6.67	5.46	< 0.001	55	11	32
	L	Central Opercular Cortex	< 0.001	78	6.46	5.33	< 0.001	− 49	− 21	21
	L	Lateral Occipital Cortex, superior division	< 0.001	729	6.27	5.22	< 0.001	− 28	− 67	31
	R	Cingulate Gyrus, anterior division	< 0.001	199	6.23	5.19	< 0.001	4	27	16
	R	Superior Frontal Gyrus	< 0.001	410	6.14	5.14	< 0.001	24	− 8	58
	L	Frontal Orbital Cortex	< 0.001	104	6.08	5.1	< 0.001	− 28	18	− 16
	R	Insular Cortex	< 0.001	120	5.76	4.9	< 0.001	40	14	− 7
	R	Frontal Orbital Cortex	< 0.001	79	5.62	4.81	< 0.001	26	15	− 18
	R	Juxtapositional Lobule Cortex	< 0.001	247	5.57	4.78	< 0.001	8	3	46
	L	Insular Cortex	< 0.001	54	5.48	4.72	< 0.001	− 37	9	− 4
	R	Supramarginal Gyrus, posterior division	< 0.001	494	5.47	4.71	< 0.001	37	− 37	42
	L	Paracingulate Gyrus	0.007	36	5.31	4.61	< 0.001	− 12	46	2
	R	Lateral Occipital Cortex, superior division	< 0.001	134	5.28	4.58	< 0.001	30	− 74	23
	R	Precuneous Cortex	0.004	39	5.07	4.44	< 0.001	4	− 66	46
	L	Intracalcarine Cortex	< 0.001	163	4.92	4.34	< 0.001	− 12	− 77	10
	L	Cingulate Gyrus, anterior division	< 0.001	207	4.85	4.28	< 0.001	− 2	31	19
	R	Intracalcarine Cortex	< 0.001	147	4.76	4.23	< 0.001	7	− 73	10
	L	Cingulate Gyrus, posterior division	0.016	32	4.76	4.22	< 0.001	− 2	− 24	43
	L	Precuneous Cortex	0.011	34	4.72	4.19	< 0.001	− 4	− 57	32
	L	Cingulate Gyrus, posterior division	< 0.001	54	4.72	4.19	< 0.001	− 2	− 50	21
	R	Lateral Occipital Cortex, superior division	< 0.001	190	4.68	4.16	< 0.001	29	− 62	53
	R	Angular Gyrus	0.036	28	4.67	4.16	< 0.001	41	− 57	17
	L	Insular Cortex	0.001	44	4.26	3.85	< 0.001	− 35	− 4	16
	R	Superior Parietal Lobule	< 0.001	76	4.09	3.72	< 0.001	28	− 48	50
Incongruent > Neutral	L	Inferior Frontal Gyrus, pars opercularis	< 0.001	67	5.33	4.62	< 0.001	− 45	16	9
	R	Postcentral Gyrus	< 0.001	91	5.31	4.6	< 0.001	46	− 30	46
	L	Supramarginal Gyrus, anterior division	< 0.001	691	5.21	4.54	< 0.001	− 52	− 30	46

Incongruent > Neutral	R	Occipital Pole	0.043	28	5.18	4.52	< 0.001	28	− 94	− 12
	L	Angular Gyrus	< 0.001	72	5.06	4.43	< 0.001	− 54	− 57	33
	R	Superior Temporal Gyrus, posterior division	0.003	42	4.94	4.35	< 0.001	63	− 24	− 5
	L	Precentral Gyrus	< 0.001	155	4.92	4.33	< 0.001	− 49	8	33
	R	Angular Gyrus	0.002	44	4.64	4.13	< 0.001	39	− 55	43
	L	Inferior Frontal Gyrus, pars opercularis	0.004	40	3.96	3.63	< 0.001	− 52	20	15
Congruent > Neutral	–	–	–	–	–	–	–	–	–	–
Stroop (Incongruent > Neutral)										
Symmetric > Asymmetric	L	Superior Frontal Gyrus	0.013	33	5.01	4.36	< 0.001	− 4	46	46
	R	Paracingulate Gyrus	0.002	43	4.84	4.24	< 0.001	5	35	30

Experiment 1; Table 2. Significant clusters of neurofunctional activity during the Numerical Stroop task. *Results obtained by comparing task conditions and by contrasting PCS asymmetry > PCS symmetry are reported. Significance threshold is set at p-uncorrected < 0.001 at the vertex level, and p-FWE < 0.05 at the cluster level. For each cluster, only the local maximum is reported. Coordinates are based on MNI standard template. L = Left hemisphere; R = Right hemisphere.*

Behavioral analyses

ANT. When examining the effect of Condition on RTs, we observed a significant effect (χ^2 (2) = 1657.79, p < 0.001). In particular, we detected faster responses for neutral (mean RTs = 552 ms ± 126) compared to congruent trials (mean RTs = 571 ± 129; *b* = - 18.84, SE = 2.86, t = − 6.59), and faster responses for congruent compared to incongruent trials (mean RTs = 667 ms ± 150, *b* = − 95.75, SE = 2.86, t = − 33.45). No effect of ACC sulcal pattern was observed (χ^2 (1) = 0.92, p = 0.34), nor a two-way interaction between ACC sulcal pattern and Condition (χ^2 (1) = 3.2, p = 0.2). Delta plots are reported in Experiment 1; Figure 3. Delta plots show that the incongruent > congruent effect (i.e., incongruency effect) increased linearly for individuals with asymmetric patterns and nonlinearly for individuals with symmetric patterns, which exhibit a flatter slope that decreases in the fifth quantile associated with the slowest responses. Similarly, the incongruent > neutral effect (i.e., interference effect) increased linearly for individuals with asymmetric patterns and nonlinearly for individuals with symmetric patterns, with a slope that flattened in the last quantile. The congruent > neutral effect was constant for individuals with asymmetric PCS, with an almost flat slope across all the quantiles, while the same effect increased linearly for individuals with symmetric PCS.

ANT

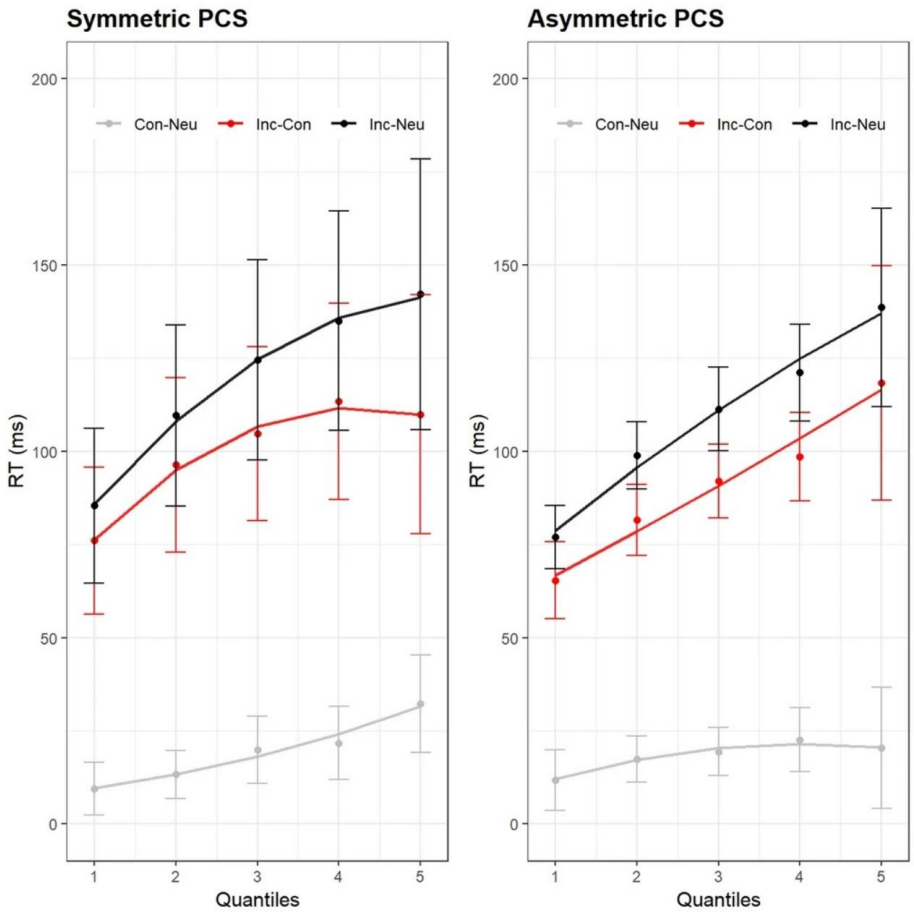

Experiment 1; Figure 3. Delta plots for the Attention Network Task (ANT). *Effects are plotted as a function of quantiles. Incong = Incongruent; Cong = Congruent; Neu = Neutral. The figure is adapted with permission from Fedeli et al. (2022) according to the Creative Commons license (http://creativecommons.org/licenses/by/4.0/).*

Numerical Stroop task. The effects of ACC sulcal pattern and Condition on RTs were tested, revealing a significant effect of Condition (χ^2 (2) = 348.12, p < 0.001). In particular, we detected faster responses for congruent (mean RTs = 639 ms ± 155) compared to neutral trials (mean RTs = 673 ms ± 164; *b* = − 33.59, SE = 3.54, t = − 9.5), and faster responses for congruent compared to incongruent trials (mean RTs = 707 ms ± 172; b = − 66.91, SE = 3.55, t = − 18.84). No effect of ACC sulcal pattern was observed (χ^2 (1) = 2, p = 0.16), nor a two-way interaction between ACC sulcal pattern and Condition (χ^2 (1) = 3.2, p = 0.2). Delta plots are reported in Experiment 1; Figure 4. The incongruent > congruent effect (i.e., incongruency effect) increased almost linearly for both individuals with asymmetric and symmetric patterns. The incongruent > neutral effect (i.e., interference effect) increased nonlinearly in individuals with an asymmetric PCS, with the slope flattening from the third quantile onwards, and linearly in individuals with symmetric PCS. The neutral > congruent effect remained stable across all quantiles for both individuals with symmetric and asymmetric PCS.

Brain-behavior correlation

In order to explore the effect of PCS symmetry detected in the incongruent > neutral contrast of the Numerical Stroop task, a correlation analysis was performed between brain activity and RTs associated with the incongruent > neutral effect (interference effect). Using the significant clusters resulting from the incongruent > neutral contrast in Numerical Stroop, the mean Blood Oxygenation Level Dependent (BOLD) signal was extracted for each participant. Then, a correlation analysis was performed between the mean BOLD activity and the interference effect associated with the slowest responses (corresponding to the fourth and fifth quantiles of the delta plots). Correlations were performed independently for individuals with asymmetric and symmetric sulcal patterns. No significant correlation was observed.

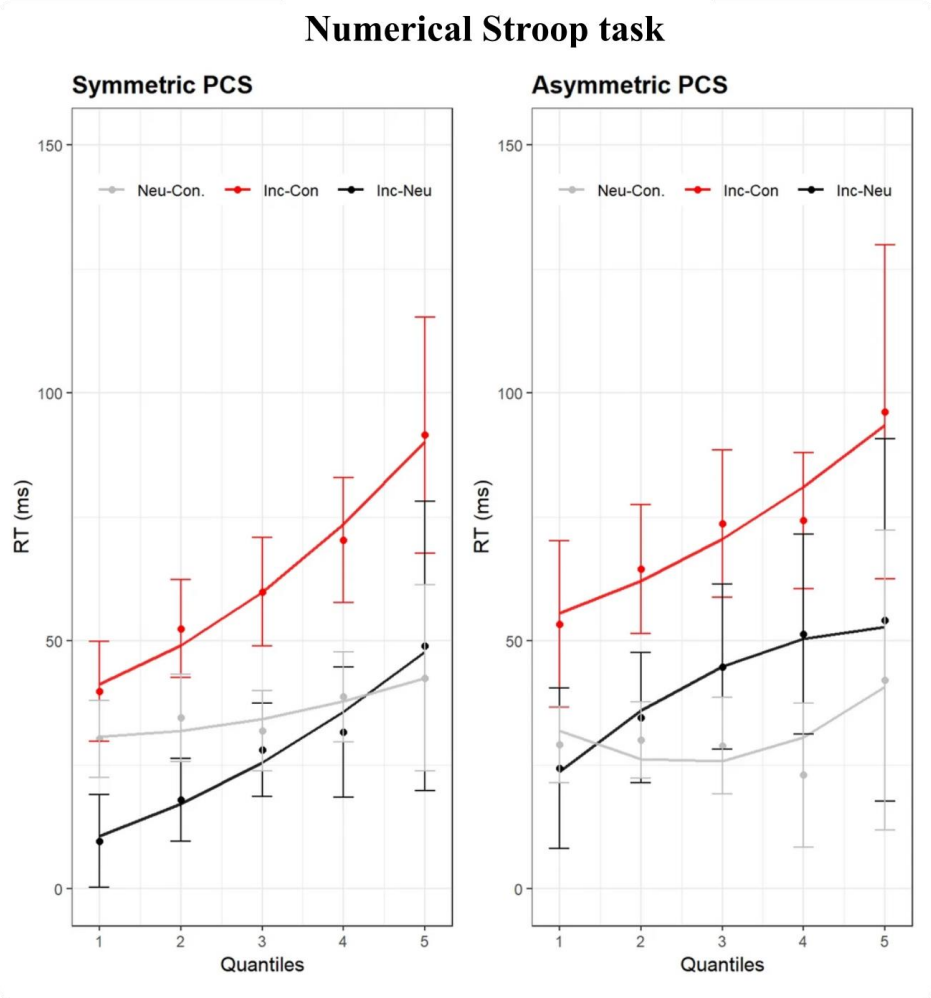

Experiment 1; Figure 4. Delta plots for the Numerical Stroop task. *Effects are plotted as a function of quantiles. Incong = Incongruent; Cong = Congruent; Neu = Neutral. The figure is adapted with permission from Fedeli et al. (2022) Creative Commons license (http://creativecommons.org/licenses/by/4.0/).*

.

Summary

The incongruent > congruent and incongruent > neutral contrasts in the ANT activated a bilateral pattern of frontal and occipital regions, including paracingulate, precentral and inferior frontal gyri, as well as lateral occipital and ventral occipitotemporal regions. In the same task, the congruent vs neutral contrast showed increased activation of bilateral occipital regions and left superior parietal lobule. Analyses on RTs revealed a significant effect of Condition (neutral > congruent > incongruent). No effect of ACC sulcal patterns was observed in neuroimaging or behavioral analyses. The delta plots of the ANT showed that PCS asymmetry was associated with an increase of the incongruency and interference effects as a function of response speed, whereas individuals with PCS symmetry showed a reduction of the same effects, pointing toward an advantage of PCS symmetry. In the Numerical Stroop task, the incongruent > congruent contrast resulted in the activation of frontal, insular, parietal, and occipital regions, including the ACC and the paracingulate gyrus, while the incongruent > neutral contrast revealed the activation of a similar pattern of regions, but no significant activation of medial frontal areas was detected. We found evidence that ACC sulcal organization affects brain functional activity associated with RI during the Numerical Stroop task. Specifically, PCS symmetry compared to PCS asymmetry was associated with increased neurofunctional activity of the medial frontal regions (i.e., left superior medial frontal gyrus and right paracingulate gyrus) in the incongruent > neutral contrast (i.e., interference effect) of the Numerical Stroop task. Analyses on RTs revealed a significant effect of Condition (congruent > neutral > incongruent), but no effect of ACC sulcal patterns. Visual inspection of the delta plots generated for the same task revealed that PCS symmetry was associated with an increase of the interference effect as a function of response speed, whereas PCS asymmetry was associated with a reduction of the same effect in correspondence with the last quantiles (i.e., slowest responses), pointing toward a PCS asymmetry advantage. No significant brain-behavior correlation was found.

3.2 Experiment 2 (Results)

In this section, we first present results concerning the association between reading ability and left OTS morphology and structural connectivity. Then, we present findings concerning whether the left OTS sulcal organization is correlated with i) reading ability; ii) left OTS morphology; iii) left OTS structural connectivity. The morphology of the sulcus was characterized using distinct indices of cortical structure, specifically GMV, SA, CT, and SD. In order to account for individual differences in brain size, each index was properly corrected using the corresponding measure of global brain structure (i.e., TIV for GMV; total SA for SA; average CT for CT). Structural connectivity analyses were performed using the Network-Based Statistics (NBS) Connectome toolbox (Zalesky et al., 2010). The effects of interest were tested using a range of network-forming thresholds: 2.4 – 2.8 (in line with recent studies, e.g., Beare et al., 2017; Çelik et al., 2020; DeSerisy et al., 2021). In the present section, we report only networks detected using a primary threshold of 2.6 (further details about the NBS statistical approach are reported in section 5.2). Effects of left OTS sulcal organization were examined by considering the possible effect of the position of the interruption (i.e., anterior and/or posterior interruption). At the end of the paragraph, we provide a short summary of the results.

Reading-related morphometric measures of left OTS

Reading ability was not associated with morphometric indices extracted from the left OTS (all ps > 0.05).

Reading-related connectivity of left OTS

Using thresholds 2.4, 2.5, 2.6 and 2.7, reading ability was positively associated with a set of nodes connected to the left OTS (p-family-wise error (FWE) corrected < 0.05). No significant networks were observed at threshold 2.8 (p-FWE > 0.05). Using a primary threshold of 2.6, we detected a network of regions positively associated with reading ability (p-FWE = 0.032), including the left superior temporal regions, insula, orbitofrontal cortex, and putamen (Experiment 2; Figure 1). The nodes included in the network and the corresponding t-values are reported in Experiment 2; Table 1. Network detected using other primary thresholds are reported in the Appendices (see Appendices; Experiment 2; Figure S1).

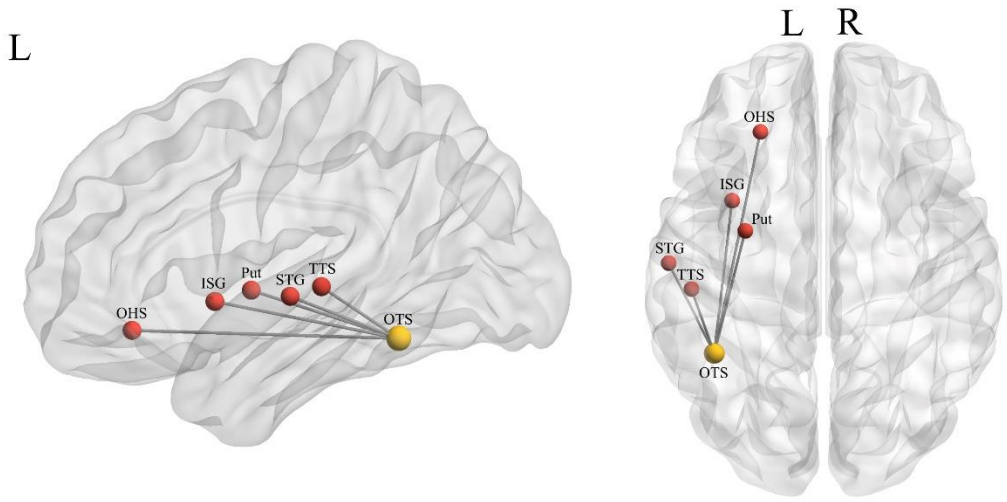

Experiment 2; Figure 1. Reading-related network. *Anatomical labels were adopted from the Destrieux Atlas (Destrieux et al., 2010). OTS = occipitotemporal sulcus; STG = superior temporal gyrus; TTS = temporal transverse sulcus; Put = putamen; ISG = insular short gyrus; OHS = orbital H-shaped sulcus; L = left hemisphere; R = right hemisphere. The figure is adapted with permission from Del Mauro, Del Maschio et al. (2022).*

Node	T-value
LH Insular short gyrus	2.77
LH Superior temporal gyrus	3.02
LH Orbital H shaped sulcus	2.90
LH Temporal transverse sulcus	2.93
LH Putamen	2.62

Experiment 2; Table 1. Reading-related network. *For each node of the network is reported the corresponding t-value. Each node is connected to the left lateral occipitotemporal sulcus (OTS). Anatomical labels were adopted from the Destrieux Atlas (Destrieux et al., 2010); LH = left hemisphere.*

Effect of left OTS sulcal pattern on reading

The sulcal organization of the left OTS was not significantly associated with reading ability. In particular, neither the anterior nor posterior interruption was associated with reading proficiency (all ps > 0.05).

Effect of left OTS sulcal pattern on morphometric measures

The posterior organization of the left OTS was significantly associated with the SD of the sulcus (t = 3.898, p-Bonferroni < 0.001). In particular, posterior continuation, rather than interruption, was correlated to increased SD of the left OTS. Similarly, the SA of the sulcus was higher when the posterior branch of the left OTS was continuous, rather than interrupted (t = 4.94, p-Bonferroni < 0.001). Moreover, the two-way interaction between posterior and anterior sulcal patterns had a significant effect on the SA of the left OTS (t = -2.589, p-Bonferroni = 0.045). The plot of the interaction is reported in Experiment 2; Figure 2. The plot suggests that a posterior interruption of the sulcus, independently from the pattern of the anterior OTS (i.e., double-interrupted and posterior-interrupted patterns), was associated to lower SA, compared to double-continuous and anterior-interrupted (posterior continuous – anterior interrupted) patterns, with the latter showing the highest SA. No significant effect of sulcal patterns was observed on GMV and CT (p > 0.05).

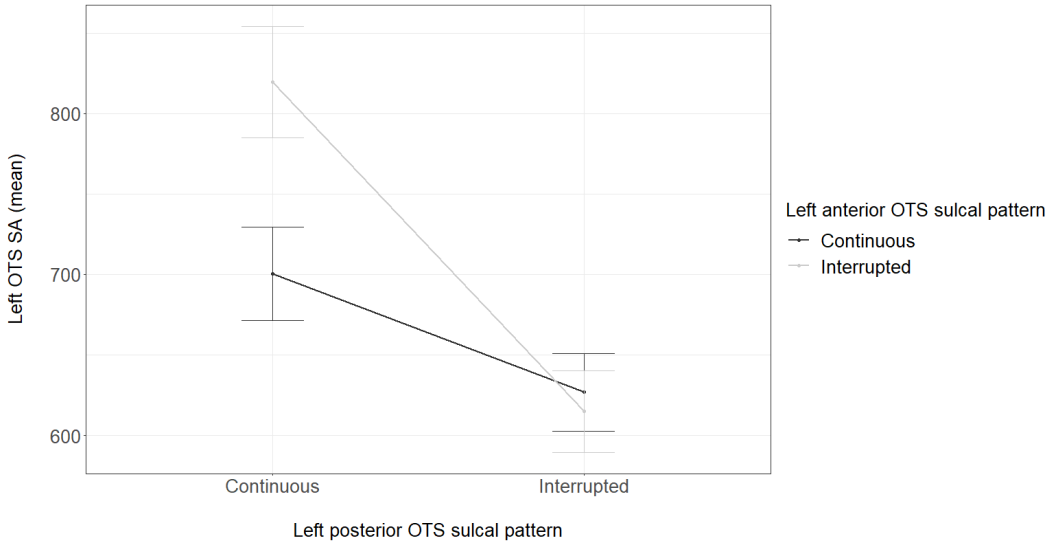

Experiment 2; Figure 2. Posterior x Anterior sulcal patterns two-way interaction. *The mean surface area (SA) is reported on the Y-axis. The posterior sulcal pattern of left occipitotemporal sulcus (OTS) is reported on the X-axis. The anterior sulcal pattern is indicated by colors: black = continuous; gray = interrupted. Double-interrupted and posterior-interrupted (posterior interrupted – anterior continuous) patterns are associated to lower SA, compared to double-continuous and anterior-interrupted (posterior continuous – anterior interrupted) patterns. Anterior-interrupted pattern exhibit the highest SA. The figure is adapted with permission from Del Mauro, Del Maschio et al. (2022).*

Effect of left OTS sulcal pattern on structural connectivity

Using thresholds 2.4, 2.5 and 2.6, posterior interruption was significantly associated with a set of nodes connected to the left OTS (p-FWE < 0.05). No significant effect was observed at thresholds 2.7 and 2.8. Using a primary threshold of 2.6, the network associated with posterior interruption (p-FWE = 0.042) included the left precuneus, the right inferior temporal sulcus and the right calcarine sulcus (see Experiment 2; Figure 3; Experiment 2; Table 2). Networks observed using thresholds 2.4 and 2.5 are reported in the Appendices (see Appendices; Experiment 2; Figure S2). No main effect of anterior sulcal pattern was observed, nor a two-way interaction between anterior and posterior sulcal patterns (p-FWE > 0.05).

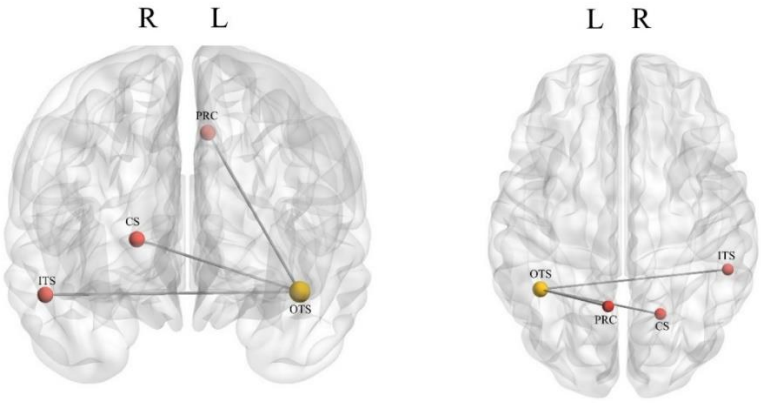

Experiment 2; Figure 3. Network associated with posterior occipitotemporal sulcus (OTS) interruption. *Anatomical labels were adopted from the Destrieux Atlas (Destrieux et al., 2010). OTS = occipitotemporal sulcus; PRC = precuneus; CS = Calcarine sulcus; ITS = inferior temporal sulcus; L = left hemisphere; R = right hemisphere. The figure is adapted with permission from Del Mauro, Del Maschio et al. (2022).*

Node	T-value
LH Precuneus	3.09
RH Inferior temporal sulcus	2.98
RH Calcarine sulcus	2.74

Experiment 2; Table 2. Network associated with posterior occipitotemporal sulcus (OTS) interruption. *For each node, the corresponding t-value is reported. Each node is connected to the left OTS. Anatomical labels were adopted from the Destrieux Atlas (Destrieux et al., 2010). LH = left hemisphere; RH = right hemisphere.*

Summary

Reading proficiency scores were not associated with cortical morphological (i.e., GMV, SA, CT, and SD) of the left OTS, hosting the so-called VWFA. However, reading ability significantly predicted the connectivity strength between the left OTS and a network of left-lateralized brain regions involved in language and reading processing, including insula, orbital sulcus, superior temporal gyrus, temporal transverse sulcus, and putamen. This result indicates that reading skills might be associated with the communication of the left OTS with other regions involved in reading. In contrast with our hypothesis, we did not detect a significant association between posterior interruption of the left OTS and reading ability. Nonetheless, we observed that the posterior interruption of the left OTS was associated with lower SA and SD of the sulcus and increased structural connectivity between the left OTS and the right inferior temporal sulcus, the right calcarine sulcus, and the left precuneus.

3.3 Experiment 3 (Results)

Sex differences in global brain structure and cortical regions

In this section, we describe sex differences using distinct indices of cortical morphology. First, we report sex differences in global brain structure, as addressed by TBV, total SA, average CT, and FD of the cortical ribbon. With regards to sex differences in brain regions, we first describe the results of the analysis performed on the global brain structure and on the cortical regions using four indices of cortical morphology (i.e., GMV, SA, CT and FD) without correcting for brain-general differences between males and females. Then, we report the results of this analysis after applying a proper correction to account for sex differences in global brain structure. In particular, local morphometric values were linearly corrected using the appropriate global measure, namely TBV for GMV, total SA for SA, average CT for CT, and FD of the cortical ribbon for FD. For each analysis, we also report the largest effect sizes calculated with the Cohen's *d*. Note that negative effect sizes denote higher brain measures in males, and vice versa. Also note that the definition of the cortical regions is based on the whole-brain parcellation atlas provided by Destrieux et al. (2010), which includes 148 regions of interest (ROIs) (Appendices; Experiment 3; Figure S1). At the end of the paragraph, we provide a short summary of the results. Further details on statistical analyses are reported in Section 5.3.

Sex differences in global brain structure. Males had significantly larger TBV (d = -1.48) and total SA (d = -1.42) than females. No difference emerged for average CT and FD of the cortical ribbon ($p > 0.05$) (Experiment 3; Table 1).

	Sample (N = 829)	Females (N = 380)	Males (N = 449)
	Mean ± SD	Mean ± SD	Mean ± SD
TBV (mm)	1253379 ± 127226.3	1168788 ± 93021.81	1324969 ± 106722.6
Total SA (mm^3)	175562.8 ± 17881.64	164007.6 ± 13591.39	185342.2 ± 15019.73
Average CT (mm^2)	2.63 ± 0.08	2.63 ± 0.08	2.64 ± 0.09
FD of the cortical ribbon	2.58 ± 0.01	2.58 ± 0.01	2.58 ± 0.01

Experiment 3; Table 1. Descriptive statistics of global brain structure. *Mean and standard deviation (SD) of total brain volume (TBV), total surface area (SA), average cortical thickness (CT), and fractal dimension (FD) of the cortical ribbon are reported for the entire sample, and for males and females separately.*

Sex differences in cortical regions. We found only limited sex differences in GMV and SA. In terms of cortical GMV, males compared to females had larger volume in 13 ROIs. In particular, large differences were found in the left (d = -0.44) and the right short insular gyri (d = -0.4). Other regions with larger volume in males included occipital poles, orbital sulci, and the left rectus.

On the other hand, 8 ROIs were larger in females compared to males. The largest differences were located in the left superior parietal gyrus (d = 0.31) and the occipital sulcus (d = 0.29). Other regions with larger volume in females included the right superior parietal gyrus, the postcentral gyrus, and the bilateral superior frontal sulcus (Experiment 3; Figures 1A) (a table including all the regions significantly different between males and females is reported in Appendices; Experiment 3; Table S1).

With regards to SA, we observed significant sex differences in 10 ROIs, which largely corresponded to the regions where we detected significantly different volumes. In particular, 6 ROIs had greater SA in males (right occipital pole; d = -0.28), and 4 ROIs had greater SA in females (left superior occipital sulcus; d = 0.3) (Experiment 3; Figures 1B) (a detailed list of significantly different regions is reported in Appendices; Experiment 3; Table S2).

On the other hand, CT displayed broad differences in both directions and distributed across the entire cerebral cortex. Specifically, 30 ROIs showed higher thickness in males compared to females (right inferior segment of the circular sulcus of the insula;

d = -0.67), and vice versa 30 ROIs were thicker in females compared to males (left angular gyrus; *d* = 0.46) (Experiment 3; Figures 1C) (a detailed list of significantly different ROIs is reported in Appendices; Experiment 3; Table S3).

When examining differences in FD, all but 11 ROIs exhibited higher FD in males (left short insular gyrus, *d* = -1.04) (Experiment 3; Figures 1D) (a list of the ROIs where no significant sex difference was detected is reported in Appendices; Experiment 3; Table S4).

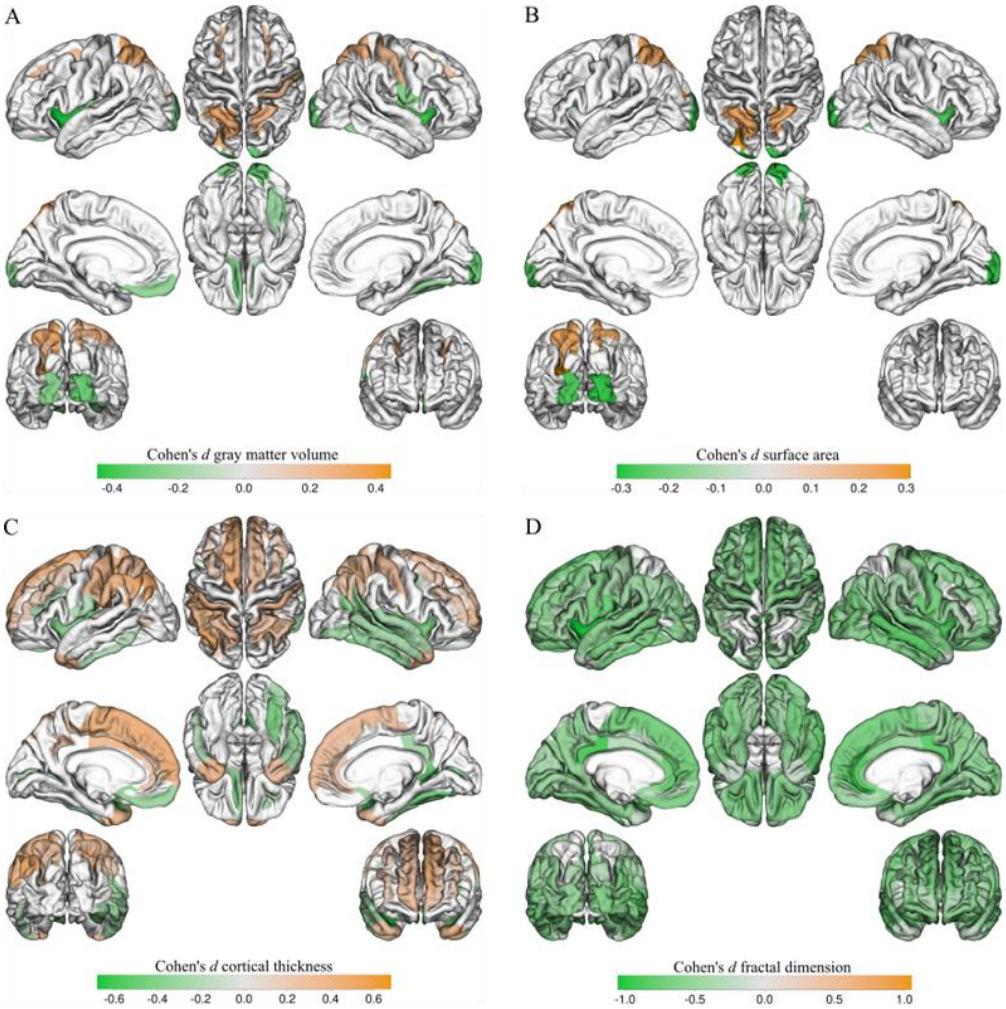

Experiment 3; Figure 1. Sex differences across regions of interest (corrected). *Sex differences in gray matter volume (A), surface area (B), cortical thickness (C), and fractal dimension (D). The colormap is based on the direction and intensity of effect sizes. Color green indicates higher local values for males (i.e., negative effect sizes), while color orange indicates higher local values for females (i.e., positive effect sizes). The figure is adapted with permission from Del Mauro, Del Maschio, Sulpizio, et al. (2022).*

Source-based morphometry

Among the 57 ICs included in the statistical analysis, 26 components were found to be significantly different as a function of sex (note that a significant group difference in an IC indicates that one group has a higher GMV in that component compared to another). Each component was converted into Z scores and thresholded at $|Z \geq 3.5|$ in order to display only clusters that were strictly related to their IC. The ICs are presented here divided into groups with similar spatial topography. For each group, we report either the mean effect size, or the effect size of each IC included in the group. Negative effect sizes denote higher GMV in males. Only representations of two groups of ICs are reported in this section as main examples. Further details about the SoBM technique are reported in Section 5.3. Detailed results are reported in Appendices; Experiment 3; Table S5.

Subcortical components (IC1, IC14, IC17). Females showed higher GMV in bilateral thalamus (IC1; d = 0.22) and caudate (IC14; d = 0.34). Males exhibited larger GMV in bilateral putamen (IC17; d = -0.33) (Experiment 3; Figure 2).

Frontal components (IC13, IC27, IC29, IC36, IC49, IC75). Females showed larger volume in all frontal components, (e.g., ACC, medial orbitofrontal cortex, dorsolateral and ventrolateral prefrontal cortex) (mean d = 0.27) (Appendices; Experiment 3; Figure S2).

Temporal and parahippocampal components (IC3, IC19, IC21, IC43). Males exhibited higher volume in lateral and medial temporal regions (e.g., inferior temporal cortices, fusiform gyri) (IC3, IC19, IC21) (mean d = -0.4). Females showed higher volume in the right superior temporal cortex, encompassing the inferior parietal lobule (IC43) (d = 0.27) (Appendices; Experiment 3; Figure S3).

Parietal and pre-postcentral components (IC18, IC31, IC51, IC73). Females had larger volume in the inferior parietal lobules, pre- and postcentral gyri (mean d = 0.32) (Experiment 3; Figure 3).

Posterior components (IC5, IC16, IC44; IC50). Precuneus and posterior/middle cingulate cortex were larger in females (IC5, IC44; mean d = 0.22), as well as superior and medial occipital regions (IC50; d = 0.21). Males exhibited larger volume in the

most inferior and rostral aspects of the occipital lobes, including calcarine scissure and lingual gyri (IC16; *d* = -0.93) (Appendices; Experiment 3; Figure S4).

Cerebellar components (IC4, IC42, IC45, IC48, and IC64). All cerebellar components were larger in males compared to females (mean *d* = -0.32) (Appendices; Experiment 3; Figure S5).

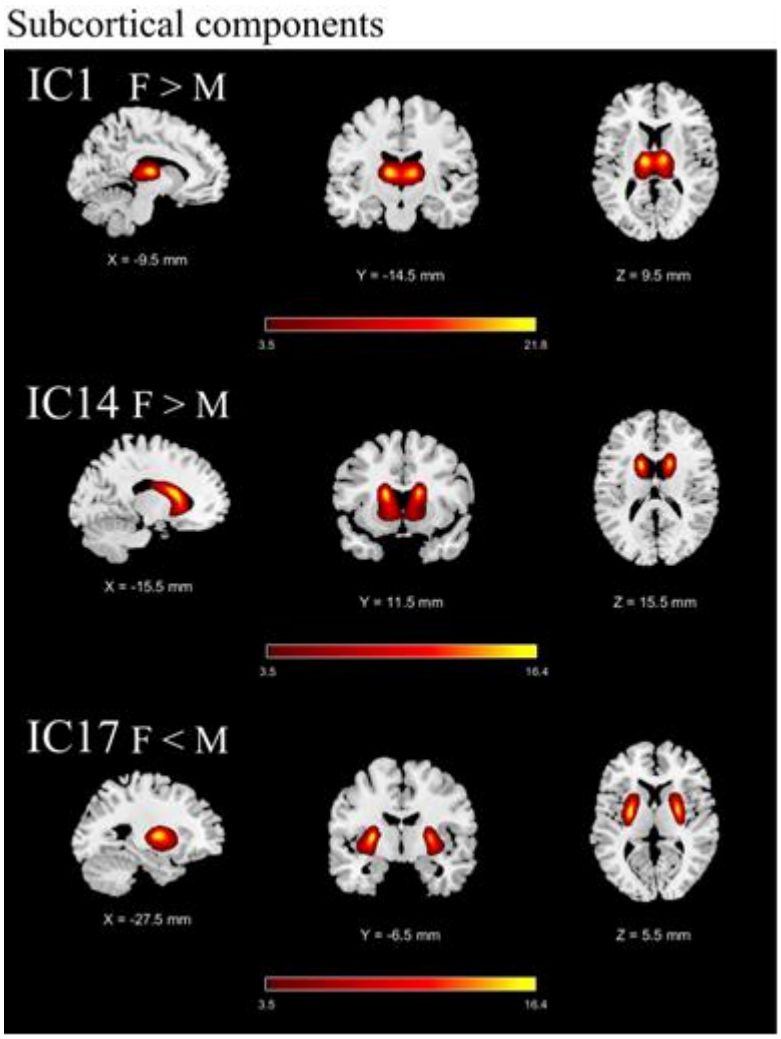

Experiment 3; Figure 2. ICs grouped as subcortical components. *Females showed larger gray matter volume (GMV) in IC1 and IC14, while males showed larger GMV in the IC17. Colormap is based on Z-score thresholded at $|Z \geq 3.5|$. The figure is adapted with permission from Del Mauro, Del Maschio, Sulpizio, et al. (2022).*

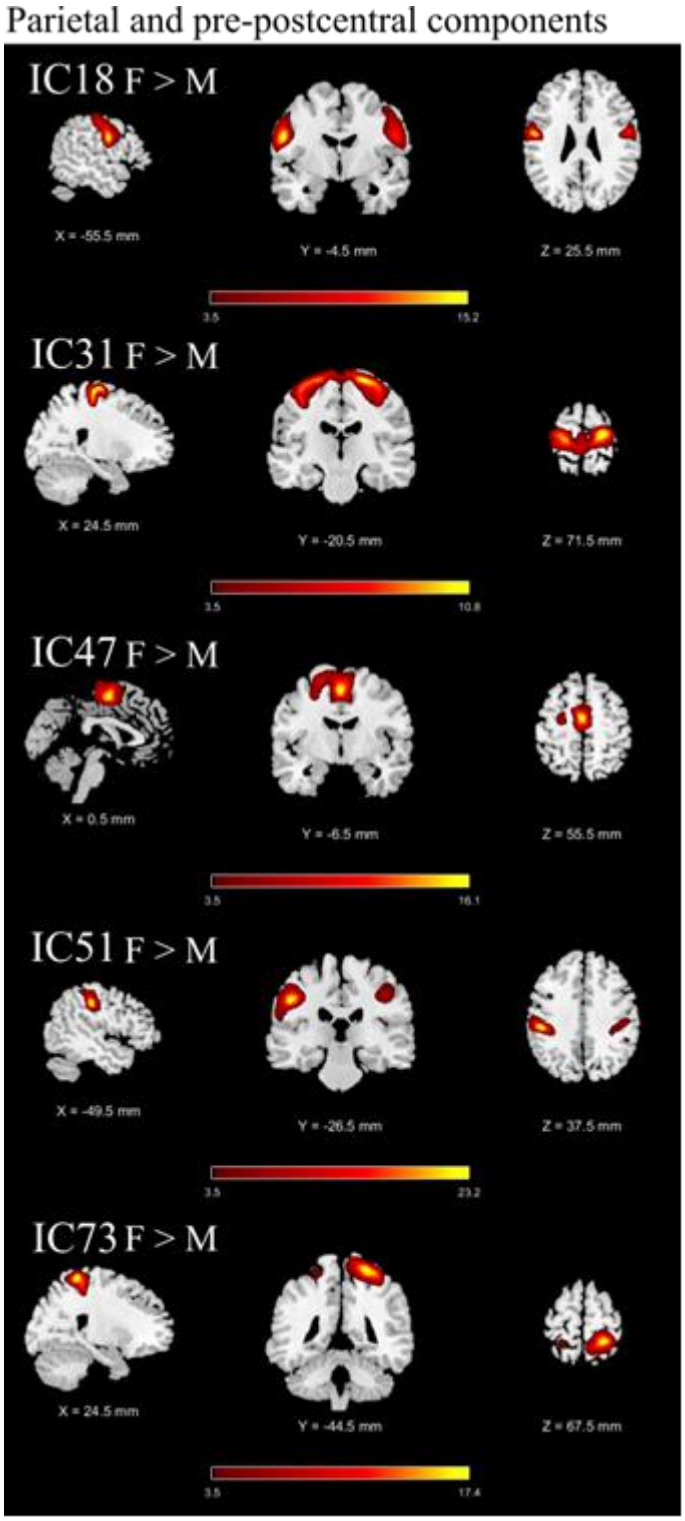

Experiment 3; Figure 3. ICs grouped as parietal and pre-postcentral components. *Females showed larger gray matter volume (GMV) in all parietal and pre-postcentral components. Colormap is based on Z-score thresholded at $|Z \geq 3.5|$. The figure is adapted with permission from Del Mauro, Del Maschio, Sulpizio, et al. (2022).*

Summary

Males compared to females showed larger TBV and total SA. When examining brain cortical regions, males and females exhibited only small differences in GMV and SA. Overall, males displayed larger values of these indices in bilateral insula, occipital pole, and orbital frontal cortex, whereas females showed larger values in superior parietal and occipital regions. With regards to CT, we did not observe a significant sex difference in the average CT. In the cortical regions, differences between males and females were more extended and equally distributed in both directions (males > females and females > males) with respect to GMV and SA. In particular, males had thicker cortex in the insular, temporal, and ventral cortices, while females displayed higher thickness in frontal, parietal, and medial regions. Values of FD were larger in males across the whole cortex. Analyses of structural ICs extracted by means of the SoBM revealed that males had larger GMV in cerebellar and temporal regions, as well as the occipital poles and putamen. In contrast females exhibited larger volume in frontal, parietal and cingulate cortices, as well as caudate and thalamus.

4. Discussion

4.1 General discussion

In the present dissertation, we investigated two key sources of brain anatomical variability, namely cortical folding patterns and biological sex. These factors are determined during fetal development by the effects of genes and hormones. In fact, on the one hand, recent evidence suggests that cortical folding patterns are arguably influenced by genetic and intra-uterine environmental factors (Amiez et al., 2018); on the other hand, a number of studies have demonstrated that steroid hormones and sex-chromosome genes can directly influence brain morphology in utero (McCarthy et al., 2017). In addition, both cortical folding patterns and biological sex are supposed to influence the development of cognitive abilities, although this relationship is far from being fixed and determined over time (e.g., see Cachia et al., 2018; Del Maschio, Sulpizio et al., 2019; Gur & Gur, 2017). In this dissertation, we described three experiments. The first two experiments examined the relationship between brain function, brain structure, and cognitive abilities by adopting early-determined and longitudinally stable individual differences in sulcal patterns as a proxy for intra-uterine events that might influence cognitive abilities. In particular, Experiment 1 focused on the anatomical variability of the PCS, and Experiment 2 examined the sulcation patterns of the left OTS.

In Experiment 1, we aimed at investigating whether PCS patterns (i.e., PCS symmetry and PCS asymmetry) were associated with differences in neurofunctional activation and behavioral performance during tasks that require inhibitory control, namely the ANT and the Numerical Stroop task. When examining the effect of ACC sulcal patterns on brain activity and behavioral performance of the ANT, no significant result was found. This result is in contrast with our hypothesis and with previous experiments where PCS asymmetry was associated with an advantage in RI assessed by means of the Flanker task (Cachia et al., 2017; Del Maschio, Sulpizio, et al., 2019). This discrepancy may be attributed to differences in the overall study design and in the group classification. Indeed, Cachia et al. (2017) adopted a two-level classification of ACC sulcal patterns (i.e., leftward asymmetry and symmetry), whereas Del Maschio, Sulpizio, et al. (2019) classified their sample using a four-level index. We suggest that,

in both studies, sample inhomogeneity may have resulted in the overestimation of the leftward asymmetry pattern.

Visual inspection of the delta plots showed that incongruent > congruent and incongruent > neutral effects (i.e., incongruency and interference effects, respectively) increased linearly in individuals with PCS asymmetry and non-linearly in individuals with PCS symmetry. In particular, the latter group was characterized by the leveling-off of the slope in the last quantiles (i.e., slower responses). This pattern has typically been associated with a reduction in RI during the Flanker task (Pratte, 2021; Ridderinkhof et al., 2005; Tieges et al., 2009). According to the activation-suppression hypothesis (Ridderinkhof, 2002; Ridderinkhof et al., 2004, 2005), incongruent trials activate inappropriate and automatic responses that have to be selectively inhibited. This selective inhibition would require time to build up in order to become effective. Hence, incongruent trials would lead to large interference when responses are fast (i.e., positive-going slope in correspondence with the first quantiles); on the contrary, selective inhibition processes would have time to develop when responses are slow, thus reducing the interference of the automatic incorrect responses (i.e., leveling-off of the slope in the last quantiles). Contrary to our expectations and to previous findings (Cachia et al., 2017; Del Maschio, Sulpizio, et al., 2019), the leveling-off of the slope observed in individuals with a symmetric PCS profile indicates that these participants were more efficient at suppressing incongruent responses in the slowest quantiles compared to individuals with PCS asymmetry. The PCS symmetry advantage observed herein may be interpreted in terms of the relationship between brain morphological symmetry and structural connectivity. Indeed, evidence suggests that the Flanker task may be associated with bilateral information processing, and specifically with symmetric neurofunctional activity and connectivity in prefrontal regions (Chen et al., 2018). Moreover, brain symmetry has been associated with greater transcallosal structural connectivity, which would enable faster inter-hemispheric information transfer compared to brain asymmetry (Doron & Gazzaniga, 2008; Nowicka & Tacikowski, 2011; Toga & Thompson, 2003). Therefore, we hypothesize that PCS symmetry may be associated with greater transcallosal structural connectivity and a more efficient bilateral information transfer and integration, which would lead to a greater RI efficiency during the ANT.

For what concerns the Numerical Stroop task, we observed a significant difference in the incongruent > neutral contrast when comparing the brain neurofunctional activity of individuals with different ACC sulcal patterns. In particular, PCS symmetry compared to PCS asymmetry was associated with greater activation of medial frontal regions, including the left superior frontal gyrus and the right paracingulate gyrus. This result is consistent with our hypothesis and with prior findings showing a PCS asymmetry advantage in inhibitory control during the Stroop task (Borst et al., 2014; Tissier et al., 2018). Indeed, increased functional activity of these regions has been associated with greater task difficulty and cognitive load (Kolling et al., 2016; Shenhav et al., 2014), and thus it may reflect greater effort in inhibiting automatic incorrect responses for participants with a symmetric PCS profile. This effect may be interpreted in terms of brain asymmetry and hemispheric specialization. In fact, evidence suggests that the Stroop task may rely upon partially lateralized processes (Chen et al., 2018). It has also been proposed that PCS asymmetry compared to PCS symmetry may be associated with faster lateralized intra-hemispheric information transfer (Cachia et al., 2014), which is supposed to be more efficient compared to processing and combining inter-hemispheric information (Doron & Gazzaniga, 2008; Nowicka & Tacikowski, 2011; Toga & Thompson, 2003). Therefore, we suggest that individuals with PCS asymmetry may take advantage of a more efficient inhibitory control during the Numerical Stroop task as a consequence of faster lateralized intra-hemispheric information transfer. In contrast, symmetric PCS profiles would be associated with slower inter-hemispheric information transfer and integration. Higher functional activity in medial frontal regions in the symmetric group may thus reflect the difficulty of integrating information processed by both simultaneously activated hemispheres. Indeed, the process of updating and combining interhemispheric information would arguably be time-consuming. We hypothesize that the asymmetric advantage recurrently reported during the Stroop task is likely a result of the increased cost associated with updating and combining information processed by the two hemispheres in individuals with a symmetric PCS profile (Borst et al., 2014; Cachia et al., 2014; Tissier et al., 2018). Differences in brain functional activity between individuals with different inter-hemispheric PCS distribution have been found only for the incongruent > neutral contrast. Possibly, incongruent > congruent and incongruent

> neutral effects may reflect different processes that underpin this specific version of the Stroop task. According to these results, individuals with distinct ACC sulcal patterns might have a modest but measurable difference in brain neurofunctional activity.

When examining the effect of ACC sulcal patterns on the RTs of the Numerical Stroop task, no significant result was found. Visual inspection and interpretation of the delta plots are consistent with the differences in brain activity herein reported. Indeed, the incongruent > neutral (interference) effect increased non-linearly in individuals with asymmetric PCS pattern, with the slope leveling-off and decreasing in the slow quantiles. This pattern may suggest a reduction of the interference effect and a more efficient inhibition of incorrect automatic responses as a function of response speed in the asymmetric group. On the contrary, the same effect increased linearly in individuals with symmetric PCS pattern, pointing toward an increasing interference effect as a function of quantiles, possibly due to greater effort to combine responses from both simultaneously active hemispheres.

Collectively, these results suggest that the strength and the direction of the association between ACC sulcal organization and EFs may depend on the degree of symmetric or asymmetric processing required by the task adopted. Moreover, a significant group difference in neurofunctional activity found only in the Numerical Stroop task indicates that individuals with an asymmetric PCS would have a more pronounced advantage when performing functionally asymmetric tasks.

Despite the delta plots suggesting that individuals with symmetric and asymmetric PCS patterns may differ with respect to the temporal dynamic of inhibitory processes, we did not replicate previous findings reporting a PCS asymmetry advantage in terms of response speed (e.g., Cachia et al., 2017; Del Maschio, Sulpizio, et al., 2019; Tissier et al., 2018). Although the use of delta plots may have revealed aspects that could have gone unnoticed in the previous experiments, we also note that these discrepancies may depend on differences in the experimental design and in the criteria adopted for sulcal patterns classification.

Similarly, in the Experiment 2 we failed to replicate previous findings reporting an association between posterior interruption of the left OTS, hosting the VWFA, and better reading ability (Borst et al., 2016; Cachia et al., 2018). We suggest that the

sociodemographic characteristics of the sample (i.e., small age range and the high educational level) and the specific task adopted to measure reading ability may account for the lack of a relationship between left OTS sulcal variability and reading ability. In particular, the TORRT, adopted herein as well as in other studies investigating the neural correlates of reading skills (Chen et al., 2019; Kristanto et al., 2020), is supposed to reflect both reading ability and verbal intelligence (Gershon et al., 2014; Grober & Sliwinski, 1991). In contrast, other recent studies have used reading fluency measures (i.e., number of words correctly read per minute) (Cachia et al., 2018), which might reflect more specific, low-level processes. Therefore, it is possible that our measure of reading proficiency, capturing multiple aspects concerning reading ability and verbal intelligence (Gershon et al., 2014; Grober & Sliwinski, 1991), may be less suited to detect the relationship between left OTS sulcal organization and reading ability as compared to the measure of reading fluency adopted by previous studies (Borst et al., 2016; Cachia et al., 2018).

Despite disconfirming previous results, we observed that the posterior interruption of the left OTS was correlated with lower SA and SD, indicating a close relationship between the morphology of the left OTS and the sulcal organization of the posterior branch of the sulcus. This result is consistent with evidence related to other brain sulci such as the PCS. Specifically, it has been shown that the occurrence of the PCS is associated with variability of gray matter morphology (e.g., SA; Fornito et al., 2008) and functional connectivity profiles (Fedeli et al., 2020) in the adjacent cingulate and parancingulate cortices. Additionally, we found that posterior interruption of the left OTS was correlated with increased connectivity between the sulcus and the left precuneus, the right calcarine sulcus, and the right inferior temporal sulcus. This is the first evidence that distinct sulcal patterns of brain sulci may be associated with differences in structural connectivity. It would be tempting to hypothesize that a posterior interruption of the left OTS may facilitate controlateral information transfer between left OTS and right hemisphere visual regions, in line with the evidence showing that the posterior aspects of the left OTS are structurally connected with both ipsi- and controlateral visual areas (Bouhali et al., 2014). Note, however, that no significant network was observed using thresholds above 2.6 (i.e., 2.7 and 2.8), and thus this result should be considered carefully.

Moreover, the interpretation of these findings is not straightforward due to the lack of a specific association between left OTS sulcal organization and reading ability. Therefore, we limit ourselves to suggest that differences in morphology and connectivity trajectories between distinct sulcal configurations of the left OTS may reflect fine-graded changes in the cortical cytology (Fischl et al., 2008; Lerma-Usabiaga et al., 2018; Palomero-Gallagher et al., 2008). Recent models of gyrification indicate that corticogenesis may be driven at a cytoarchitectonic level by non-uniform patterns of cellular growth and proliferation, as well as by the formation of cortico-cortical connections that influence the regional maturation of neuron populations (Ronan & Fletcher, 2015). One might speculate that distinct sulcation patterns of the left OTS may result from differences in neurons proliferation and connectivity patterns that ultimately influence the morphology of brain gyri and sulci during fetal development.

Adopting a different perspective, we also examined whether reading ability was associated with the morphology and structural connectivity of the left OTS. We did not observe a significant effect of reading skills on the morphological features (i.e., GMV, SA, CT, and SD) of the left OTS, suggesting no linear relationship between reading ability and GM structure of this region in typically reading adults.

On the other hand, we observed that reading ability significantly predicted the structural connectivity pattern of the left OTS. Specifically, reading scores were positively associated with increased structural connectivity linking the left OTS to the left insula, the orbitofrontal cortex, the putamen, the superior temporal gyrus (STG), and the temporal transverse sulcus. According to prior works, these regions are presumably involved in language and reading processes. In particular, the bilateral insula is implicated in reading (Bolger et al., 2005; Kristanto et al., 2020) and is significantly reduced in volume in patients with dyslexia (Richlan et al., 2013). Furthermore, the anterior VWFA exhibits a preferential connectivity with the left insula and the left STG as well as with other left perisylvian regions (see Bouhali et al., 2014). Converging evidence suggest a stable linking between the left OTS and the left superior temporal cortex. For instance, a longitudinal study conducted on children aged 7-12 reported that the linking between left OTS and left STG – connected through the ILF – increases with age and reading proficiency (Yeatman et al., 2012).

Moreover, the structural connectivity between the VWFA to the left STS was the only predictor of reading skills in a sample of adult participants (Chen et al., 2019). Overall, prior findings suggest that the left superior temporal cortex plays a significant role in language, and particularly in the phonological processing (Leonard & Chang, 2014; Skeide & Friederici, 2016). Specifically, connections between left OTS and superior temporal regions may play a critical role in the mapping of orthographic into phonological representations during reading (Chen et al., 2019). Moreover, evidence indicates that the ability to efficiently recognize written language may depend on the appropriate functional tuning of these regions (Blomert, 2011). The left putamen also participates in phonological processing during reading (Cherodath et al., 2017; Preston et al., 2010; Tettamanti et al., 2005), as suggested by the finding that the information transferred from the anterior left OTS to the left putamen increases during oral reading (Seghier & Price, 2010). Additionally, a structural connectivity analysis comparing the connectivity patterns of the VWFA and the left FFA in a sample of 5-years-old children revealed that the VWFA was more connected with the left putamen (Saygin et al., 2016).

It is worth noting that we also detected increased connectivity between the left OTS and the left orbital sulcus. Despite not being implicated in reading *per se*, the orbitofrontal cortex (OFC) may play a key role in the top-down processes guiding visual object recognition (Bar et al., 2006; Matsumoto & Kakigi, 2014). Indeed, the activation of the left OFC precedes that of the ventral occipitotemporal regions implicated in visual recognition (Bar et al., 2006). Additionally, the VWFA and the left FFA are equally connected to the left OFC, suggesting that this region plays a non-category-specific role in visual recognition (Bouhali et al., 2014). As a result of our study, we observed an increased linking between left OTS and OFC, associated with a greater reading ability, which may indicate a reinforcement of top-down processes that facilitate the visual recognition of written words.

This study provides new insights into the relationship between left language-related regions and left OTS. In particular, we found that reading skills predict structural connectivity, rather than gray matter morphology (as measured by CT, etc.), of the left OTS in typically reading adults. In accordance with the hypothesis that the functional specialization of the VWFA may be primarily determined by its proximity – and

specific connectivity – to language regions (Bouhali et al., 2014; Dehaene & Cohen, 2011), we suggest that reading skills may be closely linked with the communication of the so-called VWFA with other regions that are critical to reading.

In Experiment 3, we examined another source of prenatally determined differences in brain structure, which is biological sex. As already mentioned, sex differences in brain morphology are determined in utero by the combined action of sex-chromosome genes and steroid hormones (McCarthy et al., 2017). Crucially, sexual dimorphism in brain structure arguably underlies differences between males and females in cognitive abilities and in the phenotypical manifestation of psychiatric/neurological disorders. In addition, previous studies found that the distribution and morphological characteristics of the PCS may differ between males and females (Clark et al., 2009; Leonard et al., 2009; Yücel et al., 2001). These findings might suggest that early-determined features of brain structure associated with cortical folding and sex might be influenced by similar genetic mechanisms and intrauterine events.

In accordance with previous results (Ritchie et al., 2018; Williams et al., 2021b, 2021a), we observed higher TBV and total SA in males. However, only limited differences in local values of GMV and SA were detected. These results indicate that larger male brain size accounts for most differences in GMV and SA. In addition, in line with our initial hypothesis, males compared to females showed larger values of GMV and SA in a greater number of brain regions than females compared to males. Of note, sex-related differences in these two measures displayed similar spatial distributions, which may indicate a correlation between these indices.

With regard to the CT, the average thickness was not significantly different between males and females. Statistical analyses performed on brain cortical regions revealed extensive differences between sexes throughout the cortex. These findings indicate that sex-related differences in CT may be broader than those observed in other aspects of cortical morphology (e.g., GMV and SA), and that they may depend on region-specific, rather than whole-brain, differences. In accordance with prior studies, we observed the largest effect sizes in the right insula for males, and in the inferior parietal cortex for females (Ritchie et al., 2018). Moreover, our results are in line with Ritchie et al. (2018) and Williams et al. (2021a), who found that regional values of CT differed equally between males and females.

We suggest that these findings could provide some hint regarding the nature of distinct indices of cortical morphology. In particular, our results indicate that SA and CT are partially independent measures, as claimed by the RUH of cortical expansion (Rakic, 1995) and confirmed by genetic studies (Panizzon et al., 2009), and that GMV and SA are more associated with each other than with CT (Winkler et al., 2010).

One of the main novelties of this study is the use of the FD as index of cortical morphology. We found that the FD was higher in males across the whole cortex. The only study examining FD differences between males and females found that females had higher levels of FD bilaterally in superior frontal and parietal lobes (Luders et al., 2004). It is worth noting that the FD has been found to be strongly correlated with other metrics of cortical morphology (e.g., CT; see King et al., 2010). However, evidence suggests that it may also be sensitive to other aspects of GM structure (Madan & Kensinger, 2016). Therefore, combining the FD with other indices of cortical morphology may lead to a more comprehensive understanding of the sex differences in GM structure, rather than simply providing redundant information. We propose that higher male FD may reflect different features of GM structure compared to other metrics such as GMV, SA and CT. However, this result should be considered with caution. Indeed, the number of studies using this measure is relatively limited, and future research is needed to explore the relationship between FD and other aspects of cortical morphology.

In addition to these analyses based on a pre-defined cortical parcellation, we implemented the SoBM to investigate sex differences in GMV by adopting a voxel-wise approach based on the ICA. The pattern of sex differences that emerged from the analyses of the structural ICs is highly consistent with our hypothesis and with previous findings (e.g., Lotze et al., 2019). Indeed, females were found to have larger frontal and parietal volumes, along with the precuneus and the cingulate cortices. Compared to females, males had larger volumes in the lateral and medial temporal regions (i.e., fusiform and inferior temporal gyri, and parahippocampal cortex), as well as the cerebellum. These results support evidence that females have higher volume in fronto-parietal regions, whereas males have higher volume in temporal and cerebellar regions (Chen et al., 2007; Lotze et al., 2019; Ruigrok et al., 2014).

The absence of cognitive and behavioral measures represents a limitation of this study. However, we hypothesize that differences in structural ICs may partially reflect sex-specific advantages reported for some cognitive abilities. For instance, it is worth noting that regions where females showed higher GMV are also core components of the DMN, including medial prefrontal cortex, posterior cingulate cortex/precuneus, and inferior parietal lobules (Raichle, 2015). Therefore, our results may expand prior findings reporting higher functional connectivity in females within the DMN (Biswal et al., 2010; Ritchie et al., 2018). Crucially, the DMN has been proposed to play a crucial role in social cognition (Amft et al., 2015; Mars et al., 2012). Greater volume, as well as higher functional connectivity (Biswal et al., 2010; Ritchie et al., 2018), in the regions that form the DMN may underpin the putative female advantage in social cognition (Gur & Gur, 2017).

Similarly, larger male volume in regions subserving motor functions, specifically the cerebellum and the putamen bilaterally (Caligiore et al., 2017; Koziol et al., 2014; Marchand et al., 2008), may be related to the putative male advantage in motor tasks (Gur & Gur, 2017). While this result is in line with prior studies (Rijpkema et al., 2012; Ruigrok et al., 2014), we did not observe higher volume in frontal motor cortices for males as reported previously (Lotze et al., 2019; Ruigrok et al., 2014).

The results of this study partially support evidence of higher occipital lobe volumes in males. Indeed, we observed higher volume for males in inferior and lateral occipital regions, including the calcarine scissure and the lingual gyri (see also Chen et al., 2007; Lotze et al., 2019). Crucially, the large effect size observed for this component (d = -0.93) suggests the presence of broad group differences in these regions. Females, on the other hand, displayed larger volumes within the superior and medial occipital regions, including the calcarine scissure and the cuneus. Future studies should explore whether such structural differences between males and females are associated with differences in the visual system (Vanston & Strother, 2017) or in visuospatial abilities (Gur & Gur, 2017; Moreno-Briseño et al., 2010).

4.2 Future directions

Despite being a promising tool, the relationship between sulcal patterns and cognitive abilities should be further delineated. For instance, future studies may investigate this association by adopting a longitudinal approach. In fact, although the sulcal patterns are life-stable characteristics of brain structure, longitudinal studies may reveal whether this relationship changes over time as a consequence of environmental influences. In addition, the use of structural equation modeling or path analysis should be considered to investigate the potential indirect effects of folding patterns on cognitive abilities. For instance, folding patterns may not directly influence cognitive abilities, but rather impact on the morphology, connectivity or neurofunctional activity of other brain regions, which in turn may affect cognitive abilities.

In experiment 1, we reported that ACC sulcal patterns modulate the topology of functional brain activity during the Numerical Stroop task, which is reflected in the temporal dynamic of the inhibitory process. While completing this dissertation, we are performing a new neuroimaging experiment that investigates the relationship between ACC sulcal patterns and EFs, and in particular inhibitory control, in a sample of bilingual speakers. Indeed, numerous evidence suggests that bilinguals rely upon EFs to detect linguistic conflicts, inhibit linguistic intrusions, and switch from one language to another (i.e., language switching) (Abutalebi & Green, 2008, 2016; Green & Abutalebi, 2013), and therefore language background should be considered alongside ACC sulcal morphology as a factor that may influence inhibitory control. In particular, language switching involves the activation of several regions underpinning EFs, including prefrontal and parietal regions, as well as the ACC (Abutalebi & Green, 2008). The aim of this experiment is to investigate whether the occurrence and inter-hemispheric distribution of the PCS modulate the brain neurofunctional activity associated with language switching during a picture-naming task, as well as the structural connectivity of the cingulate and paracingulate cortices.

Previous findings showed that altered morphology and distribution of the PCS are associated with lower executive functioning in patients with schizophrenia (Fornito et al., 2006). We suggest that the results of Experiment 1, showing differences between PCS patterns in the neurofunctional activity and temporal dynamic of inhibitory

processes, may provide useful insights to understand the relationship between ACC sulcal patterns and altered cognitive control in schizophrenia.

In Experiment 2, we did not find a significant association between sulcal patterns of the left OTS and reading ability. However, we are currently working on a new experiment whose main goal is to elucidate this relationship using a measure of reading fluency, which has been previously associated with the left OTS sulcal pattern (Cachia et al., 2018), instead of the TORRT adopted herein. In this new experiment, we also aim at examining whether the sulcal organization of the left OTS modulates the functional connectivity and neurofunctional activity patterns of the VWFA while performing a reading task.

Finally, in Experiment 3 we explored sex differences in brain morphology. We found that males had increased FD throughout the cerebral cortex. We suggest that future studies should clarify the neurobiological meaning of the FD, how it relates to other indices of cortical morphology, and what are the implications of the sex differences in FD reported hereby. Moreover, we showed that the SoBM may represent a valuable instrument to investigate sex differences in GMV. In our study, we did not provide cognitive and behavioral measures. However, our results may provide useful insights for future studies that aim at investigating the neural correlates of the repeatedly reported sex differences in cognitive abilities and psychiatric/neurological disorders. Further investigations may also examine whether structural ICs are associated with specific cognitive abilities and psychiatric/neurological disorders as a function of sex.

4.3 Conclusions

In the present dissertation, we investigated early-determined differences in brain structure and their relationship with cortical morphology, structural connectivity, brain functional activity, and cognitive abilities. In two experiments we focused on the sulcal pattern variability of the PCS and left OTS. Taken together, our results provide novel insights into how individual differences in cortical folding patterns relate to brain functional activity, cortical morphology, structural connectivity, and cognitive abilities. Our results showed that the folding pattern variability of the ACC is related to individual differences in the topology of neurofunctional activity associated with inhibitory control, which is reflected in the temporal dynamic of cognitive processes. Moreover, we found that the sulcal organization of the left OTS modulates the morphology and the structural connectivity pattern of the sulcus. In both studies, we failed to replicate previous findings suggesting that specific sulcal patterns may confer an advantage in inhibitory control (in terms of response speed) and reading ability (e.g., Cachia et al., 2017, 2018; Tissier et al., 2018). These discrepancies presumably reflect differences in the experimental design (e.g., the tasks adopted) and in the criteria adopted for the sample classification (e.g., two- or four-level PCS classification), as well as differences in the socio-demographic characteristics of the participants (e.g., age and educational level). Crucially, the small (although significant) variance in behavioral performance accounted for by sulcal patterns variability (e.g., see Borst et al., 2014; Cachia et al., 2018; Tissier et al., 2018) suggests that contingent factors related to experimental design and sample characteristics might represent powerful confounding factors that should be taken into account in future studies. It is also important bearing in mind that the influence of sulcal patterns on cognitive abilities appears to be modulated by experiential factors, such as bilingual background, as showed by Cachia et al. (2017) and Del Maschio, Sulpizio, et al. (2019). Overall, despite new and promising findings that add to the available data, we found some inconsistencies with previous studies that should be taken into account for future investigations. Although we were not able to replicate the association between reading ability and left OTS folding patterns, we observed that reading ability significantly predicted the structural connectivity pattern of the left OTS. This result highlights the great importance of the individual experience as a source of individual

variability in brain morphology, compared to which the role played by folding patterns appears to be limited. Nonetheless, our findings suggest that sulcal patterns represent a source – albeit limited – of variance and should be taken into account in future investigations.

We also explored brain structural differences between males and females by means of multiple indices and techniques that collectively provide a multidimensional picture of the brain structure. The origin of the sex differences in brain structure reported herein must presumably be traced back to genetic and hormonal events that take place during fetal development. Crucially, previous evidence showed that the distribution and morphological characteristics of the PCS are different among males and females (Clark et al., 2009; Leonard et al., 2009; Yücel et al., 2001). This finding suggests that some of the pre-natal events above may partially overlap with those that influence the morphology of brain sulci during the gyrification process. Our results showed that MRI techniques and neuroimaging analysis tools provide the instruments to investigate distinct facets of brain morphology, each bringing unique and valuable information. Overall, we observed limited sex differences in GMV and SA, with a greater number of regions showing increased GMV or SA in males compared to females, rather than vice versa. On the other hand, sex differences in CT were more extended and equally distributed in both directions. In addition, FD values were higher in males throughout the cerebral cortex. We also speculated that sex differences in structural ICs may partially reflect differences between females and males in some cognitive abilities. For instance, female-biased structural ICs include regions that play a crucial role in the DMN, and may underlie the repeatedly reported female advantage in social cognitive skills (Amft et al., 2015; Biswal et al., 2010; Gur & Gur, 2017). Similarly, higher male volume in motor regions (i.e., putamen and cerebellum) may be associated with the putative male advantage in motor tasks (Caligiore et al., 2017; Gur & Gur, 2017; Koziol et al., 2014).

5. Materials and methods

5.1 Experiment 1 (Materials and methods)

Participants

Forty-two Italian young adult participants volunteered to participle in the study. One subject was excluded from the sample due to white matter hyperintensity, resulting in a final sample of 42 participants (mean age = 25.19 ± 4.89; 30 F). All participants had no history of psychiatric or neurological disorders, had normal or corrected-to-normal vision, and were right-handed (Oldfield, 1971). For each participant, sociodemographic and cognitive measures were collected, including SES (The MacArthur Scale of Subjective Social Status, https://macses.ucsf.edu/research/psychosocial/subjective.php#measurement), years of formal education, fluid intelligence quotient (Raven's Standard Progressive Matrices for adults) (Basso et al., 1987), and visuo-spatial working memory (Corsi test) (Monaco et al., 2013). No participants were discarded because of low intelligence quotient or low working memory score. Descriptive statistics of sociodemographic and cognitive measures are reported in Experiment 1; Table 3. The study was carried out in accordance with the Declaration of Helsinki and with the ethical approval from the Human Research Ethics Committee of the Vita-Salute San Raffaele University, Milan, Italy. All participants gave written informed consent.

	Mean ± St.Dev.
Personal Income	1.52 ± 0.77
Family Income	3.62 ± 1.08
Education (Years)	16.62 ± 1.45
Raven's Matrices (corrected scores)	33.54 ± 2.52
Corsi test	6.27 ± 1.16

Experiment 1; Table 3. Descriptive statistics of sociodemographic and cognitive measures. *Mean and Standard Deviation (St.Dev.) are reported for Socio-Economic Status (SES), including Personal and Family incomes, years of formal education, Raven's Matrices and Corsi test.*

Procedure

Participants performed the ANT and the Numerical Stroop task inside an MRI scanner. The order of the tasks was counterbalanced across participants, and the two tasks were separated from each other by the acquisition of a T1-weighted image (T1w) (duration = 7.83 minutes).

The ANT (Fan et al., 2002, 2005), which we adapted from Abutalebi et al. (2012), is an extension of the Flanker task (Eriksen & Eriksen, 1974) that allows to investigate three distinct dimensions of attentional functions: alerting, orienting and executive control. Alerting is the ability to reach and sustain an alerted state; orienting represents the ability to select specific information from an input based on its relevance; executive control is the ability to select the appropriate response among two or more conflicting responses conjointly activated. Since previous experiments investigated the relationship between ACC sulcal patterns and executive control, with a particular focus on RI (Cachia et al., 2017; Del Maschio, Sulpizio, et al., 2019), the present study examined only the executive control dimension of this task, and therefore alerting and orienting functions were not considered in the following analyses. Each participant completed two runs, separated from each other by a small break of ~30 s, each including 96 trials and lasting 7 m and 43 s. In addition, the two runs were preceded by a practice session of 16 trials. In each trial, participants were presented with a central horizontal arrow flanked on each side by two horizontal arrows oriented in the same direction with respect to the central arrow (e.g., →→→→→) (i.e., congruent trials), in the opposite direction with respect to the central arrow (e.g., →→←→→) (i.e., incongruent trials), or by two lines (e.g., – – → – –) (i.e., neutral trials). Trials were equally distributed among conditions (i.e., 32 trials for each condition). Participants were asked to indicate as fast and accurately as possible the direction of the central arrow, by pressing the left or the right button of an MR-compatible response box in the MRI scanner (Experiment 1; Figure 5). Trials were preceded by a fixation cross (+) at the center of the screen (duration = 400 ms), and by a visual cue (duration = 100 ms). In each condition, 50% of trials were presented above the fixation cross (up), and 50% below the fixation cross (down). In addition, four visual cue conditions were adopted: in the "no cue" condition, participants saw only the central fixation cross for 100 ms in addition to the original duration of 400 ms; in the "center cue" condition,

an asterisk (*) was presented at the center of the screen for 100 ms in place of the fixation cross; in the “double cue” condition, two asterisks were simultaneously presented above and below the fixation cross for 100 ms, corresponding to the two possible target positions; in the “spatial cue” condition, an asterisk was presented above or below the fixation cross for 100 ms (spatial cues always correctly anticipated the target position). Trials were randomly interspersed in an event-related sequence. Target stimuli lasted 1700 ms. Following participant’s response, target stimuli remained displayed on the screen until the end of the presentation time. Trials were interleaved by a black screen and the inter-stimulus interval (ISI) was jittered following Dale’s exponential function (Dale, 1999) (mean ISI = 2797.66 ms; min ISI = 1873; max ISI = 4964 ms).

The Numerical Stroop task (Stroop, 1935; Windes, 1968) was adapted from Hernández et al. (2010). Each participant completed two runs, separated from each other by a small break of ~30 s, each including 108 trials and lasting 7 m and 48 s. in addition, the two runs were preceded by a practice session of 16 trials. In each trial, participants were presented with a sequence of one, two, three or four identical numbers (or alphabetical characters). In the congruent trials, the number of digits corresponded to the number values (e.g., 1; 22; 333; 444); in the incongruent condition, the number of digits was different from the number values (e.g., 2; 44; 111; 3333); in the neutral condition, a sequence of alphabetical characters was presented (e.g., G; ZZ; MMM; ZZZZ). Trials were equally distributed among conditions (i.e., 36 trials in each condition). Participants were asked to indicate as fast as possible the number of items that composed the sequence, by pressing one of four buttons on a MR-compatible response box in the MRI scanner (Experiment 1; Figure 6). Trials were preceded by a fixation cross (+) at the center of the screen (duration = 500 ms). Trials were randomly interspersed in an event-related sequence and interleaved by a black screen and the ISI was jittered following Dale’s exponential function (Dale, 1999) (mean ISI = 1770.11 ms; min ISI = 1036 ms; max ISI = 4113 ms).

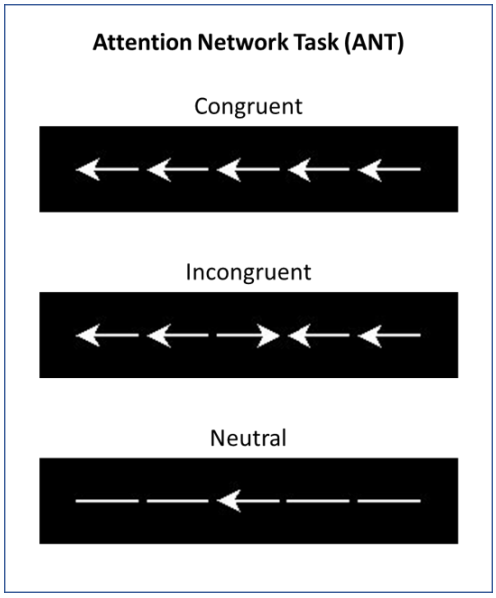

Experiment 1; Figure 5. Conditions of the Attention Network Task. *Participants were presented with a central horizontal arrow flanked on each side by two horizontal arrows oriented in the same direction with respect to the central arrow (top row), in the opposite direction with respect to the central arrow (middle row), or by two lines (bottom row).*

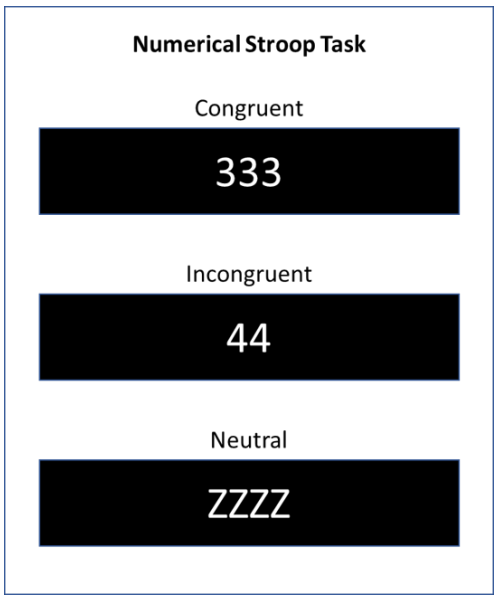

Experiment 1; Figure 6. Conditions of the Numerical Stroop Task. *Participants were presented with a sequence of one, two, three or four identical numbers (top and middle rows) or alphabetical characters (bottom row). The number of digits corresponded to the number values (top row) or was different from the number values (middle row).*

MRI acquisition

MRI acquisition was performed at the Centro di Eccellenza Risonanza Magnetica ad Alto Campo (C.E.R.M.A.C., Unit of Neuroradiology) San Raffaele Hospital, Milan (Italy) with a 3 Tesla Philips Ingenia CX MR scanner (Philips Medical Systems, Best, Netherlands) with a 32 channels SENSE head coil. For both the ANT and the Numerical Stroop tasks, functional scans were acquired with a fast speed Echo Planar Imaging (EPI) sequence (Echo Time [TE] = 33 ms; Repetition Time [TR] = 2000 ms; Flip Angle = 85°; number of volumes per run = 236 (ANT); 256 (Numerical Stroop); Field of View [FOV] = 240 × 240; matrix size = 80 × 80; 35 axial slices per volume; slice thickness = 3; interslice gap = 0.75; voxel size = 3 × 3 × 3; Phase Encoding direction [PE] = A/P; SENSE factor = 2; whole brain coverage). In order to optimize EPI image signal, each run was preceded by five dummy scans. A high-resolution Magnetization Prepared Rapid Gradient Echo (MPRAGE) T1w anatomical image was acquired for each participant with the following parameters: TR = 9.9 ms, TE = 4.9 ms, Flip Angle = 8°, FOV = 269 mm, matrix size = 384 × 384, number of axial slices = 243, slice thickness = 1.4 mm, voxel size = 0.7 × 0.7 × 0.7 mm 3, Phase Encoding direction (PE) = A/P, SENSE factor = 2, with whole brain coverage.

ACC sulcal pattern classification

The origin of all T1w images was manually set to match the bicommissural line (anterior commissure-posterior commissure; AC-PC). Sulcal pattern classification was carried out following the procedure described by Garrison et al. (2019). T1w images were visually inspected on MANGO (Multi-image Analysis GUI, v4.0, http://ric.uthscsa.edu/mango/mango.html), and the PCS was identified as the sulcus running dorsal and parallel to the CS. The anterior limit of the PCS was set on the sagittal plane at x = -5 for the left hemisphere and x = +5 for right hemisphere, starting from the point at which the sulcus begins to move on a rostro-caudal direction along the imaginary extension of the AC-PC line. The posterior limit of the PCS was identified as a line passing through the posterior commissure and perpendicular to the AC-PC line. The PCS was measured and classified as either present (PCS ≥ 20 mm) or absent (PCS ≤ 20 mm). In case of interrupted PCS, fragments were considered for the computation of the total length only if the interruptions were ≤ 19 mm. Interruptions were not included in the computation of the PCS total length. Participants

were classified as asymmetric when the PCS was present in one hemisphere and absent in the other, and symmetric when the PCS was bilaterally present or absent.

fMRI preprocessing

The surface-based fMRI pipeline described by Brodoehl et al. (2020) was adopted for both the ANT and the Numerical Stroop task. The surface-based fMRI is supposed to enhance the anatomical precision of clusters of neurofunctional activity compared to the standard volumetric preprocessing. Evidence suggests that the use of spatial smoothing in volumetric processing is associated with an increase in signal contamination between contiguous (but functionally distinct) regions of the brain (Yan et al., 2009). For instance, this happens for the cingulate and paracingulate gyri when the PCS is present, since these two regions lie adjacent in the folded cortex (i.e., volumetric space) but separate in the unfolded cortex (i.e., surface space). Therefore, surface-based fMRI may allow disentangling the specific functional contributions of neighboring regions in the ACC by accounting for individual variability in sulcal organization. Additionally, the relatively large smoothing kernel used in the classic volumetric pipeline (e.g., 8 x 8 x 8 mm^3) can often result in bilateral activation of ACC since the left and right ACC are very close to one another. Even though this procedure improves the signal-to-noise ratio, it increases the risk of functional activity spreading between hemispheres. By using a smaller smoothing kernel (3 x 3 x 3 mm^3), surface-based fMRI may prevent inter-hemispheric contamination of ACC functional activity. Preprocessing pipeline included the following steps: individual surface estimation; slice-timing correction of functional data; spatial realignment and coregistration to skull-stripped and bias-corrected T1w images; General Linear Model (GLM) estimation; mapping of functional contrast-images in the native volumetric space onto the individual surface; normalization and smoothing. T1w images were segmented and skull-stripped by means of the Computational Analysis Toolbox v12 (CAT12; http://www.neuro.uni-jena.de/cat/index.html) (Gaser et al., 2022). Specifically, individual structural images were segmented into GM, WM and cerebrospinal fluid (CSF), resulting in separate images for each tissue class. CAT12 segmentation approach adopt a spatial adaptive non-local mean (SANLM) denoising filter, and a local adaptive segmentation (LAS) approach that applies a local intensity transformation of tissue classes to correct for regional inhomogeneities and intensity

variations. Additionally, an Adaptive Maximum A Posterior (AMAP) technique (Rajapakse et al., 1997) and a Partial Volume Estimation (PVE) (Tohka et al., 2004) were carried out in order to obtain a more accurate segmentation. Central surface reconstruction was carried out for each hemispheres by adopting a projection-based thickness (PBT) computational approach included in CAT12 (Dahnke et al., 2013). The central surface mesh, consisting in vertex connected by edges (instead of voxels), is calculated as the average distance between the inner (GM/WM) and outer (GM/CSF) boundaries of the brain surface. Functional volumes were slice-time corrected using the first slice as reference point, then realigned to the first volume and unwarped to correct for motion artifacts and geometric distortions. Realigned functional volumes were coregistered to the bias-corrected and skull-stripped structural image. Then, functional volumes of each task were entered into a separated GLM. The BOLD signal was modelled with the canonical hemodynamic response function (HRF). Serial correlations were accounted for using the AR (1) model during parameter estimation. Trial onsets for the incongruent, congruent, and neutral conditions of each task were entered into the model, while realignment parameters were included as nuisance covariates. Based on previous fMRI studies (Blasi et al., 2006; Geissler et al., 2020; Huang et al., 2020), the following t-contrasts were estimated for both tasks: incongruent > congruent, incongruent > neutral, and congruent > neutral. Then, contrast-images resulting from first-level analysis were mapped onto each individual central surface. Surface images were resampled to the standard 32 k HCP template provided by CAT12, and smoothed with a 3 x 3 x3 Full-Width at Half-Maximum (FWHM) gaussian kernel (Brodoehl et al., 2020).

Statistical analyses

Behavioral analyses. Statistical analyses were run to test the effect of the ACC sulcal pattern on executive performance (i.e., inhibitory control). Since accuracy scores were very high for both ANT (mean accuracy = 99.65%) and Numerical Stroop task (mean accuracy = 99.10%) (i.e., ceiling effect), only RTs were considered for the analyses. All behavioral analyses were performed on R v.4.0.2. using the lmer function implemented in the lme4 package (De Jong et al., 1994; Ridderinkhof, 2002).

For each task, participants' RTs to correct responses were entered into a linear mixed-effects model as dependent variable. Task conditions (congruent, incongruent, and

neutral), ACC sulcal patterns (PCS symmetry and PCS asymmetry), and their two-way interaction were entered into the model as predictors, with the participants modelled as random intercepts. Likelihood ratio tests were performed to test the significance of the fixed effects. Each fixed effect was tested for its significance by comparing a model which included the fixed term of interest against a model in which it was not present. Fixed effects were retained when increased the goodness of fit. In case of significant interactions, all the lower-order terms involved were retained. Coefficients were considered significant when $t \geq |2|$.

In addition, RTs were sorted by speed from fastest to slowest in bins of equal size (i.e., quantiles) in order to investigate differences in the distribution of RTs between conditions by means of delta plots (De Jong et al., 1994; Ridderinkhof, 2002; Ridderinkhof et al., 2004). Delta plots are informative about the temporal dynamics of cognitive processing by plotting task's effect size (i.e., difference between the RTs of different task conditions) as a function of response speed (i.e., quantiles) (Ridderinkhof et al., 2004), and have been used to investigate executive control between populations or across experimental conditions. For instance, by visually comparing the slopes of the incongruency effect (i.e., incongruent > congruent) between quantile points, delta plots can reveal difference in the modalities and extent of inhibitory control processes taking place during the task. In particular, the incongruency effect associated with interference tasks (e.g., Simon, Flanker and Stroop tasks) usually decreases as RTs lengthen. Specifically, delta plots typically show an initial increase of the incongruency effect (i.e., the slope increases) associated with faster responses, followed by a decrease of the incongruency effect (i.e., the slope flattens or decreases) in the rightmost part of the distribution associated with slower responses (Burle et al., 2014; Pratte, 2021; Ridderinkhof et al., 2005; Ridderinkhof et al., 2004). The reduction of the incongruency effect for the slowest responses is supposed to reflect the use of a slow but effective mechanism of inhibition (Pratte, 2021; Ridderinkhof et al., 2005; Ridderinkhof et al., 2004).

Delta plots were used here to examine whether the temporal dynamics of the inhibitory control differ between individuals with different ACC sulcal patterns. For each participant, the RTs of correct responses in each condition were grouped into five bins based on the response speed. In particular, for a given participant in a specific

condition, the 1st quantile included the fastest 20% of the responses; the 2nd quantile included the next fastest 20%, and so on until the 5th quantile, which included the slowest 20% of the responses. Based on previous studies, the following effects were computed for each task separately to explore the temporal dynamic of RI: incongruency (incongruent > congruent) effect (Ridderinkhof et al., 2005) and interference (incongruent > neutral) effect (Shao et al., 2015). For illustrative purposes, the congruent and the neutral conditions were also compared. A delta plot representing task effects as a function of RT quantiles was generated independently for each task and for individuals with symmetric and asymmetric PCS profiles separately.

Neuroimaging analyses. Smoothed and resampled individual surfaces were entered into a GLM. First, one-sample t-tests were used to investigate the effects of task conditions irrespective of ACC sulcal pattern. Then, a full factorial design was estimated to investigate differences in brain activity between individuals with asymmetric and symmetric PCS profiles. Since we were only interested in investigating the impact of ACC sulcal organization on the functional activity of the cingulate/prefrontal cortex, analyses were performed within an inclusive mask created using the following bilateral regions from Harvard-Oxford atlas (Smith et al., 2004): Cingulate Gyrus, anterior division; Paracingulate Gyrus; Superior Frontal Gyrus; Frontal Pole. Atlas regions were mapped onto surface with CAT12 using the standard 32k HCP template as reference. Based on previous evidence suggesting that the PCS distribution may vary among males and females (Leonard et al., 2009; Yücel et al., 2001), and that education impact on Stroop RTs (Van der Elst et al., 2006), sex and years of formal education were entered as nuisance covariates into the model. Since age was highly correlated with years of formal education (r = 0.61; p < 0.001), this variable was not included into the model to avoid multicollinearity. Significance threshold was set at p-FWE < 0.05 at the cluster level, and p-uncorrected < 0.001 at the vertex level (note that surface-based fMRI is based on vertex, rather than voxels).

Brain-behavior correlations. A correlation analysis was performed to address whether the functional activity of each participant, extracted from significant clusters resulting from the group contrasts, was correlated to mean RTs associated with that effect in the two tasks. In addition, the same correlation was performed considering mean RTs from the 4th and 5th quantiles (corresponding to the slowest responses), since flattening of

the slope for these quantiles is typically associated with the efficiency of RI (Ridderinkhof et al., 2005; Ridderinkhof et al., 2004; van den Wildenberg et al., 2010).

5.2 Experiment 2 (Materials and methods)

Participants

A sample of 100 young adult participants was drawn from the Wu-Minn HCP dataset (Van Essen et al., 2013). The sample is available as a pre-defined group of unrelated participants on ConnectomeDB (https://db.humanconnectome.org), the online dissemination platform for the HCP (Hodge et al., 2016). Participants had no psychiatric or neurological disorders (Van Essen et al., 2013). Sociodemographic variables, including age, years of formal education, and income were collected for each participant by means of the Semi-Structured Assessment for the Genetics of Alcoholism (SSAGA; Bucholz et al., 1994). Participants rated their income on a 9-point Likert scale, indicating which category best matched their current economic situation. Left-handed participants (Edinburgh Handedness Questionnaire < 0; Oldfield, 1971) were excluded from the sample, leading to a final sample of 86 participants (F = 46). The descriptive statistics of sociodemographic variables are reported in Experiment 2; Table 3.

Reading proficiency

The NIH Toolbox Oral Reading Recognition Test (TORRT) (Gershon et al., 2014) was used to assess English reading proficiency in the adult population. It is worth noting that reading ability as assessed by the TORRT is influenced by a variety of factors, including general and specific cognitive skills related to reading, level of exposure to written material, and whether the individual's environment provided the opportunity to develop basic or complex reading skills (Gershon et al., 2013). This test was administered using the computer adaptive testing (CAT) approach, which allows for adjusting the difficulty of the items according to the individual's ability. In this task, participants were instructed to pronounce as accurately as possible single printed letters or words, including irregular and low-frequency words, without any time limitations. Scores are automatically calculated. Higher scores indicate better reading ability (details on score conversion are reported in Gershon et al., 2014). Descriptive statistics of the TORRT scores are reported in Experiment 2; Table 3.

	Mean ± St.Dev. (range)
Age	29.24 ± 3.64 (22-36)
Education (Years)	15 ± 1.88 (11-17)
Income	5.02 ± 2.09 (1-8)
TORRT (age-adjusted)	105.82 ± 14.34 (71-130)

Experiment 2; Table 3. Descriptive statistics of sociodemographic variables and reading ability*. Mean, standard deviation (St.Dev.) and range are reported for participants' age, years of formal education, income, and NIH Toolbox Oral Reading Recognition Test (TORRT) scores. TORRT scores were adjusted for age.*

Image acquisition

T1w and DW images were included in the HCP dataset. A detailed description of the acquisition protocols is reported in Glasser et al. (2013) and Sotiropoulos et al. (2013).

Structural MRI preprocessing

A detailed overview of the structural preprocessing pipeline performed by the HCP is reported in Glasser et al. (2013). Briefly, distortion correction, bias correction, and registration to the MNI space were performed by means of the FMRIB Software Library (FSL) v.5.0.9 (Jenkinson et al., 2012). Using Freesurfer v.5.2 (Fischl, 2012), the segmentation of the T1w images was carried out, and then the individual white and pial surfaces were generated and registered to the fsaverage template using the standard folding-based surface registration (Glasser et al., 2013). Three indexes of cortical morphometry were extracted from the individual surfaces, and specifically from the left OTS as defined by Destrieux brain parcellation (Destrieux et al., 2010): GMV (mm^3), SA (mm^2) and CT (mm). The SA was calculated as the sum of the areas of all vertices within a brain region, while the CT was measured as the average distance between the GM/WM boundary and the pial surface (note that the GMV is the product between SA and CT) (Vuoksimaa et al., 2015).

In order to obtain a reconstruction of the central surface for each participant, raw T1w images were further preprocessed using CAT12 standard pipeline (Gaser et al., 2022). Then, the SD (mm) of the left OTS, defined as the Euclidean distance between the central surface and its convex hull, was extracted from each individual central surface.

Diffusion MRI preprocessing

Minimally preprocessed DW images were provided by the HCP. Preprocessing steps were performed using FSL v.5.0.9 (Jenkinson et al., 2012), including b0 intensity normalization, EPI distortion correction, eddy current and subject motion correction, and resampling of DW images to 1.25 mm native structural space. A detailed description of the HCP's DW images preprocessing pipeline is reported in Glasser et al. (2013). Additional preprocessing steps were carried out by using MRtrix3, an open-source software optimized for processing, analysis, and visualization of DW data (Tournier et al., 2019). For each participant, the Fiber Orientation Distribution (FOD) (Tournier et al., 2019) was estimated using the Dhollander algorithm, which adopt a multi-shell multi-tissue constrained spherical deconvolution (MSMT-CSD; Jeurissen et al., 2014) approach to decompose DW images signal in separate tissue contribution (i.e., WM, GM and CSF), while accounting for potential biases occurring in voxels with partial volumes (Dhollander et al., 2016, 2019). Intensity normalization was also performed to correct for global intensity differences.

Anatomical Constrained Tractography and connectome construction

Anatomical Constrained Tractography (ACT) and connectome construction were carried out using MRtrix3 (Tournier et al., 2019). ACT (Smith et al., 2012) enables to enhance biological plausibility of streamline generation (e.g., by rejecting streamlines that terminates in the CSF). ACT requires T1w images to be segmented into five different tissue types (i.e., cortical GM, subcortical GM, WM, CSF, and pathological tissue), which were registered to diffusion space using FSL. For each participant, 1 million streamlines were generated, seeding from the GM/WM boundary, using the Second-order Integration over Fiber Orientation Distributions (iFOD2), a probabilistic algorithm that takes the FOD images previously generated as input (Tournier et al., 2010). In order to overcome the non-quantitative nature of the streamlines, spherical-deconvolution informing filtering of tractograms (SIFT2) (Smith et al., 2015) was performed to assign a weight to each streamline, thus obtaining a biologically accurate measure of fiber connectivity whilst retaining the complete streamlines reconstruction. Using Freesurfer, a volumetric parcellation image based on the Destrieux atlas (Destrieux et al., 2010), including cerebellum and subcortical structures, was created and registered to each participant's tractogram in diffusion space. Finally, a 164x164

structural connectivity (SC) matrix was generated for each participant, whose cells contain the sum of the streamline weights, scaled by regional volume, connecting each node and representing the strength of the structural connectivity between each node.

OTS identification and sulcal pattern classification

Sulcal surface was generated for each participant by means of the standard preprocessing pipeline of the Morphologist toolbox implemented in BrainVISA v.5 (https://brainvisa.info/web/). Based on the sulcal surface, the left and right OTS were identified and classified as either continuous or interrupted depending on the continuous or fragmented morphology of the sulcus (Cachia et al., 2018). To investigate the possible effect of the position of the OTS interruption, we identified whether the interruption was located in the anterior and/or posterior branch of the sulcus (the latter hosting the VWFA). The Y-coordinate of the posterior extremity of the brainstem was used as anatomical criterion to define the anterior and posterior branches of both the left and right OTS (Cachia et al., 2018) (Experiment 2; Figure 4). Note that, when the OTS was interrupted and both the anterior and posterior fragments crossed the posterior extremity of the brainstem, the OTS was classified as both anteriorly and posteriorly interrupted. The classification of the left and right OTS was carried out independently by two blind co-authors (GDM and NDM). Six participants had ambiguous OTS folding patterns, which rendered identification of the sulcal pattern particularly difficult. However, inter-rater agreement was above 95%. Since all ambiguous cases were resolved by author JA, participants were maintained in the sample for subsequent analyses. The distribution of the sulcal patterns in the sample is reported in Experiment 2; Table 4.

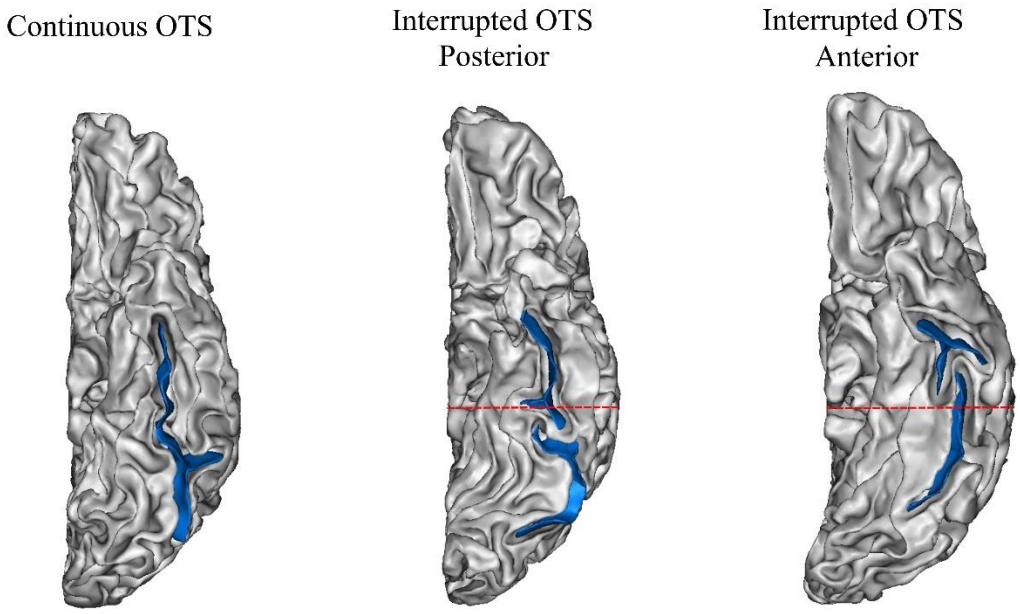

Experiment 2; Figure 4. Example of continuous or interrupted occipitotemporal sulcus (OTS). *Sulcal interruption was classified as located either in the anterior or posterior part of the sulcus. The Y-coordinate of the posterior extremity of the brainstem (red dashed line) was used as anatomical criterion to define the anterior and posterior part of the sulcus. The same procedure has been used for the left and right OTS. The figure is adapted with permission from Del Mauro, Del Maschio et al. (2022).*

	Left OTS		Right OTS	
	Anterior	Posterior	Anterior	Posterior
Continuous	54	43	50	35
Interrupted	32	43	36	51

Experiment 2; Table 4. Distribution of left and right occipitotemporal sulcus (OTS). *The anterior and posterior parts of the sulcus are classified as either continuous or interrupted.*

Statistical analyses

Correlation analyses. To avoid multicollinearity in the subsequent analyses, Pearson's correlations were computed between reading proficiency scores, education, age, and income. Results are reported in Experiment 2; Table 5.

	Reading proficiency	Income	Age	Educational history
Reading proficiency	_	r = 0.1	r = -0.01	r = 0.37*
Income	r = 0.1	_	r = 0.37*	r = 0.44*
Age	r = -0.01	r = 0.37*	_	r = 0.13
Education (Years)	r = 0.37*	r = 0.44*	r = 0.13	_

Experiment 2; Table 5. Correlation analyses. *Pearson's correlation analyses between reading proficiency, years of formal educational, age, and income. R = Pearson's correlation coefficient; * = significant correlation ($p < 0.05$).*

Effect of reading ability on the morphology of the left OTS. All statistical analyses on morphometric measures were performed on R v.4.0.2. To investigate the effect of reading proficiency on the morphology of the left OTS, a separate GLM was estimated for each morphometric index, namely GMV, CT, SA, and SD. The morphometric index was entered into the model as dependent variable and the reading proficiency as predictor. Based on evidence that males and females differ in brain morphology (Williams et al., 2021a) and that SES impacts on brain structure (Brito et al., 2014), sex and income were included into the model as nuisance variables. In order to account for individual differences in brain-general morphology, a measure of global brain structure was also entered into the model as nuisance covariate (TIV for GMV, total SA for SA, average CT for CT).

Effect of reading ability on the structural connectivity of the left OTS. The NBS Connectome toolbox v.1.2 (Zalesky et al., 2010) running on Matlab v.2019a was used to investigate the effect of reading ability on the structural connectivity of the left OTS. In the NBS Connectome toolbox, hypotheses about human connectome are tested using connectivity matrices, which are analyzed using a nonparametric permutation-based statistical approach to deal with the multiple comparison problem on graphs. Because we were interested in studying the relationship between reading ability and structural connectivity of the left OTS, we restricted the analysis to this region by setting the cells of the previously calculated SC matrices (containing the sum of the

streamline weights connecting each pair of nodes) to 0, except for the row and the column corresponding to the left OTS. The NBS Connectome toolbox requires the statistical model to be specified as a GLM. Therefore, these newly generated matrices were entered into a GLM as dependent variable, whereas reading proficiency scores and the model intercept were included as regressors. Based on evidence that income and sex influence white matter connectivity (Bell et al., 2021; Ingalhalikar et al., 2014), these variables were entered as nuisance covariates into the model. We tested the effect of reading proficiency on the structural connectivity pattern of the left OTS. In the NBS analysis, a user-defined t-value is used as primary threshold to independently test the effect of interest at each connection (i.e., edge) (Zalesky et al., 2010). Note that the threshold value affects the specificity, but not the sensitivity of the NBS method (see Fornito et al., 2016). As recommended by NBS guidelines, primary-thresholds were selected to balance network extension (i.e., avoiding excessive connections) with effect strength (see Zalesky et al., 2010). In addition, since the value of the primary threshold can significantly affect the results, we tested the effect of reading proficiency a range of thresholds (in line with recent studies, e.g., Beare et al., 2017; Çelik et al., 2020; DeSerisy et al., 2021): 2.4, 2.5, 2.6, 2.7 and 2.8. Supra-threshold connections are used to identify connected components (i.e., connected clusters in the topological space). To determine the significance of the components, 5,000 permutations were performed and a FWE corrected p-value of 0.05 was used. The FWE-corrected p-value was estimated based on the component intensity, calculated as the sum of the test values of each of connection within the component, which is suited to detect strong and focal effects confined to few connections (Zalesky et al., 2010).

Effect of the left OTS sulcal pattern on reading ability. To investigate the effect of the left OTS sulcal pattern on reading ability, reading proficiency scores were entered as dependent variable in a GLM with two dichotomous predictors: left anterior OTS (continuous vs interrupted) and left posterior OTS (continuous vs interrupted). Moreover, the sulcal pattern of the right OTS was included into the model as nuisance variable with two other dichotomous variables: right anterior OTS (continuous vs interrupted) and right posterior OTS (continuous vs interrupted). Based on the results of a previous study (Cachia et al., 2018), the income was also entered into the model as nuisance variable. Since males and females did not differ significantly in reading

proficiency scores ($p > 0.05$), sex was not included into the model as nuisance variable. Statistical analyses were performed on R v.4.0.2.

Effect of left OTS sulcal pattern on morphometric measures. To investigate whether the sulcal pattern of the left OTS is associated with the morphology of the sulcus, a separate GLM was estimated for each morphometric index (i.e., GMV, CT, SA, and SD). The morphometric index was entered into the model as dependent variable. Two dichotomous variables (i.e., left anterior OTS: continuous vs interrupted; left posterior OTS: continuous vs interrupted) were included as predictors, while income and sex were entered as nuisance variables (Brito et al., 2014; Williams et al., 2021a). The effect of anterior and posterior sulcal patterns was explored. To account for individual differences in brain-general morphology, a measure of global brain structure was included into the model as nuisance covariate (TIV for GMV, total SA for SA, average CT for CT). All results were corrected for multiple comparisons using Bonferroni correction.

Effect of the left OTS sulcal pattern on structural connectivity. The effect of the left OTS sulcal pattern on the structural connectivity of the sulcus was investigated by means of the NBS Connectome toolbox (Zalesky et al., 2010), following the same procedure described above. SC matrices were entered into the GLM as dependent variable, with left anterior and posterior OTS sulcal patterns (continuous vs interrupted), income (Bell et al., 2021), sex (Ingalhalikar et al., 2014), and the model intercept as regressors. First, the main effects of anterior and posterior sulcal patterns were tested. Then, the interaction between anterior and posterior sulcal patterns was examined by adding the interaction term into the model.

5.3 Experiment 3 (Materials and methods)

Participants

The sample of this study was provided by the Wu-Minn HCP dataset (Van Essen et al., 2013), including 1206 participants with no history of psychiatric or neurological disorders. We excluded participants who: (1) did not have MRI data; (2) had missing information; (3) had an Edinburgh Handedness Questionnaire score < 0 (Oldfield, 1971). In addition, in line with evidence suggesting that the use of hormonal contraceptive might have a considerable impact on female's brain structure (Lisofsky et al., 2016; Pletzer et al., 2010), we also excluded female participants that declared to use birth control methods or did not report this information.

The final sample included 829 participants (380 F). Independent sample t-tests were performed to test differences between females and males in sociodemographic variables. Females were significantly older than males ($t = 7.43$, $p < 0.001$), while no difference emerged between the two groups for years of formal education and income ($p > 0.05$). Descriptive statistics of sociodemographic variables are reported in Experiment 3; Table 2.

	Sample (N = 829)	Females (N = 380)	Males (N = 449)
	Mean ± St.Dev. (range)	Mean ± St.Dev. (range)	Mean ± St.Dev. (range)
Age	28.77 ± 3.75 (22-36)	29.79 ± 3.65 (22-36)	27.91 ± 3.61 (22-36)
Education (Years)	14.85 ± 1.81 (11-17)	14.91 ± 1.84 (11-17)	14.8 ± 1.78 (11-17)
Income	4.98 ± 2.19 (1-8)	4.99 ± 2.21 (1-8)	4.98 ± 2.16 (1-8)

Experiment 3; Table 2. Descriptive statistics of sociodemographic variables. *Mean, standard deviation (St.Dev.) and range of sociodemographic variables are reported for the entire sample, and for males and females separately.*

Image acquisition

T1w images were included in the HCP dataset. A detailed description of the acquisition protocols is reported in Glasser et al. (2013).

Preprocessing

Detailed information on structural preprocessing is reported in Glasser et al. (2013). T1w images were preprocessed using FSL version 5.0.9 (Jenkinson et al., 2012) and FreeSurfer version 5.2 (Fischl, 2012). In summary, the structural preprocessing pipeline included the following steps: distortion and bias correction; registration to MNI space; segmentation of the volume into predefined structures; reconstruction of white and pial cortical surfaces; registration of the surfaces to the fsaverage template using the standard folding-based surface registration (Glasser et al., 2013).

Estimation of cortical measures

For each measure of interest (i.e., GMV, SA, CT and FD), we extracted local values for the 148 cortical regions of the Destrieux cortical parcellation (Destrieux et al., 2010), and an index of global brain structure, including TBV, average CT, total SA, and FD of the cortical ribbon.

The FD was calculated using the calcFD toolbox, a publicly available Matlab toolbox designed to measure the fractal dimensionality of a 3D structure using the intermediate files resulting from the FreeSurfer pipeline (Madan & Kensinger, 2016; https://github.com/cMadan/calcFD) (a definition of the other morphometric indices is reported in paragraph 5.2).

Source-based morphometry

The Group ICA of an fMRI Toolbox (GIFT; https://trendscenter.org/software/gift/) was used to identify networks of GM covariance. Prior to performing SoBM, segmented GM images were generated using CAT12 (http://www.neuro.uni-jena.de/cat/index.html) (Gaser et al., 2022). GM images were resampled to 2 x 2 x 2 mm voxels (Segall et al., 2012) and smoothed with an 8 x 8 x 8 mm FWHM Gaussian kernel. The number of ICs was automatically computed by GIFT using the 'minimum description length' (MDL) criterion (Li et al., 2007). The ICA was performed using the Infomax algorithm (Bell & Sejnowski, 1995). The ICA algorithm generates two matrices: a subject by component matrix (i.e., mixing matrix) and a component by

voxel matrix (i.e., source matrix). The mixing matrix represents the contribution of each participant to each individual component (expressed as loading coefficients), whereas each voxel's contribution to an individual component is represented by the source matrix (Xu et al., 2009). In order to increase components stability, we adopted the ICASSO algorithm (http://research.ics.aalto.fi/ica/icasso/). Using this approach, the ICA was performed 100 times using bootstrapping and permutations. ICASSO produced a quality index (*Iq*) ranging from 0 to 1, which reflects the compactness and repeatability of each component. Based on this index, components with low stability and repeatability were identified and excluded for subsequent analyses. Then, statistical analyses were performed by extracting from the mixing matrix of each component the loading coefficients of the participants.

Statistical analyses

Sex differences in global brain structure and cortical regions. All statistical analyses were performed on R v4.0.2. For each measure of interest, a GLM was estimated with morphometric values as dependent variable and sex as group factor. Based on previous evidence showing that age impacts brain structure (Gennatas et al., 2017), this variable was included into the model as nuisance covariate. To control whether regional differences were a by-product of a brain-general difference between males and females, a measure of global brain structure was also included into the model as nuisance variable (Ritchie et al., 2018): TBV for GMV, total SA for SA, average CT for CT, and FD of the cortical ribbon for FD.

P-values of each index were independently adjusted using the false-discovery rate (FDR) correction. Cohen's d was calculated as the t-value multiplied by 2 and divided by the square root of the degrees of freedom (Ritchie et al., 2018). Note that negative t-values and effect sizes denote higher brain measures in males. For each cortical measure and cortical region, effect sizes were projected onto the fsaverage template using the *fsbrain* library running on R v4.0.2 (Schäfer & Ecker, 2020).

Source-based morphometry. We extracted 95 ICs according to the MDL criterion (Li et al., 2007). Before running statistical analyses, the *Iq* was used to assess the repeatability of each component ($Iq \geq 0.9$). Thirty-five ICs were excluded due to this criterion ($Iq < 0.9$). Three components including large white matter clusters were also

excluded, leading to a final number of 57 ICs. Sex differences were tested separately for each IC. Loading coefficients were entered into a GLM as dependent variable, with sex as group factor and TBV and age as nuisance variables. Negative t-values and effect sizes indicate higher GMV in males. All p-values were adjusted for multiple comparisons using FDR correction.

6. References

Abutalebi, J., Della Rosa, P. A., Green, D. W., Hernandez, M., Scifo, P., Keim, R., Cappa, S. F., & Costa, A. (2012). Bilingualism Tunes the Anterior Cingulate Cortex for Conflict Monitoring. *Cerebral Cortex*, *22*(9), 2076–2086. https://doi.org/10.1093/cercor/bhr287

Abutalebi, J., & Green, D. W. (2008). Control mechanisms in bilingual language production: Neural evidence from language switching studies. *Language and Cognitive Processes*, *23*(4), 557–582. https://doi.org/10.1080/01690960801920602

Abutalebi, J., & Green, D. W. (2016). Neuroimaging of language control in bilinguals: neural adaptation and reserve. *Bilingualism: Language and Cognition*, *19*(4), 689–698. https://doi.org/10.1017/S1366728916000225

Amft, M., Bzdok, D., Laird, A. R., Fox, P. T., Schilbach, L., & Eickhoff, S. B. (2015). Definition and characterization of an extended social-affective default network. *Brain Structure and Function*, *220*(2), 1031–1049. https://doi.org/10.1007/s00429-013-0698-0

Amiez, C., Neveu, R., Warrot, D., Petrides, M., Knoblauch, K., & Procyk, E. (2013). The location of feedback-related activity in the midcingulate cortex is predicted by local morphology. *Journal of Neuroscience*, *33*(5), 2217–2228. https://doi.org/10.1523/JNEUROSCI.2779-12.2013

Amiez, C., & Petrides, M. (2014). Neuroimaging evidence of the anatomo-functional organization of the human cingulate motor areas. *Cerebral Cortex*, *24*(3), 563–578. https://doi.org/10.1093/cercor/bhs329

Amiez, C., Sallet, J., Hopkins, W. D., Meguerditchian, A., Hadj-Bouziane, F., Ben Hamed, S., Wilson, C. R. E., Procyk, E., & Petrides, M. (2019). Sulcal organization in the medial frontal cortex provides insights into primate brain evolution. *Nature Communications*, *10*(1). https://doi.org/10.1038/s41467-019-11347-x

Amiez, C., Wilson, C. R. E., & Procyk, E. (2018). Variations of cingulate sulcal organization and link with cognitive performance. *Scientific Reports*, *8*(1), 1–13. https://doi.org/10.1038/s41598-018-32088-9

Andersson, M. (1994). *Sexual Selection*. Princeton University Press. https://doi.org/10.1515/9780691207278

Andreano, J. M., & Cahill, L. (2009). Sex influences on the neurobiology of learning and memory. *Learning & Memory*, *16*(4), 248–266. https://doi.org/10.1101/lm.918309

Arnold, A. P. (2012). The end of gonad-centric sex determination in mammals. *Trends in Genetics*, *28*(2), 55–61. https://doi.org/10.1016/j.tig.2011.10.004

Azevedo, F. A. C., Carvalho, L. R. B., Grinberg, L. T., Farfel, J. M., Ferretti, R. E. L., Leite, R. E. P., Filho, W. J., Lent, R., & Herculano-Houzel, S. (2009). Equal numbers of neuronal and nonneuronal cells make the human brain an isometrically scaled-up primate brain. *Journal of Comparative Neurology*, *513*(5), 532–541.

https://doi.org/10.1002/cne.21974

Ball, G. F., Balthazart, J., & McCarthy, M. M. (2014). Is it useful to view the brain as a secondary sexual characteristic? *Neuroscience and Biobehavioral Reviews*, *46*(P4), 628–638. https://doi.org/10.1016/j.neubiorev.2014.08.009

Bar, M., Kassam, K. S., Ghuman, A. S., Boshyan, J., Schmidt, A. M., Dale, A. M., Hämäläinen, M. S., Marinkovic, K., Schacter, D. L., Rosen, B. R., & Halgren, E. (2006). Top-down facilitation of visual recognition. *Proceedings of the National Academy of Sciences of the United States of America*, *103*(2), 449–454. https://doi.org/10.1073/pnas.0507062103

Barkovich, A. J., Guerrini, R., Kuzniecky, R. I., Jackson, G. D., & Dobyns, W. B. (2012). A developmental and genetic classification for malformations of cortical development: Update 2012. *Brain*, *135*(5), 1348–1369. https://doi.org/10.1093/brain/aws019

Barnes, L. L., Wilson, R. S., Bienias, J. L., Schneider, J. A., Evans, D. A., & Bennett, D. A. (2005). Sex differences in the clinical manifestations of Alzheimer disease pathology. *Archives of General Psychiatry*, *62*(6), 685–691. https://doi.org/10.1001/archpsyc.62.6.685

Baron-Cohen, S., Knickmeyer, R. C., Belmonte, M. K., Jack, C. R., Wiste, H. J., Weigand, S. D., Knopman, D. S., Vemuri, P., Mielke, M. M., Lowe, V., Senjem, M. L., Gunter, J. L., Machulda, M. M., Gregg, B. E., Pankratz, V. S., Rocca, W. A., Petersen, R. C., Kong, L., Chen, K., … Solso, S. (2005). Sex differences in the brain: Implications for explaining autism. *Brain Research*, *1380*(5749), 819–823. https://doi.org/10.1016/j.jpsychires.2013.02.003

Baron-Cohen, S., Lombardo, M. V., Auyeung, B., Ashwin, E., Chakrabarti, B., & Knickmeyer, R. (2011). Why are Autism Spectrum conditions more prevalent in Males? *PLoS Biology*, *9*(6). https://doi.org/10.1371/journal.pbio.1001081

Basso, A., Capitani, E., & Laiacona, M. (1987). Raven's coloured progressive matrices: normative values on 305 adult normal controls. *Functional Neurology*, *2*(2), 189–194. http://www.ncbi.nlm.nih.gov/pubmed/3666548

Bava, S., Boucquey, V., Goldenberg, D., Thayer, R. E., Ward, M., Jacobus, J., & Tapert, S. F. (2011). Sex differences in adolescent white matter architecture. *Brain Research*, *1375*(0603), 41–48. https://doi.org/10.1016/j.brainres.2010.12.051

Bayer, S. A., & Altman, J. (1991). *Neocortical development (Vol. 1)*. Raven Press.

Beacher, F. D., Minati, L., Baron-Cohen, S., Lombardo, M. V., Lai, M. C., Gray, M. A., Harrison, N. A., & Critchley, H. D. (2012). Autism attenuates sex differences in brain structure: A combined voxel-based morphometry and diffusion tensor imaging study. *American Journal of Neuroradiology*, *33*(1), 83–89. https://doi.org/10.3174/ajnr.A2880

Beare, R., Adamson, C., Bellgrove, M. A., Vilgis, V., Vance, A., Seal, M. L., & Silk, T. J. (2017). Altered structural connectivity in ADHD: a network based analysis. *Brain Imaging and Behavior*, *11*(3), 846–858. https://doi.org/10.1007/s11682-016-9559-9

Beckmann, M., Johansen-Berg, H., & Rushworth, M. F. S. (2009). Connectivity-based parcellation of human cingulate cortex and its relation to functional specialization. *Journal of Neuroscience*, *29*(4), 1175–1190. https://doi.org/10.1523/JNEUROSCI.3328-08.2009

Bell, A. J., & Sejnowski, T. J. (1995). An Information-Maximization Approach to Blind Separation and Blind Deconvolution. *Neural Computation*, *7*(6), 1129–1159. https://doi.org/10.1162/neco.1995.7.6.1129

Bell, K. L., Purcell, J. B., Harnett, N. G., Goodman, A. M., Mrug, S., Schuster, M. A., Elliott, M. N., Emery, S. T., & Knight, D. C. (2021). White Matter Microstructure in the Young Adult Brain Varies with Neighborhood Disadvantage in Adolescence. Neuroscience, 466, 162-172. https://doi.org/10.1016/j.neuroscience.2021.05.012

Birur, B., Kraguljac, N. V., Shelton, R. C., & Lahti, A. C. (2017). Brain structure, function, and neurochemistry in schizophrenia and bipolar disorder- A systematic review of the magnetic resonance neuroimaging literature. *Npj Schizophrenia*, *3*(1), 1–14. https://doi.org/10.1038/s41537-017-0013-9

Biswal, B. B., Mennes, M., Zuo, X. N., Gohel, S., Kelly, C., Smith, S. M., Beckmann, C. F., Adelstein, J. S., Buckner, R. L., Colcombe, S., Dogonowski, A. M., Ernst, M., Fair, D., Hampson, M., Hoptman, M. J., Hyde, J. S., Kiviniemi, V. J., Kötter, R., Li, S. J., … Milham, M. P. (2010). Toward discovery science of human brain function. *Proceedings of the National Academy of Sciences of the United States of America*, *107*(10), 4734–4739. https://doi.org/10.1073/pnas.0911855107

Blackmon, K., Barr, W. B., Kuzniecky, R., DuBois, J., Carlson, C., Quinn, B. T., Blumberg, M., Halgren, E., Hagler, D. J., Mikhly, M., Devinsky, O., McDonald, C. R., Dale, A. M., & Thesen, T. (2010). Phonetically irregular word pronunciation and cortical thickness in the adult brain. *NeuroImage*, *51*(4), 1453–1458. https://doi.org/10.1016/j.neuroimage.2010.03.028

Blasi, G., Goldberg, T. E., Weickert, T., Das, S., Kohn, P., Zoltick, B., Bertolino, A., Callicott, J. H., Weinberger, D. R., & Mattay, V. S. (2006). Brain regions underlying response inhibition and interference monitoring and suppression. *European Journal of Neuroscience*, *23*(6), 1658–1664. https://doi.org/10.1111/j.1460-9568.2006.04680.x

Blomert, L. (2011). The neural signature of orthographic-phonological binding in successful and failing reading development. *NeuroImage*, *57*(3), 695–703. https://doi.org/10.1016/j.neuroimage.2010.11.003

Bolger, D. J., Perfetti, C. A., & Schneider, W. (2005). Cross-cultural effect on the brain revisited: Universal structures plus writing system variation. *Human Brain Mapping*, *25*(1), 92–104. https://doi.org/10.1002/hbm.20124

Bora, E., Fornito, A., Radua, J., Walterfang, M., Seal, M., Wood, S. J., Yücel, M., Velakoulis, D., & Pantelis, C. (2011). Neuroanatomical abnormalities in schizophrenia: A multimodal voxelwise meta-analysis and meta-regression analysis. *Schizophrenia Research*, *127*(1–3), 46–57. https://doi.org/10.1016/j.schres.2010.12.020

Borst, G., Cachia, A., Tissier, C., Ahr, E., Simon, G., & Houdé, O. (2016). Early

Cerebral Constraints on Reading Skills in School-Age Children: An MRI Study. *Mind, Brain, and Education*, *10*(1), 47–54. https://doi.org/10.1111/mbe.12098

Borst, G., Cachia, A., Vidal, J., Simon, G., Fischer, C., Pineau, A., Poirel, N., Mangin, J. F., & Houdé, O. (2014). Folding of the anterior cingulate cortex partially explains inhibitory control during childhood: A longitudinal study. *Developmental Cognitive Neuroscience*, *9*, 126–135. https://doi.org/10.1016/j.dcn.2014.02.006

Botvinick, M. M., Cohen, J. D., & Carter, C. S. (2004). Conflict monitoring and anterior cingulate cortex: An update. *Trends in Cognitive Sciences*, *8*(12), 539–546. https://doi.org/10.1016/j.tics.2004.10.003

Bouhali, F., de Schotten, M. T., Pinel, P., Poupon, C., Mangin, J. F., Dehaene, S., & Cohen, L. (2014). Anatomical connections of the visual word form area. *Journal of Neuroscience*, *34*(46), 15402–15414. https://doi.org/10.1523/JNEUROSCI.4918-13.2014

Brain Development Cooperative group. (2012). Total and regional brain volumes in a population-based normative sample from 4 to 18 years: The NIH MRI study of normal brain development. *Cerebral Cortex*, *22*(1), 1–12. https://doi.org/10.1093/cercor/bhr018

Brito, N. H., & Noble, K. G. (2014). Socioeconomic status and structural brain development. Frontiers in Neuroscience, 8. https://doi.org/10.3389/fnins.2014.00276

Brodoehl, S., Gaser, C., Dahnke, R., Witte, O. W., & Klingner, C. M. (2020). Surface-based analysis increases the specificity of cortical activation patterns and connectivity results. *Scientific Reports*, *10*(1), 5737. https://doi.org/10.1038/s41598-020-62832-z

Broere-Brown, Z. A., Baan, E., Schalekamp-Timmermans, S., Verburg, B. O., Jaddoe, V. W. V., & Steegers, E. A. P. (2016). Sex-specific differences in fetal and infant growth patterns: A prospective population-based cohort study. *Biology of Sex Differences*, *7*(1), 1–9. https://doi.org/10.1186/s13293-016-0119-1

Bucholz, K. K., Cadoret, R., Cloninger, C. R., Dinwiddie, S. H., Hesselbrock, V. M., Nurnberger, J. I., Reich, T., Schmidt, I., & Schuckit, M. A. (1994). A new, semi-structured psychiatric interview for use in genetic linkage studies: a report on the reliability of the SSAGA. *Journal of Studies on Alcohol*, *55*(2), 149–158. https://doi.org/10.15288/jsa.1994.55.149

Budday, S., Steinmann, P., & Kuhl, E. (2015). Physical biology of human brain development. *Frontiers in Cellular Neuroscience*, *9*(JULY), 1–17. https://doi.org/10.3389/fncel.2015.00257

Burle, B., Spieser, L., Servant, M., & Hasbroucq, T. (2014). Distributional reaction time properties in the Eriksen task: marked differences or hidden similarities with the Simon task? *Psychonomic Bulletin & Review*, *21*(4), 1003–1010. https://doi.org/10.3758/s13423-013-0561-6

Bush, G., Frazier, J. A., Rauch, S. L., Seidman, L. J., Whalen, P. J., Jenike, M. A., Rosen, B. R., & Biederman, J. (1999). Anterior cingulate cortex dysfunction in attention-deficit/hyperactivity disorder revealed by fMRI and the counting stroop. *Biological Psychiatry*, *45*(12), 1542–1552. https://doi.org/10.1016/S0006-

3223(99)00083-9

Bush, G., Whalen, P. J., Rosen, B. R., Jenike, M. A., McInerney, S. C., & Rauch, S. L. (1998). The counting stroop: An interference task specialized for functional neuroimaging-validation study with functional MRI. *Human Brain Mapping*, *6*(4), 270–282. https://doi.org/10.1002/(SICI)1097-0193(1998)6:4<270::AID-HBM6>3.0.CO;2-0

Cachia, A., Borst, G., Jardri, R., Raznahan, A., Murray, G. K., Mangin, J. F., & Plaze, M. (2021). Towards Deciphering the Fetal Foundation of Normal Cognition and Cognitive Symptoms From Sulcation of the Cortex. *Frontiers in Neuroanatomy*, *15*(September), 1–13. https://doi.org/10.3389/fnana.2021.712862

Cachia, A., Borst, G., Tissier, C., Fisher, C., Plaze, M., Gay, O., Rivière, D., Gogtay, N., Giedd, J., Mangin, J. F., Houdé, O., & Raznahan, A. (2016). Longitudinal stability of the folding pattern of the anterior cingulate cortex during development. *Developmental Cognitive Neuroscience*, *19*, 122–127. https://doi.org/10.1016/j.dcn.2016.02.011

Cachia, A., Borst, G., Vidal, J., Fischer, C., Pineau, A., Mangin, J.-F., & Houdé, O. (2014). The Shape of the ACC Contributes to Cognitive Control Efficiency in Preschoolers. *Journal of Cognitive Neuroscience*, *26*(1), 96–106. https://doi.org/10.1162/jocn_a_00459

Cachia, A., Del Maschio, N., Borst, G., Della Rosa, P. A., Pallier, C., Costa, A., Houdé, O., & Abutalebi, J. (2017). Anterior cingulate cortex sulcation and its differential effects on conflict monitoring in bilinguals and monolinguals. *Brain and Language*, *175*(October), 57–63. https://doi.org/10.1016/j.bandl.2017.09.005

Cachia, A., Roell, M., Mangin, J. F., Sun, Z. Y., Jobert, A., Braga, L., Houde, O., Dehaene, S., & Borst, G. (2018). How interindividual differences in brain anatomy shape reading accuracy. *Brain Structure and Function*, *223*(2), 701–712. https://doi.org/10.1007/s00429-017-1516-x

Caligiore, D., Pezzulo, G., Baldassarre, G., Bostan, A. C., Strick, P. L., Doya, K., Helmich, R. C., Dirkx, M., Houk, J., Jörntell, H., Lago-Rodriguez, A., Galea, J. M., Miall, R. C., Popa, T., Kishore, A., Verschure, P. F. M. J., Zucca, R., & Herreros, I. (2017). Consensus Paper: Towards a Systems-Level View of Cerebellar Function: the Interplay Between Cerebellum, Basal Ganglia, and Cortex. *Cerebellum*, *16*(1), 203–229. https://doi.org/10.1007/s12311-016-0763-3

Cao, B., Mwangi, B., Passos, I. C., Wu, M. J., Keser, Z., Zunta-Soares, G. B., Xu, Di., Hasan, K. M., & Soares, J. C. (2017). Lifespan Gyrification Trajectories of Human Brain in Healthy Individuals and Patients with Major Psychiatric Disorders. *Scientific Reports*, *7*(1), 1–8. https://doi.org/10.1038/s41598-017-00582-1

Cárdenas, E. F., Kujawa, A., & Humphreys, K. L. (2020). Neurobiological changes during the peripartum period: Implications for health and behavior. *Social Cognitive and Affective Neuroscience*, *15*(10), 1097–1110. https://doi.org/10.1093/scan/nsz091

Çelik, Z. Ç., Çolak, Ç., Di Biase, M. A., Zalesky, A., Zorlu, N., Bora, E., Kitiş, Ö., & Yüncü, Z. (2020). Structural connectivity in adolescent synthetic cannabinoid users

with and without ADHD. *Brain Imaging and Behavior*, *14*(2), 505–514. https://doi.org/10.1007/s11682-018-0023-x

Chen, L., Wassermann, D., Abrams, D. A., Kochalka, J., Gallardo-Diez, G., & Menon, V. (2019). The visual word form area (VWFA) is part of both language and attention circuitry. *Nature Communications*, *10*(1), 1–12. https://doi.org/10.1038/s41467-019-13634-z

Chen, X., Sachdev, P. S., Wen, W., & Anstey, K. J. (2007). Sex differences in regional gray matter in healthy individuals aged 44-48 years: A voxel-based morphometric study. *NeuroImage*, *36*(3), 691–699. https://doi.org/10.1016/j.neuroimage.2007.03.063

Chen, Z., Zhao, X., Fan, J., & Chen, A. (2018). Functional cerebral asymmetry analyses reveal how the control system implements its flexibility. *Human Brain Mapping*, *39*(12), 4678–4688. https://doi.org/10.1002/hbm.24313

Cherodath, S., Rao, C., Midha, R., Sumathi, T. A., & Singh, N. C. (2017). A role for putamen in phonological processing in children. *Bilingualism*, *20*(2), 318–326. https://doi.org/10.1017/S1366728916000614

Chi, J. G., Dooling, E. C., & Gilles, F. H. (1977). Gyral development of the human brain. *Annals of Neurology*, *1*(1), 86–93. https://doi.org/10.1002/ana.410010109

Christov-Moore, L., Simpson, E. A., Coudé, G., Grigaityte, K., Iacoboni, M., & Ferrari, P. F. (2014). Empathy: Gender effects in brain and behavior. *Neuroscience and Biobehavioral Reviews*, *46*(P4), 604–627. https://doi.org/10.1016/j.neubiorev.2014.09.001

Clark, G. M., Mackay, C. E., Davidson, M. E., Iversen, S. D., Collinson, S. L., James, A. C., Roberts, N., & Crow, T. J. (2010). Paracingulate sulcus asymmetry; Sex difference, correlation with semantic fluency and change over time in adolescent onset psychosis. Psychiatry Research: Neuroimaging, 184(1), 10-15. https://doi.org/10.1016/j.pscychresns.2010.06.012

Clouchoux, C., Kudelski, D., Gholipour, A., Warfield, S. K., Viseur, S., Bouyssi-Kobar, M., Mari, J. L., Evans, A. C., Du Plessis, A. J., & Limperopoulos, C. (2012). Quantitative in vivo MRI measurement of cortical development in the fetus. *Brain Structure and Function*, *217*(1), 127–139. https://doi.org/10.1007/s00429-011-0325-x

Clutton-Brock, T., & Huchard, E. (2013). Social competition and its consequences in female mammals. *Journal of Zoology*, *289*(3), 151–171. https://doi.org/10.1111/jzo.12023

Cohen, L., & Dehaene, S. (2004). Specialization within the ventral stream: The case for the visual word form area. *NeuroImage*, *22*(1), 466–476. https://doi.org/10.1016/j.neuroimage.2003.12.049

Courchesne, E., Campbell, K., & Solso, S. (2011). Brain growth across the life span in autism: Age-specific changes in anatomical pathology. *Brain Research*, *1380*, 138–145. https://doi.org/10.1016/j.brainres.2010.09.101

Crosson, B., Saclek, J. R., Bobholz, J. A., Gökçay, D., Mohr, C. M., Leonard, C. M.,

Maron, L., Auerbach, E. J., Browd, S. R., Freeman, A. J., & Briggs, R. W. (1999). Activity in the paracingulate and cingulate sulci during word generation: An fMRI study of functional anatomy. *Cerebral Cortex*, *9*(4), 307–316. https://doi.org/10.1093/cercor/9.4.307

Dahnke, R., Yotter, R. A., & Gaser, C. (2013). Cortical thickness and central surface estimation. *NeuroImage*, *65*, 336–348. https://doi.org/10.1016/j.neuroimage.2012.09.050

Dale, A. M. (1999). Optimal experimental design for event-related fMRI. *Human Brain Mapping*, *8*(2–3), 109–114. https://doi.org/10.1002/(SICI)1097-0193(1999)8:2/3<109::AID-HBM7>3.0.CO;2-W

Darwin, C. (1871). *The Descent of Man and Selection in Relation to Sex*. John Murray.

Dawes, P., Cruickshanks, K. J., Moore, D. R., Fortnum, H., Edmondson-Jones, M., McCormack, A., & Munro, K. J. (2015). The effect of prenatal and childhood development on hearing, vision and cognition in adulthood. *PLoS ONE*, *10*(8), 1–16. https://doi.org/10.1371/journal.pone.0136590

Dawkins, R. (1989). *The selfish gene*. Oxford University Press.

De Frias, C., Nilsson, L. G., & Herlitz, A. (2006). Sex differences in cognition are stable over a 10-year period in adulthood and old age. *Aging, Neuropsychology, and Cognition*, *13*(3–4), 574–587. https://doi.org/10.1080/13825580600678418

De Jong, R., Liang, C.-C., & Lauber, E. (1994). Conditional and unconditional automaticity: A dual-process model of effects of spatial stimulus-response correspondence. *Journal of Experimental Psychology: Human Perception and Performance*, *20*(4), 731–750. https://doi.org/10.1037/0096-1523.20.4.731

Decasien, A. R., Guma, E., Liu, S., & Raznahan, A. (2022). Sex differences in the human brain : a roadmap for more careful analysis and interpretation of a biological reality. *Biology of Sex Differences*, 1–21. https://doi.org/10.1186/s13293-022-00448-w

Dehaene, S., & Cohen, L. (2011). The unique role of the visual word form area in reading. *Trends in Cognitive Sciences*, *15*(6), 254–262. https://doi.org/10.1016/j.tics.2011.04.003

Dehaene, S., Pegado, F., Braga, L. W., Ventura, P., Nunes Filho, G., Jobert, A., Dehaene-Lambertz, G., Kolinsky, R., Morais, J., & Cohen, L. (2010). How learning to read changes the cortical networks for vision and language. *Science*, *330*(6009), 1359–1364. https://doi.org/10.1126/science.1194140

Dehay, C., Horsburgh, G., Berland, M., Killackey, H., & Kennedy, H. (1991). The effects of bilateral enucleation in the primate fetus on the parcellation of visual cortex. *Developmental Brain Research*, *62*(1), 137–141. https://doi.org/10.1016/0165-3806(91)90199-S

Del Maschio, N., Fedeli, D., Sulpizio, S., & Abutalebi, J. (2019). The relationship between bilingual experience and gyrification in adulthood: A cross-sectional surface-based morphometry study. *Brain and Language*, *198*(March), 104680.

https://doi.org/10.1016/j.bandl.2019.104680

Del Maschio, N., Sulpizio, S., Fedeli, D., Ramanujan, K., Ding, G., Weekes, B. S., Cachia, A., Abutalebi, J., Del Maschio, N., Sulpizio, S., Fedeli, D., Ramanujan, K., Ding, G., Weekes, B. S., Cachia, A., & Abutalebi, J. (2019). ACC sulcal patterns and their modulation on cognitive control efficiency across lifespan: A neuroanatomical study on bilinguals and monolinguals. *Cerebral Cortex*, *29*(7), 3091–3101. https://doi.org/10.1093/cercor/bhy175

Del Mauro, G., Del Maschio, N., & Abutalebi, J. (2022). The relationship between reading abilities and the left occipitotemporal sulcus: A dual perspective study. *Brain and Language*, *235*, 105189. https://doi.org/10.1016/j.bandl.2022.105189

Del Mauro, G., Del Maschio, N., Sulpizio, S., Fedeli, D., Perani, D., & Abutalebi, J. (2022). Investigating sexual dimorphism in human brain structure by combining multiple indexes of brain morphology and source-based morphometry. *Brain Structure and Function*, *227*(1), 11–21. https://doi.org/10.1007/s00429-021-02376-8

DeSerisy, M., Ramphal, B., Pagliaccio, D., Raffanello, E., Tau, G., Marsh, R., Posner, J., & Margolis, A. E. (2021). Frontoparietal and default mode network connectivity varies with age and intelligence. *Developmental Cognitive Neuroscience*, *48*, 100928. https://doi.org/10.1016/j.dcn.2021.100928

Destrieux, C., Fischl, B., Dale, A., & Halgren, E. (2010). Automatic parcellation of human cortical gyri and sulci using standard anatomical nomenclature. *NeuroImage*, *53*(1), 1–15. https://doi.org/10.1016/j.neuroimage.2010.06.010

Dhollander, T., Mito, R., Raffelt, D., & Connelly, A. (2019). Improved white matter response function estimation for 3-tissue constrained spherical deconvolution. *Proc. Intl. Soc. Mag. Reson. Med*, *555*.

Dhollander, T., Raffelt, D., & Connelly, A. (2016). Unsupervised 3-tissue response function estimation from single-shell or multi-shell diffusion MR data without a co-registered T1 image Predicting stroke impairment using machine learning techniques View project A novel sparse partial correlation method fo. *ISMRM Workshop on Breaking the Barriers of Diffusion MRI*, *35*(September), 1–2. https://www.researchgate.net/publication/307863133

Di Ieva, A., Esteban, F. J., Grizzi, F., Klonowski, W., & Martín-Landrove, M. (2015). Fractals in the neurosciences, part II: Clinical applications and future perspectives. *Neuroscientist*, *21*(1), 30–43. https://doi.org/10.1177/1073858413513928

Di Ieva, A., Grizzi, F., Jelinek, H., Pellionisz, A. J., & Losa, G. A. (2014). Fractals in the neurosciences, part I: General principles and basic neurosciences. *Neuroscientist*, *20*(4), 403–417. https://doi.org/10.1177/1073858413513927

Diamond, A. (2013). Executive Functions. *Annual Review of Psychology*, *64*(1), 135–168. https://doi.org/10.1146/annurev-psych-113011-143750

Doron, K., & Gazzaniga, M. (2008). Neuroimaging techniques offer new perspectives on callosal transfer and interhemispheric communication. *Cortex*, *44*(8), 1023–1029. https://doi.org/10.1016/j.cortex.2008.03.007

Dubois, J., Benders, M., Cachia, A., Lazeyras, F., Ha-Vinh Leuchter, R., Sizonenko, S. V., Borradori-Tolsa, C., Mangin, J. F., & Hüppi, P. S. (2008). Mapping the early cortical folding process in the preterm newborn brain. *Cerebral Cortex*, *18*(6), 1444–1454. https://doi.org/10.1093/cercor/bhm180

Dubois, J., Lefèvre, J., Angleys, H., Leroy, F., Fischer, C., Lebenberg, J., Dehaene-Lambertz, G., Borradori-Tolsa, C., Lazeyras, F., Hertz-Pannier, L., Mangin, J. F., Hüppi, P. S., & Germanaud, D. (2019). The dynamics of cortical folding waves and prematurity-related deviations revealed by spatial and spectral analysis of gyrification. *NeuroImage*, *185*(September 2017), 934–946. https://doi.org/10.1016/j.neuroimage.2018.03.005

Dubol, M., Epperson, C. N., Sacher, J., Pletzer, B., Derntl, B., Lanzenberger, R., Sundström-Poromaa, I., & Comasco, E. (2021). Neuroimaging the menstrual cycle: A multimodal systematic review. *Frontiers in Neuroendocrinology*, *60*, 100878. https://doi.org/10.1016/j.yfrne.2020.100878

Duerden, E. G., Chakravarty, M. M., Lerch, J. P., & Taylor, M. J. (2020). Sex-Based Differences in Cortical and Subcortical Development in 436 Individuals Aged 4-54 Years. *Cerebral Cortex*, *30*(5), 2854–2866. https://doi.org/10.1093/cercor/bhz279

Eliot, L., Ahmed, A., Khan, H., & Patel, J. (2021). Dump the "dimorphism": Comprehensive synthesis of human brain studies reveals few male-female differences beyond size. *Neuroscience and Biobehavioral Reviews*, *125*, 667–697. https://doi.org/10.1016/j.neubiorev.2021.02.026

Eriksen, B. A., & Eriksen, C. W. (1974). Effects of noise letters upon the identification of a target letter in a nonsearch task. *Perception & Psychophysics*, *16*(1), 143–149. https://doi.org/10.3758/BF03203267

Escorial, S., Román, F. J., Martínez, K., Burgaleta, M., Karama, S., & Colom, R. (2015). Sex differences in neocortical structure and cognitive performance: A surface-based morphometry study. *NeuroImage*, *104*, 355–365. https://doi.org/10.1016/j.neuroimage.2014.09.035

Fan, J., McCandliss, B. D., Fossella, J., Flombaum, J., & Posner, M. (2005). The activation of attentional networks. *NeuroImage*, *26*(2), 471–479. https://doi.org/10.1016/j.neuroimage.2005.02.004

Fan, J., McCandliss, B. D., Sommer, T., Raz, A., & Posner, M. I. (2002). Testing the Efficiency and Independence of Attentional Networks. *Journal of Cognitive Neuroscience*, *14*(3), 340–347. https://doi.org/10.1162/089892902317361886

Fedeli, D., Del Maschio, N., Caprioglio, C., Sulpizio, S., & Abutalebi, J. (2020). Sulcal Pattern Variability and Dorsal Anterior Cingulate Cortex Functional Connectivity across Adult Age. *Brain Connectivity*, *10*(6), 267–278. https://doi.org/10.1089/brain.2020.0751

Fernández, V., Llinares-Benadero, C., & Borrell, V. (2016). Cerebral cortex expansion and folding: what have we learned? *The EMBO Journal*, *35*(10), 1021–1044. https://doi.org/10.15252/embj.201593701

Ferretti, M. T., Iulita, M. F., Cavedo, E., Chiesa, P. A., Dimech, A. S., Chadha, A. S.,

Baracchi, F., Girouard, H., Misoch, S., Giacobini, E., Depypere, H., & Hampel, H. (2018). Sex differences in Alzheimer disease — The gateway to precision medicine. *Nature Reviews Neurology*, *14*(8), 457–469. https://doi.org/10.1038/s41582-018-0032-9

Ferri, S. L., Abel, T., & Brodkin, E. S. (2018). Sex Differences in Autism Spectrum Disorder: a Review. *Current Psychiatry Reports*, *20*(2), 9. https://doi.org/10.1007/s11920-018-0874-2

Fischl, B. (2012). FreeSurfer. *NeuroImage*, *62*(2), 774–781. https://doi.org/10.1016/j.neuroimage.2012.01.021

Fischl, B., Rajendran, N., Busa, E., Augustinack, J., Hinds, O., Yeo, B. T. T., Mohlberg, H., Amunts, K., & Zilles, K. (2008). Cortical folding patterns and predicting cytoarchitecture. *Cerebral Cortex*, *18*(8), 1973–1980. https://doi.org/10.1093/cercor/bhm225

Fisher, R. A. (1930). *The Genetical theory of Natural Selection*. Clarendon.

Fjell, A. M., Walhovd, K. B., Brown, T. T., Kuperman, J. M., Chung, Y., Hagler, D. J., Venkatraman, V., Cooper Roddey, J., Erhart, M., McCabe, C., Akshoomoff, N., Amaral, D. G., Bloss, C. S., Libiger, O., Darst, B. F., Schork, N. J., Casey, B. J., Chang, L., Ernst, T. M., … Dale, A. M. (2012). Multimodal imaging of the self-regulating developing brain. *Proceedings of the National Academy of Sciences of the United States of America*, *109*(48), 19620–19625. https://doi.org/10.1073/pnas.1208243109

Fornito, A., Yücel, M., Wood, S. J., Proffitt, T., McGorry, P. D., Velakoulis, D., & Pantelis, C. (2006). Morphology of the paracingulate sulcus and executive cognition in schizophrenia. Schizophrenia Research, 88(1-3), 192-197. https://doi.org/10.1016/j.schres.2006.06.034

Fornito, A., Malhi, G. S., Lagopoulos, J., Ivanovski, B., Wood, S. J., Velakoulis, D., ... & Yücel, M. (2007). In vivo evidence for early neurodevelopmental anomaly of the anterior cingulate cortex in bipolar disorder. Acta Psychiatrica Scandinavica, 116(6), 467-472. https://doi.org/10.1111/j.1600-0447.2007.01069.x

Fornito, A., Wood, S. J., Whittle, S., Fuller, J., Adamson, C., Saling, M. M., Velakoulis, D., Pantelis, C., & Yücel, M. (2008). Variability of the paracingulate sulcus and morphometry of the medial frontal cortex: Associations with cortical thickness, surface area, volume, and sulcal depth. *Human Brain Mapping*, *29*(2), 222–236. https://doi.org/10.1002/hbm.20381

Fornito, A., Zalesky, A., & Bullmore, E. (2016). *Fundamentals of brain network analysis*. Academic Press.

Frye, R. E., Liederman, J., Malmberg, B., McLean, J., Strickland, D., & Beauchamp, M. S. (2010). Surface area accounts for the relation of gray matter volume to reading-related skills and history of dyslexia. *Cerebral Cortex*, *20*(11), 2625–2635. https://doi.org/10.1093/cercor/bhq010

Garrison, J. R., Fernyhough, C., McCarthy-Jones, S., Haggard, M., Carr, V., Schall, U., Scott, R., Jablensky, A., Mowry, B., Michie, P., Catts, S., Henskens, F., Pantelis, C., Loughland, C., & Simons, J. S. (2015). Paracingulate sulcus morphology is

associated with hallucinations in the human brain. *Nature Communications*, *6*, 2–7. https://doi.org/10.1038/ncomms9956

Garrison, J. R., Fernyhough, C., McCarthy-Jones, S., Simons, J. S., & Sommer, I. E. C. (2019). Paracingulate sulcus morphology and hallucinations in clinical and nonclinical groups. *Schizophrenia Bulletin*, *45*(4), 733–741. https://doi.org/10.1093/schbul/sby157

Gaser, C., Dahnke, R., Thompson, P. M., Kurth, F., & Luders, E. (2022). CAT-a computational anatomy toolbox for the analysis of structural MRI data. *BioRxiv*. https://doi.org/https://doi.org/10.1101/2022.06.11.495736

Gaulin, S. J. C. (1995). Does evolutionary theory predict sex differences in the brain? In *The cognitive neurosciences* (pp. 1211–1225). The MIT Press.

Geissler (Geißler), C. F., Hofmann, M. J., & Frings, C. (2020). It is more than Interference: Examining the neurohemodynamic correlates of the flanker task with functional near-infrared spectroscopy. *European Journal of Neuroscience*, *52*(3), 3022–3031. https://doi.org/10.1111/ejn.14708

Gennatas, E. D., Avants, B. B., Wolf, D. H., Satterthwaite, T. D., Ruparel, K., Ciric, R., ... & Gur, R. C. (2017). Age-related effects and sex differences in gray matter density, volume, mass, and cortical thickness from childhood to young adulthood. Journal of Neuroscience, 37(20), 5065-5073. https://doi.org/10.1523/JNEUROSCI.3550-16.2017

Gershon, R. C., Cook, K. F., Mungas, D., Manly, J. J., Slotkin, J., Beaumont, J. L., & Weintraub, S. (2014). Language Measures of the NIH Toolbox Cognition Battery. *Journal of the International Neuropsychological Society*, *20*(6), 642–651. https://doi.org/10.1017/S1355617714000411

Gershon, R. C., Slotkin, J., Manly, J. J., Blitz, D. L., Beaumont, J. L., Schnipke, D., Wallner-Allen, K., Golinkoff, R. M., Gleason, J. B., Hirsh-Pasek, K., Adams, M. J., & Weintraub, S. (2013). IV. NIH Toolbox Cognition Battery (CB): measuring language (vocabulary comprehension and reading decoding). *Monographs of the Society for Research in Child Development*, *78*(4), 49–69. https://doi.org/10.1111/mono.12034

Giedd, J. N., & Rapoport, J. L. (2010). Structural MRI of Pediatric Brain Development: What Have We Learned and Where Are We Going? *Neuron*, *67*(5), 728–734. https://doi.org/10.1016/j.neuron.2010.08.040

Giedd, J. N., Raznahan, A., Alexander-Bloch, A., Schmitt, E., Gogtay, N., & Rapoport, J. L. (2015). Child psychiatry branch of the national institute of mental health longitudinal structural magnetic resonance imaging study of human brain development. *Neuropsychopharmacology*, *40*(1), 43–49. https://doi.org/10.1038/npp.2014.236

Gilmore, J. H., Lin, W., Prastawa, M. W., Looney, C. B., Vetsa, Y. S. K., Knickmeyer, R. C., Evans, D. D., Smith, J. K., Hamer, R. M., Lieberman, J. A., & Gerig, G. (2007). Regional gray matter growth, sexual dimorphism, and cerebral asymmetry in the neonatal brain. *Journal of Neuroscience*, *27*(6), 1255–1260. https://doi.org/10.1523/JNEUROSCI.3339-06.2007

Glasser, M. F., Goyal, M. S., Preuss, T. M., Raichle, M. E., & Van Essen, D. C. (2014). Trends and properties of human cerebral cortex: Correlations with cortical myelin content. *NeuroImage*, *93*, 165–175. https://doi.org/10.1016/j.neuroimage.2013.03.060

Glasser, M. F., Sotiropoulos, S. N., Wilson, J. A., Coalson, T. S., Fischl, B., Andersson, J. L., Xu, J., Jbabdi, S., Webster, M., Polimeni, J. R., Van Essen, D. C., & Jenkinson, M. (2013). The minimal preprocessing pipelines for the Human Connectome Project. *NeuroImage*, *80*, 105–124. https://doi.org/10.1016/j.neuroimage.2013.04.127

Gobinath, A. R., Choleris, E., & Galea, L. A. M. (2017). Sex, hormones, and genotype interact to influence psychiatric disease, treatment, and behavioral research. *Journal of Neuroscience Research*, *95*(1–2), 50–64. https://doi.org/10.1002/jnr.23872

Goldman, J. G., & Manis, F. R. (2013). Relationships Among Cortical Thickness, Reading Skill, and Print Exposure in Adults. *Scientific Studies of Reading*, *17*(3), 163–176. https://doi.org/10.1080/10888438.2011.620673

Gong, G., Rosa-Neto, P., Carbonell, F., Chen, Z. J., He, Y., & Evans, A. C. (2009). Age- and gender-related differences in the cortical anatomical network. *Journal of Neuroscience*, *29*(50), 15684–15693. https://doi.org/10.1523/JNEUROSCI.2308-09.2009

Green, D. W., & Abutalebi, J. (2013). Language control in bilinguals: The adaptive control hypothesis. *Journal of Cognitive Psychology*, *25*(5), 515–530. https://doi.org/10.1080/20445911.2013.796377

Grober, E., & Sliwinski, M. (1991). Development and validation of a model for estimating premorbid verbal intelligence in the elderly. *Journal of Clinical and Experimental Neuropsychology*, *13*(6), 933–949. https://doi.org/10.1080/01688639108405109

Gupta, C. N., Turner, J. A., & Calhoun, V. D. (2019). Source-based morphometry: a decade of covarying structural brain patterns. *Brain Structure and Function*, *224*(9), 3031–3044. https://doi.org/10.1007/s00429-019-01969-8

Gur, R. C., & Gur, R. E. (2017). Complementarity of sex differences in brain and behavior: From laterality to multimodal neuroimaging. *Journal of Neuroscience Research*, *95*(1–2), 189–199. https://doi.org/10.1002/jnr.23830

Gur, R. C., Richard, J., Calkins, M. E., Chiavacci, R., Hansen, J. A., Bilker, W. B., Loughead, J., Connolly, J. J., Qiu, H., Mentch, F. D., Abou-Sleiman, P. M., Hakonarson, H., & Gur, R. E. (2012). Age group and sex differences in performance on a computerized neurocognitive battery in children age 8-21. *Neuropsychology*, *26*(2), 251–265. https://doi.org/10.1037/a0026712

Haijma, S. V., Van Haren, N., Cahn, W., Koolschijn, P. C. M. P., Hulshoff Pol, H. E., & Kahn, R. S. (2013). Brain volumes in schizophrenia: A meta-analysis in over 18 000 subjects. *Schizophrenia Bulletin*, *39*(5), 1129–1138. https://doi.org/10.1093/schbul/sbs118

Hart, S. J., Green, S. R., Casp, M., & Belger, A. (2010). Emotional priming effects during Stroop task performance. *NeuroImage*, *49*(3), 2662–2670.

https://doi.org/10.1016/j.neuroimage.2009.10.076

Haubensak, W., Attardo, A., Denk, W., & Huttner, W. B. (2004). Neurons arise in the basal neuroepithelium of the early mammalian telencephalon: A major site of neurogenesis. *Proceedings of the National Academy of Sciences of the United States of America*, *101*(9), 3196–3201. https://doi.org/10.1073/pnas.0308600100

Heilbronner, S. R., & Hayden, B. Y. (2016). Dorsal Anterior Cingulate Cortex: A Bottom-Up View. *Annual Review of Neuroscience*, *39*(April), 149–170. https://doi.org/10.1146/annurev-neuro-070815-013952

Hernández, M., Costa, A., Fuentes, L. J., Vivas, A. B., & Sebastián-Gallés, N. (2010). The impact of bilingualism on the executive control and orienting networks of attention. *Bilingualism: Language and Cognition*, *13*(3), 315–325. https://doi.org/10.1017/S1366728909990010

Herting, M. M., Maxwell, E. C., Irvine, C., & Nagel, B. J. (2012). The impact of sex, puberty, and hormones on white matter microstructure in adolescents. *Cerebral Cortex*, *22*(9), 1979–1992. https://doi.org/10.1093/cercor/bhr246

Hodge, M. R., Horton, W., Brown, T., Herrick, R., Olsen, T., Hileman, M. E., McKay, M., Archie, K. A., Cler, E., Harms, M. P., Burgess, G. C., Glasser, M. F., Elam, J. S., Curtiss, S. W., Barch, D. M., Oostenveld, R., Larson-Prior, L. J., Ugurbil, K., Van Essen, D. C., & Marcus, D. S. (2016). ConnectomeDB—Sharing human brain connectivity data. *NeuroImage*, *124*, 1102–1107. https://doi.org/10.1016/j.neuroimage.2015.04.046

Hoekzema, E., Barba-müller, E., Pozzobon, C., Picado, M., Lucco, F., García-garcía, D., Soliva, J. C., Tobeña, A., Desco, M., Crone, E. A., Ballesteros, A., Carmona, S., & Vilarroya, O. (2017). *Pregnancy leads to long-lasting changes in human brain structure*. *20*(2), 1097–1110. https://doi.org/10.1038/nn.4458

Houdé, O., Rossi, S., Lubin, A., & Joliot, M. (2010). Mapping numerical processing, reading, and executive functions in the developing brain: An fMRI meta-analysis of 52 studies including 842 children. *Developmental Science*, *13*(6), 876–885. https://doi.org/10.1111/j.1467-7687.2009.00938.x

Hu, X., Zhang, L., Liang, K., Cao, L., Liu, J., Li, H., Gao, Y., Hu, X., Hu, Y., Kuang, W., Sweeney, J. A., Gong, Q., & Huang, X. (2022). Sex-specific alterations of cortical morphometry in treatment-naïve patients with major depressive disorder. *Neuropsychopharmacology*. https://doi.org/10.1038/s41386-021-01252-7

Huang, Y., Su, L., & Ma, Q. (2020). The Stroop effect: An activation likelihood estimation meta-analysis in healthy young adults. *Neuroscience Letters*, *716*, 134683. https://doi.org/10.1016/j.neulet.2019.134683

Hung, Y., Gaillard, S. L., Yarmak, P., & Arsalidou, M. (2018). Dissociations of cognitive inhibition, response inhibition, and emotional interference: Voxelwise ALE meta-analyses of fMRI studies. *Human Brain Mapping*, *39*(10), 4065–4082. https://doi.org/10.1002/hbm.24232

Im, K., Lee, J. M., Yoon, U., Shin, Y. W., Soon, B. H., In, Y. K., Juo, S. K., & Kim, S. I. (2006). Fractal dimension in human cortical surface: Multiple regression analysis

with cortical thickness, sulcal depth, and folding area. *Human Brain Mapping*, *27*(12), 994–1003. https://doi.org/10.1002/hbm.20238

Ingalhalikar, M., Smith, A., Parker, D., Satterthwaite, T. D., Elliott, M. A., Ruparel, K., Hakonarson, H., Gur, R. E., Gur, R. C., & Verma, R. (2014). Sex differences in the structural connectome of the human brain. *Proceedings of the National Academy of Sciences of the United States of America*, *111*(2), 823–828. https://doi.org/10.1073/pnas.1316909110

Jack, C. R., Wiste, H. J., Weigand, S. D., Knopman, D. S., Vemuri, P., Mielke, M. M., Lowe, V., Senjem, M. L., Gunter, J. L., Machulda, M. M., Gregg, B. E., Pankratz, V. S., Rocca, W. A., & Petersen, R. C. (2015). Age, sex, and APOE ϵ4 effects on memory, brain structure, and β-Amyloid across the adult life Span. *JAMA Neurology*, *72*(5), 511–519. https://doi.org/10.1001/jamaneurol.2014.4821

Jahn, A., Nee, D. E., Alexander, W. H., & Brown, J. W. (2016). Distinct regions within medial prefrontal cortex process pain and cognition. *Journal of Neuroscience*, *36*(49), 12385–12392. https://doi.org/10.1523/JNEUROSCI.2180-16.2016

Jenkinson, M., Beckmann, C. F., Behrens, T. E. J., Woolrich, M. W., & Smith, S. M. (2012). Fsl. *NeuroImage*, *62*, 782–790. https://doi.org/10.1016/j.neuroimage.2011.09.015

Jeurissen, B., Tournier, J. D., Dhollander, T., Connelly, A., & Sijbers, J. (2014). Multi-tissue constrained spherical deconvolution for improved analysis of multi-shell diffusion MRI data. *NeuroImage*, *103*, 411–426. https://doi.org/10.1016/j.neuroimage.2014.07.061

Johns, C. L., Jahn, A. A., Jones, H. R., Kush, D., Molfese, P. J., Van Dyke, J. A., Magnuson, J. S., Tabor, W., Mencl, W. E., Shankweiler, D. P., & Braze, D. (2018). Individual differences in decoding skill, print exposure, and cortical structure in young adults. *Language, Cognition and Neuroscience*, *33*(10), 1275–1295. https://doi.org/10.1080/23273798.2018.1476727

Jones, D. K., Knösche, T. R., & Turner, R. (2013). White matter integrity, fiber count, and other fallacies: The do's and don'ts of diffusion MRI. *NeuroImage*, *73*, 239–254. https://doi.org/10.1016/j.neuroimage.2012.06.081

Jones, D. T., MacHulda, M. M., Vemuri, P., McDade, E. M., Zeng, G., Senjem, M. L., Gunter, J. L., Przybelski, S. A., Avula, R. T., Knopman, D. S., Boeve, B. F., Petersen, R. C., & Jack, C. R. (2011). Age-related changes in the default mode network are more advanced in Alzheimer disease. *Neurology*, *77*(16), 1524–1531. https://doi.org/10.1212/WNL.0b013e318233b33d

Kaczkurkin, A. N., Raznahan, A., & Satterthwaite, T. D. (2019). Sex differences in the developing brain: insights from multimodal neuroimaging. *Neuropsychopharmacology*, *44*(1), 71–85. https://doi.org/10.1038/s41386-018-0111-z

Kalmanti, E., & Maris, T. G. (2007). Fractal dimension as an index of brain cortical changes throughout life. *In Vivo*, *21*(4), 641–646.

Kanai, R., & Rees, G. (2011). The structural basis of inter-individual differences in

human behaviour and cognition. *Nature Reviews Neuroscience*, *12*(4), 231–242. https://doi.org/10.1038/nrn3000

Kašpárek, T., Mareček, R., Schwarz, D., Přikryl, R., Vaníček, J., Mikl, M., & Češková, E. (2010). Source-based morphometry of gray matter volume in men with first-episode schizophrenia. *Human Brain Mapping*, *31*(2), 300–310. https://doi.org/10.1002/hbm.20865

Kaufmann, L., Ischebeck, A., Weiss, E., Koppelstaetter, F., Siedentopf, C., Vogel, S. E., Gotwald, T., Marksteiner, J., & Wood, G. (2008). An fMRI study of the numerical Stroop task in individuals with and without minimal cognitive impairment. *Cortex*, *44*(9), 1248–1255. https://doi.org/10.1016/j.cortex.2007.11.009

Kaufmann, L., Koppelstaetter, F., Delazer, M., Siedentopf, C., Rhomberg, P., Golaszewski, S., Felber, S., & Ischebeck, A. (2005). Neural correlates of distance and congruity effects in a numerical Stroop task: an event-related fMRI study. *NeuroImage*, *25*(3), 888–898. https://doi.org/10.1016/j.neuroimage.2004.12.041

King, R. D., Brown, B., Hwang, M., Jeon, T., & George, A. T. (2010). Fractal dimension analysis of the cortical ribbon in mild Alzheimer's disease. *NeuroImage*, *53*(2), 471–479. https://doi.org/10.1016/j.neuroimage.2010.06.050

King, R. D., George, A. T., Jeon, T., Hynan, L. S., Youn, T. S., Kennedy, D. N., & Dickerson, B. (2009). Characterization of atrophic changes in the cerebral cortex using fractal dimensional analysis. *Brain Imaging and Behavior*, *3*(2), 154–166. https://doi.org/10.1007/s11682-008-9057-9

Knickmeyer, R. C., Xia, K., Lu, Z., Ahn, M., Jha, S. C., Zou, F., Zhu, H., Styner, M., & Gilmore, J. H. (2017). Impact of Demographic and Obstetric Factors on Infant Brain Volumes: A Population Neuroscience Study. *Cerebral Cortex*, *27*(12), 5616–5625. https://doi.org/10.1093/cercor/bhw331

Kolling, N., Behrens, T., Wittmann, M., & Rushworth, M. (2016). Multiple signals in anterior cingulate cortex. *Current Opinion in Neurobiology*, *37*, 36–43. https://doi.org/10.1016/j.conb.2015.12.007

Kong, L., Chen, K., Womer, F., Jiang, W., Luo, X., Driesen, N., Liu, J., Blumberg, H., Tang, Y., Xu, K., & Wang, F. (2013). Sex differences of gray matter morphology in cortico-limbic-striatal neural system in major depressive disorder. *Journal of Psychiatric Research*, *47*(6), 733–739. https://doi.org/10.1016/j.jpsychires.2013.02.003

Koran, M. E. I., Wagener, M., & Hohman, T. J. (2017). Sex differences in the association between AD biomarkers and cognitive decline. *Brain Imaging and Behavior*, *11*(1), 205–213. https://doi.org/10.1007/s11682-016-9523-8

Koziol, L. F., Budding, D., Andreasen, N., D'Arrigo, S., Bulgheroni, S., Imamizu, H., Ito, M., Manto, M., Marvel, C., Parker, K., Pezzulo, G., Ramnani, N., Riva, D., Schmahmann, J., Vandervert, L., & Yamazaki, T. (2014). Consensus paper: The cerebellum's role in movement and cognition. *Cerebellum*, *13*(1), 151–177. https://doi.org/10.1007/s12311-013-0511-x

Kranz, G. S., Zhang, B. B. B., Handschuh, P., Ritter, V., & Lanzenberger, R. (2020).

Gender-affirming hormone treatment – A unique approach to study the effects of sex hormones on brain structure and function. *Cortex*, *129*, 68–79. https://doi.org/10.1016/j.cortex.2020.04.005

Kristanto, D., Liu, M., Liu, X., Sommer, W., & Zhou, C. (2020). Predicting reading ability from brain anatomy and function: From areas to connections. *NeuroImage*, *218*(May). https://doi.org/10.1016/j.neuroimage.2020.116966

Kroenke, C. D., & Bayly, P. V. (2018). How forces fold the cerebral cortex. *Journal of Neuroscience*, *38*(4), 767–775. https://doi.org/10.1523/JNEUROSCI.1105-17.2017

Krogsrud, S. K., Fjell, A. M., Tamnes, C. K., Grydeland, H., Mork, L., Due-Tønnessen, P., Bjørnerud, A., Sampaio-Baptista, C., Andersson, J., Johansen-Berg, H., & Walhovd, K. B. (2016). Changes in white matter microstructure in the developing brain-A longitudinal diffusion tensor imaging study of children from 4 to 11years of age. *NeuroImage*, *124*, 473–486. https://doi.org/10.1016/j.neuroimage.2015.09.017

Labonté, B., Engmann, O., Purushothaman, I., Menard, C., Wang, J., Tan, C., Scarpa, J. R., Moy, G., Loh, Y.-H. E., Cahill, M., Lorsch, Z. S., Hamilton, P. J., Calipari, E. S., Hodes, G. E., Issler, O., Kronman, H., Pfau, M., Obradovic, A. L. J., Dong, Y., … Nestler, E. J. (2017). Sex-specific transcriptional signatures in human depression. *Nature Medicine*, *23*(9), 1102–1111. https://doi.org/10.1038/nm.4386

Le Gros Clark, W. E. (1945). *Deformation patterns in the cerebral cortex* (J. Johnson (Ed.)). Oxford University Press.

Lebel, C., Caverhill-Godkewitsch, S., & Beaulieu, C. (2010). Age-related regional variations of the corpus callosum identified by diffusion tensor tractography. *NeuroImage*, *52*(1), 20–31. https://doi.org/10.1016/j.neuroimage.2010.03.072

Lebel, C., Gee, M., Camicioli, R., Wieler, M., Martin, W., & Beaulieu, C. (2012). Diffusion tensor imaging of white matter tract evolution over the lifespan. *NeuroImage*, *60*(1), 340–352. https://doi.org/10.1016/j.neuroimage.2011.11.094

Lenroot, R. K., Blumenthal, J. D., Wallace, G. L., Clasen, L. S., Lee, N. R., & Giedd, J. N. (2014). A case-control study of brain structure and behavioral characteristics in 47,XXX syndrome. *Genes, Brain and Behavior*, *13*(8), 841–849. https://doi.org/10.1111/gbb.12180

Lenroot, Rhoshel K., Gogtay, N., Greenstein, D. K., Wells, E. M., Wallace, G. L., Clasen, L. S., Blumenthal, J. D., Lerch, J., Zijdenbos, A. P., Evans, A. C., Thompson, P. M., & Giedd, J. N. (2007). Sexual dimorphism of brain developmental trajectories during childhood and adolescence. *NeuroImage*, *36*(4), 1065–1073. https://doi.org/10.1016/j.neuroimage.2007.03.053

Leonard, C. M., Towler, S., Welcome, S., & Chiarello, C. (2009). Paracingulate asymmetry in anterior and midcingulate cortex: Sex differences and the effect of measurement technique. *Brain Structure and Function*, *213*(6), 553–569. https://doi.org/10.1007/s00429-009-0210-z

Leonard, M. K., & Chang, E. F. (2014). Dynamic speech representations in the human temporal lobe. *Trends in Cognitive Sciences*, *18*(9), 472–479. https://doi.org/10.1016/j.tics.2014.05.001

Lerma-Usabiaga, G., Carreiras, M., & Paz-Alonso, P. M. (2018). Converging evidence for functional and structural segregation within the left ventral occipitotemporal cortex in reading. *Proceedings of the National Academy of Sciences of the United States of America*, *115*(42), E9981–E9990. https://doi.org/10.1073/pnas.1803003115

Li, G., Wang, L., Shi, F., Lyall, A. E., Lin, W., Gilmore, J. H., & Shen, D. (2014). Mapping longitudinal development of local cortical gyrification in infants from birth to 2 years of age. *Journal of Neuroscience*, *34*(12), 4228–4238. https://doi.org/10.1523/JNEUROSCI.3976-13.2014

Li, R., Ma, X., Wang, G., Yang, J., & Wang, C. (2016). Why sex differences in schizophrenia? *Journal of Translational Neuroscience*, *1*(1), 37–42. http://www.ncbi.nlm.nih.gov/pubmed/29152382

Li, S., Xia, M., Pu, F., Li, D., Fan, Y., Niu, H., Pei, B., & He, Y. (2011). Age-related changes in the surface morphology of the central sulcus. *NeuroImage*, *58*(2), 381–390. https://doi.org/10.1016/j.neuroimage.2011.06.041

Li, Y.-O., Adalı, T., & Calhoun, V. D. (2007). Estimating the number of independent components for functional magnetic resonance imaging data. *Human Brain Mapping*, *28*(11), 1251–1266. https://doi.org/10.1002/hbm.20359

Liao, Z., Patel, Y., Khairullah, A., Parker, N., & Paus, T. (2021). Pubertal Testosterone and the Structure of the Cerebral Cortex in Young Men. *Cerebral Cortex (New York, N.Y. : 1991)*, *31*(6), 2812–2821. https://doi.org/10.1093/cercor/bhaa389

Liesinger, A. M., Graff-Radford, N. R., Duara, R., Carter, R. E., Hanna Al-Shaikh, F. S., Koga, S., Hinkle, K. M., DiLello, S. K., Johnson, M. K. F., Aziz, A., Ertekin-Taner, N., Ross, O. A., Dickson, D. W., & Murray, M. E. (2018). Sex and age interact to determine clinicopathologic differences in Alzheimer's disease. *Acta Neuropathologica*, *136*(6), 873–885. https://doi.org/10.1007/s00401-018-1908-x

Lindenfors, P., & Tullberg, B. S. (2011). *Evolutionary Aspects of Aggression* (pp. 7–22). https://doi.org/10.1016/B978-0-12-380858-5.00009-5

Lisofsky, N., Riediger, M., Gallinat, J., Lindenberger, U., & Kühn, S. (2016). Hormonal contraceptive use is associated with neural and affective changes in healthy young women. *NeuroImage*, *134*, 597–606. https://doi.org/10.1016/j.neuroimage.2016.04.042

Liu, S., Seidlitz, J., Blumenthal, J. D., Clasen, L. S., & Raznahan, A. (2020). Integrative structural, functional, and transcriptomic analyses of sex-biased brain organization in humans. *Proceedings of the National Academy of Sciences of the United States of America*, *117*(31), 18788–18798. https://doi.org/10.1073/pnas.1919091117

Lombardo, M. V., Ashwin, E., Auyeung, B., Chakrabarti, B., Taylor, K., Hackett, G., Bullmore, E. T., & Baron-Cohen, S. (2012). Fetal testosterone influences sexually dimorphic gray matter in the human brain. *Journal of Neuroscience*, *32*(2), 674–680. https://doi.org/10.1523/JNEUROSCI.4389-11.2012

Lotze, M., Domin, M., Gerlach, F. H., Gaser, C., Lueders, E., Schmidt, C. O., & Neumann, N. (2019). Novel findings from 2,838 Adult Brains on Sex Differences in

Gray Matter Brain Volume. *Scientific Reports*, *9*(1), 1–7. https://doi.org/10.1038/s41598-018-38239-2

Luders, E., Gaser, C., Narr, K. L., & Toga, A. W. (2009). Why sex matters: Brain size independent differences in gray matter distributions between men and women. *Journal of Neuroscience*, *29*(45), 14265–14270. https://doi.org/10.1523/JNEUROSCI.2261-09.2009

Luders, E., Narr, K. L., Thompson, P. M., Rex, D. E., Jancke, L., Steinmetz, H., & Toga, A. W. (2004). Gender differences in cortical complexity. *Nature Neuroscience*, *7*(8), 799–800. https://doi.org/10.1038/nn1277

Madan, C. R., & Kensinger, E. A. (2016). Cortical complexity as a measure of age-related brain atrophy. *NeuroImage*, *134*, 617–629. https://doi.org/10.1016/j.neuroimage.2016.04.029

Mak, L. E., Minuzzi, L., MacQueen, G., Hall, G., Kennedy, S. H., & Milev, R. (2017). The Default Mode Network in Healthy Individuals: A Systematic Review and Meta-Analysis. *Brain Connectivity*, *7*(1), 25–33. https://doi.org/10.1089/brain.2016.0438

Mandelbrot, B. (1967). How long is the coast of Britain? Statistical self-similarity and fractional dimension. *Science*, *156*(3775), 636–638. https://doi.org/10.1126/science.156.3775.636

Mangin, J. F., Jouvent, E., & Cachia, A. (2010). In-vivo measurement of cortical morphology: Means and meanings. *Current Opinion in Neurology*, *23*(4), 359–367. https://doi.org/10.1097/WCO.0b013e32833a0afc

Marchand, W. R., Lee, J. N., Thatcher, J. W., Hsu, E. W., Rashkin, E., Suchy, Y., Chelune, G., Starr, J., & Barbera, S. S. (2008). Putamen coactivation during motor task execution. *NeuroReport*, *19*(9), 957–960. https://doi.org/10.1097/WNR.0b013e328302c873

Mars, R. B., Neubert, F.-X., Noonan, M. P., Sallet, J., Toni, I., & Rushworth, M. F. S. (2012). On the relationship between the "default mode network" and the "social brain." *Frontiers in Human Neuroscience*, *6*. https://doi.org/10.3389/fnhum.2012.00189

Martin, A., Schurz, M., Kronbichler, M., & Richlan, F. (2015). Reading in the brain of children and adults: A meta-analysis of 40 functional magnetic resonance imaging studies. *Human Brain Mapping*, *36*(5), 1963–1981. https://doi.org/10.1002/hbm.22749

Matelli, M., & Umiltà, C. (2007). *Il cervello: anatomia e funzione del sistema nervoso centrale*. il Mulino.

Matsumoto, A., & Kakigi, R. (2014). Subliminal Semantic Priming Changes the Dynamic Causal Influence between the Left Frontal and Temporal Cortex. *Journal of Cognitive Neuroscience*, *26*(1), 165–174. https://doi.org/10.1162/jocn_a_00472

McCarrey, A. C., An, Y., Kitner-Triolo, M. H., Ferrucci, L., & Resnick, S. M. (2016). Sex differences in cognitive trajectories in clinically normal older adults. *Psychology and Aging*, *31*(2), 166–175. https://doi.org/10.1037/pag0000070

McCarthy, M. M., & Arnold, A. P. (2011). Reframing sexual differentiation of the

brain. *Nature Neuroscience*, *14*(6), 677–683. https://doi.org/10.1038/nn.2834

McCarthy, M. M., Nugent, B. M., & Lenz, K. M. (2017). Neuroimmunology and neuroepigenetics in the establishment of sex differences in the brain. *Nature Reviews Neuroscience*, *18*(8), 471–484. https://doi.org/10.1038/nrn.2017.61

McEwen, B. S., & Milner, T. A. (2017). Understanding the broad influence of sex hormones and sex differences in the brain. *Journal of Neuroscience Research*, *95*(1–2), 24–39. https://doi.org/10.1002/jnr.23809

Mellerio, C., Roca, P., Chassoux, F., Danière, F., Cachia, A., Lion, S., Naggara, O., Devaux, B., Meder, J. F., & Oppenheim, C. (2015). The power button sign: A newly described central sulcal pattern on surface rendering MR images of type 2 focal cortical dysplasia. *Radiology*, *274*(2), 500–507. https://doi.org/10.1148/radiol.14140773

Mielke, M. M. (2020). Consideration of Sex Differences in the Measurement and Interpretation of Alzheimer Disease-Related Biofluid-Based Biomarkers. *The Journal of Applied Laboratory Medicine*, *5*(1), 158–169. https://doi.org/10.1373/jalm.2019.030023

Miller, K. L., Alfaro-Almagro, F., Bangerter, N. K., Thomas, D. L., Yacoub, E., Xu, J., Bartsch, A. J., Jbabdi, S., Sotiropoulos, S. N., Andersson, J. L. R., Griffanti, L., Douaud, G., Okell, T. W., Weale, P., Dragonu, I., Garratt, S., Hudson, S., Collins, R., Jenkinson, M., … Smith, S. M. (2016). Multimodal population brain imaging in the UK Biobank prospective epidemiological study. *Nature Neuroscience*, *19*(11), 1523–1536. https://doi.org/10.1038/nn.4393

Mills, K. L., Goddings, A. L., Herting, M. M., Meuwese, R., Blakemore, S. J., Crone, E. A., Dahl, R. E., Güroğlu, B., Raznahan, A., Sowell, E. R., & Tamnes, C. K. (2016). Structural brain development between childhood and adulthood: Convergence across four longitudinal samples. *NeuroImage*, *141*, 273–281. https://doi.org/10.1016/j.neuroimage.2016.07.044

Miyake, A., & Friedman, N. P. (2012). The nature and organization of individual differences in executive functions: Four general conclusions. *Current Directions in Psychological Science*, *21*(1), 8–14. https://doi.org/10.1177/0963721411429458

Miyata, T., Kawaguchi, D., Kawaguchi, A., & Gotoh, Y. (2010). Mechanisms that regulate the number of neurons during mouse neocortical development. *Current Opinion in Neurobiology*, *20*(1), 22–28. https://doi.org/10.1016/j.conb.2010.01.001

Monaco, M., Costa, A., Caltagirone, C., & Carlesimo, G. A. (2013). Forward and backward span for verbal and visuo-spatial data: standardization and normative data from an Italian adult population. *Neurological Sciences*, *34*(5), 749–754. https://doi.org/10.1007/s10072-012-1130-x

Moreno-Briseño, P., Díaz, R., Campos-Romo, A., & Fernandez-Ruiz, J. (2010). Sex-related differences in motor learning and performance. *Behavioral and Brain Functions*, *6*, 2–5. https://doi.org/10.1186/1744-9081-6-74

Mountcastle, V. (1997). The columnar organization of the neocortex. *Brain*, *120*(4), 701–722. https://doi.org/10.1093/brain/120.4.701

Mustafa, N., Ahearn, T. S., Waiter, G. D., Murray, A. D., Whalley, L. J., & Staff, R. T. (2012). Brain structural complexity and life course cognitive change. *NeuroImage*, *61*(3), 694–701. https://doi.org/10.1016/j.neuroimage.2012.03.088

Narvacan, K., Treit, S., Camicioli, R., Martin, W., & Beaulieu, C. (2017). Evolution of deep gray matter volume across the human lifespan. *Human Brain Mapping*, *38*(8), 3771–3790. https://doi.org/10.1002/hbm.23604

Neufang, S., Specht, K., Hausmann, M., Güntürkün, O., Herpertz-Dahlmann, B., Fink, G. R., & Konrad, K. (2009). Sex differences and the impact of steroid hormones on the developing human brain. *Cerebral Cortex*, *19*(2), 464–473. https://doi.org/10.1093/cercor/bhn100

Nishikuni, K., & Ribas, G. C. (2013). Study of fetal and postnatal morphological development of the brain sulci: Laboratory investigation. *Journal of Neurosurgery: Pediatrics*, *11*(1), 1–11. https://doi.org/10.3171/2012.9.PEDS12122

Nowicka, A., & Tacikowski, P. (2011). Transcallosal transfer of information and functional asymmetry of the human brain. *Laterality: Asymmetries of Body, Brain and Cognition*, *16*(1), 35–74. https://doi.org/10.1080/13576500903154231

Oldfield, R. C. (1971). The assessment and analysis of handedness: The Edinburgh inventory. *Neuropsychologia*, *9*(1), 97–113. https://doi.org/10.1016/0028-3932(71)90067-4

Ono, M., Kubik, S., & Abarnathey, C. (1990). *Atlas of the cerebral sulci*. New York: Georg Thieme Publisher.

Palomero-Gallagher, N., Mohlberg, H., Zilles, K., & Vogt, B. (2008). Cytology and receptor architecture of human anterior cingulate cortex. *Journal of Comparative Neurology*, *508*(6), 906–926. https://doi.org/10.1002/cne.21684

Palomero-Gallagher, N., Vogt, B. A., Schleicher, A., Mayberg, H. S., & Zilles, K. (2009). Receptor architecture of human cingulate cortex: Evaluation of the four-region neurobiological model. *Human Brain Mapping*, *30*(8), 2336–2355. https://doi.org/10.1002/hbm.20667

Panizzon, M. S., Fennema-Notestine, C., Eyler, L. T., Jernigan, T. L., Prom-Wormley, E., Neale, M., Jacobson, K., Lyons, M. J., Grant, M. D., Franz, C. E., Xian, H., Tsuang, M., Fischl, B., Seidman, L., Dale, A., & Kremen, W. S. (2009). Distinct genetic influences on cortical surface area and cortical thickness. *Cerebral Cortex*, *19*(11), 2728–2735. https://doi.org/10.1093/cercor/bhp026

Panning, B. (2008). X-chromosome inactivation: the molecular basis of silencing. *Journal of Biology*, *7*(8), 30. https://doi.org/10.1186/jbiol95

Paus, T., Tomaiuolo, F., Otaky, N., MacDonald, D., Petrides, M., Atlas, J., Morris, R., & Evans, A. C. (1996). Human Cingulate and Paracingulate Sulci: Pattern, Variability, Asymmetry, and Probabilistic Map. *Cerebral Cortex*, *6*(2), 207–214. https://doi.org/10.1093/cercor/6.2.207

Peper, J. S., Hulshoff Pol, H. E., Crone, E. A., & van Honk, J. (2011). Sex steroids and brain structure in pubertal boys and girls: A mini-review of neuroimaging studies.

Neuroscience, *191*, 28–37. https://doi.org/10.1016/j.neuroscience.2011.02.014

Peper, Jiska S., Burke, S. M., & Wierenga, L. M. (2020). Sex differences and brain development during puberty and adolescence. In *Handbook of Clinical Neurology* (1st ed., Vol. 175). Elsevier B.V. https://doi.org/10.1016/B978-0-444-64123-6.00003-5

Perdue, M. V, Mednick, J., Pugh, K. R., & Landi, N. (2020). Gray Matter Structure Is Associated with Reading Skill in Typically Developing Young Readers. *Cerebral Cortex*, *30*(10), 5449–5459. https://doi.org/10.1093/cercor/bhaa126

Pernet, C., Andersson, J., Paulesu, E., & Demonet, J. F. (2009). When all hypotheses are right: A multifocal account of dyslexia. *Human Brain Mapping*, *30*(7), 2278–2292. https://doi.org/10.1002/hbm.20670

Pietschnig, J., Penke, L., Wicherts, J. M., Zeiler, M., & Voracek, M. (2015). Meta-analysis of associations between human brain volume and intelligence differences: How strong are they and what do they mean? *Neuroscience and Biobehavioral Reviews*, *57*, 411–432. https://doi.org/10.1016/j.neubiorev.2015.09.017

Pletzer, B., Kronbichler, M., Aichhorn, M., Bergmann, J., Ladurner, G., & Kerschbaum, H. H. (2010). Menstrual cycle and hormonal contraceptive use modulate human brain structure. *Brain Research*, *1348*, 55–62. https://doi.org/10.1016/j.brainres.2010.06.019

Poluch, S., & Juliano, S. L. (2015). Fine-tuning of neurogenesis is essential for the evolutionary expansion of the cerebral cortex. *Cerebral Cortex*, *25*(2), 346–364. https://doi.org/10.1093/cercor/bht232

Pontious, A., Kowalczyk, T., Englund, C., & Hevner, R. F. (2007). Role of intermediate progenitor cells in cerebral cortex development. *Developmental Neuroscience*, *30*(1–3), 24–32. https://doi.org/10.1159/000109848

Pratte, M. S. (2021). Eriksen flanker delta plot shapes depend on the stimulus. *Attention, Perception, & Psychophysics*, *83*(2), 685–699. https://doi.org/10.3758/s13414-020-02166-0

Preston, J. L., Frost, S. J., Mencl, W. E., Fulbright, R. K., Landi, N., Grigorenko, E., Jacobsen, L., & Pugh, K. R. (2010). Early and late talkers: School-age language, literacy and neurolinguistic differences. *Brain*, *133*(8), 2185–2195. https://doi.org/10.1093/brain/awq163

Raichle, M. E. (2015). The Brain's Default Mode Network. *Annual Review of Neuroscience*, *38*, 433–447. https://doi.org/10.1146/annurev-neuro-071013-014030

Rajapakse, J. C., Giedd, J. N., & Rapoport, J. L. (1997). Statistical approach to segmentation of single-channel cerebral MR images. *IEEE Transactions on Medical Imaging*, *16*(2), 176–186. https://doi.org/10.1109/42.563663

Rakic, P. (1972). Mode of cell migration to the superficial layers of fetal monkey neocortex. *Journal of Comparative Neurology*, *145*(1), 61–83. https://doi.org/10.1002/cne.901450105

Rakic, P. (1995). A small step for the cell, a giant leap for mankind: a hypothesis of neocortical expansion during evolution. *Trends in Neurosciences*, *18*(9), 383–388.

https://doi.org/10.1016/0166-2236(95)93934-P

Raznahan, A., & Disteche, C. M. (2021). X-chromosome regulation and sex differences in brain anatomy. *Neuroscience and Biobehavioral Reviews*, *120*(October 2020), 28–47. https://doi.org/10.1016/j.neubiorev.2020.10.024

Raznahan, A., Greenstein, D., Lee, N. R., Clasen, L. S., & Giedd, J. N. (2012). Prenatal growth in humans and postnatal brain maturation into late adolescence. *Proceedings of the National Academy of Sciences of the United States of America*, *109*(28), 11366–11371. https://doi.org/10.1073/pnas.1203350109

Raznahan, A., Lee, N. R., Greenstein, D., Wallace, G. L., Blumenthal, J. D., Clasen, L. S., & Giedd, J. N. (2016). Globally Divergent but Locally Convergent X- and Y-Chromosome Influences on Cortical Development. *Cerebral Cortex*, *26*(1), 70–79. https://doi.org/10.1093/cercor/bhu174

Raznahan, A., Shaw, P., Lalonde, F., Stockman, M., Wallace, G. L., Greenstein, D., Clasen, L., Gogtay, N., & Giedd, J. N. (2011). How does your cortex grow? *Journal of Neuroscience*, *31*(19), 7174–7177. https://doi.org/10.1523/JNEUROSCI.0054-11.2011

Raznahan, A., Shaw, P. W., Lerch, J. P., Clasen, L. S., Greenstein, D., Berman, R., Pipitone, J., Chakravarty, M. M., Giedd, J. N., Narvacan, K., Treit, S., Camicioli, R., Martin, W., & Beaulieu, C. (2014). Longitudinal four-dimensional mapping of subcortical anatomy in human development. *Human Brain Mapping*, *111*(4), 1592–1597. https://doi.org/10.1073/pnas.1316911111

Reillo, I., De Juan Romero, C., García-Cabezas, M. Á., & Borrell, V. (2011). A Role for intermediate radial glia in the tangential expansion of the mammalian cerebral cortex. *Cerebral Cortex*, *21*(7), 1674–1694. https://doi.org/10.1093/cercor/bhq238

Richlan, F., Kronbichler, M., & Wimmer, H. (2013). Structural abnormalities in the dyslexic brain: A meta-analysis of voxel-based morphometry studies. *Human Brain Mapping*, *34*(11), 3055–3065. https://doi.org/10.1002/hbm.22127

Richman, D. P., Stewart, R. M., Hutchinson, J. W., & Caviness, V. S. (1975). Mechanical model of brain convolutional development. *Science*, *189*(4196), 18–21. https://doi.org/10.1126/science.1135626

Ridderinkhof, R. K. (2002). Micro- and macro-adjustments of task set: activation and suppression in conflict tasks. *Psychological Research*, *66*(4), 312–323. https://doi.org/10.1007/s00426-002-0104-7

Ridderinkhof, R. K., Scheres, A., Oosterlaan, J., & Sergeant, J. A. (2005). Delta Plots in the Study of Individual Differences: New Tools Reveal Response Inhibition Deficits in AD/HD That Are Eliminated by Methylphenidate Treatment. *Journal of Abnormal Psychology*, *114*(2), 197–215. https://doi.org/10.1037/0021-843X.114.2.197

Ridderinkhof, R. K., van den Wildenberg, W. P. M., Wijnen, J., & Burle, B. (2004). Response Inhibition in Conflict Tasks Is Revealed in Delta Plots. In *Cognitive neuroscience of attention* (pp. 369–377). The Guilford Press.

Rijpkema, M., Everaerd, D., van der Pol, C., Franke, B., Tendolkar, I., & Fernández,

G. (2012). Normal sexual dimorphism in the human basal ganglia. *Human Brain Mapping*, *33*(5), 1246–1252. https://doi.org/10.1002/hbm.21283

Ritchie, S. J., Cox, S. R., Shen, X., Lombardo, M. V., Reus, L. M., Alloza, C., Harris, M. A., Alderson, H. L., Hunter, S., Neilson, E., Liewald, D. C. M., Auyeung, B., Whalley, H. C., Lawrie, S. M., Gale, C. R., Bastin, M. E., McIntosh, A. M., & Deary, I. J. (2018). Sex differences in the adult human brain: Evidence from 5216 UK biobank participants. *Cerebral Cortex*, *28*(8), 2959–2975. https://doi.org/10.1093/cercor/bhy109

Roell, M., Bellon, E., Polspoel, B., Declercq, M., & De Smedt, B. (2021). No Evidence for an Association Between Variability in Sulcal Pattern and Academic Achievement. *Research Square*, 1–16.

Ronan, L., & Fletcher, P. C. (2015). From genes to folds: a review of cortical gyrification theory. *Brain Structure and Function*, *220*(5), 2475–2483. https://doi.org/10.1007/s00429-014-0961-z

Ronan, L., Voets, N., Rua, C., Alexander-Bloch, A., Hough, M., Mackay, C., Crow, T. J., James, A., Giedd, J. N., & Fletcher, P. C. (2014). Differential tangential expansion as a mechanism for cortical gyrification. *Cerebral Cortex*, *24*(8), 2219–2228. https://doi.org/10.1093/cercor/bht082

Rubinow, D. R., & Schmidt, P. J. (2019). Sex differences and the neurobiology of affective disorders. *Neuropsychopharmacology*, *44*(1), 111–128. https://doi.org/10.1038/s41386-018-0148-z

Ruigrok, A. N. V., Salimi-Khorshidi, G., Lai, M. C., Baron-Cohen, S., Lombardo, M. V., Tait, R. J., & Suckling, J. (2014). A meta-analysis of sex differences in human brain structure. *Neuroscience and Biobehavioral Reviews*, *39*, 34–50. https://doi.org/10.1016/j.neubiorev.2013.12.004

Sanchis-Segura, C., Ibañez-Gual, M. V., Adrián-Ventura, J., Aguirre, N., Gómez-Cruz, Á. J., Avila, C., & Forn, C. (2019). Sex differences in gray matter volume: How many and how large are they really? *Biology of Sex Differences*, *10*(1), 1–19. https://doi.org/10.1186/s13293-019-0245-7

Sanchis-Segura, C., Ibañez-Gual, M. V., Aguirre, N., Gómez-Cruz, Á. J., & Forn, C. (2020). Effects of different intracranial volume correction methods on univariate sex differences in grey matter volume and multivariate sex prediction. *Scientific Reports*, *10*(1), 1–15. https://doi.org/10.1038/s41598-020-69361-9

Saygin, Z. M., Osher, D. E., Norton, E. S., Youssoufian, D. A., Beach, S. D., Feather, J., Gaab, N., Gabrieli, J. D. E., & Kanwisher, N. (2016). Connectivity precedes function in the development of the visual word form area. *Nature Neuroscience*, *19*(9), 1250–1255. https://doi.org/10.1038/nn.4354

Schäfer, T., & Ecker, C. (2020). fsbrain: an R package for the visualization of structural neuroimaging data. *BioRxiv*.

Schmidt, P. J., Nieman, L. K., Danaceau, M. A., Adams, L. F., & Rubinow, D. R. (1998). Differential Behavioral Effects of Gonadal Steroids in Women with and in Those without Premenstrual Syndrome. *New England Journal of Medicine*, *338*(4),

209–216. https://doi.org/10.1056/NEJM199801223380401

Schnack, H. G., Van Haren, N. E. M., Brouwer, R. M., Evans, A., Durston, S., Boomsma, D. I., Kahn, R. S., & Hulshoff Pol, H. E. (2015). Changes in thickness and surface area of the human cortex and their relationship with intelligence. *Cerebral Cortex*, *25*(6), 1608–1617. https://doi.org/10.1093/cercor/bht357

Schork, A. J., Won, H., Appadurai, V., Nudel, R., Gandal, M., Delaneau, O., Revsbech Christiansen, M., Hougaard, D. M., Bækved-Hansen, M., Bybjerg-Grauholm, J., Giørtz Pedersen, M., Agerbo, E., Bøcker Pedersen, C., Neale, B. M., Daly, M. J., Wray, N. R., Nordentoft, M., Mors, O., Børglum, A. D., … Werge, T. (2019). A genome-wide association study of shared risk across psychiatric disorders implicates gene regulation during fetal neurodevelopment. *Nature Neuroscience*, *22*(3), 353–361. https://doi.org/10.1038/s41593-018-0320-0

Segall, J. M., Allen, E. A., Jung, R. E., Erhardt, E. B., Arja, S. K., Kiehl, K., & Calhoun, V. D. (2012). Correspondence between structure and function in the human brain at rest. *Frontiers in Neuroinformatics*, *6*(MARCH), 1–17. https://doi.org/10.3389/fninf.2012.00010

Seghier, M. L., & Price, C. J. (2010). Reading aloud boosts connectivity through the putamen. *Cerebral Cortex*, *20*(3), 570–582. https://doi.org/10.1093/cercor/bhp123

Sey, N. Y. A., Hu, B., Mah, W., Fauni, H., McAfee, J. C., Rajarajan, P., Brennand, K. J., Akbarian, S., & Won, H. (2020). A computational tool (H-MAGMA) for improved prediction of brain-disorder risk genes by incorporating brain chromatin interaction profiles. *Nature Neuroscience*, *23*(4), 583–593. https://doi.org/10.1038/s41593-020-0603-0

Shah, D. S., Prados, J., Gamble, J., De Lillo, C., & Gibson, C. L. (2013). Sex differences in spatial memory using serial and search tasks. *Behavioural Brain Research*, *257*, 90–99. https://doi.org/10.1016/j.bbr.2013.09.027

Shao, Z., Roelofs, A., Martin, R. C., & Meyer, A. S. (2015). Selective inhibition and naming performance in semantic blocking, picture-word interference, and color–word Stroop tasks. *Journal of Experimental Psychology: Learning, Memory, and Cognition*, *41*(6), 1806–1820. https://doi.org/10.1037/a0039363

Sheline, Y. I., Barch, D. M., Price, J. L., Rundle, M. M., Vaishnavi, S. N., Snyder, A. Z., Mintun, M. A., Wang, S., Coalson, R. S., & Raichle, M. E. (2009). The default mode network and self-referential processes in depression. *Proceedings of the National Academy of Sciences of the United States of America*, *106*(6), 1942–1947. https://doi.org/10.1073/pnas.0812686106

Shenhav, A., Straccia, M. A., Cohen, J. D., & Botvinick, M. M. (2014). Anterior cingulate engagement in a foraging context reflects choice difficulty, not foraging value. *Nature Neuroscience*, *17*(9), 1249–1254. https://doi.org/10.1038/nn.3771

Shim, G., Jung, W. H., Choi, J. S., Jung, M. H., Jang, J. H., Park, J. Y., ... & Kwon, J. S. (2009). Reduced cortical folding of the anterior cingulate cortex in obsessive–compulsive disorder. Journal of Psychiatry and Neuroscience, 34(6), 443-449.

Silverman, I., Choi, J., & Peters, M. (2007). The Hunter-Gatherer Theory of Sex

Differences in Spatial Abilities: Data from 40 Countries. *Archives of Sexual Behavior*, *36*(2), 261–268. https://doi.org/10.1007/s10508-006-9168-6

Skakkebæk, A., Gravholt, C. H., Rasmussen, P. M., Bojesen, A., Jensen, J. S., Fedder, J., Laurberg, P., Hertz, J. M., Stergaard, J. R., Pedersen, A. D., & Wallentin, M. (2014). Neuroanatomical correlates of Klinefelter syndrome studied in relation to the neuropsychological profile. *NeuroImage: Clinical*, *4*, 1–9. https://doi.org/10.1016/j.nicl.2013.10.013

Skeide, M. A., & Friederici, A. D. (2016). The ontogeny of the cortical language network. *Nature Reviews Neuroscience*, *17*(5), 323–332. https://doi.org/10.1038/nrn.2016.23

Smaers, J. B., Gómez-Robles, A., Parks, A. N., & Sherwood, C. C. (2017). Exceptional Evolutionary Expansion of Prefrontal Cortex in Great Apes and Humans. *Current Biology*, *27*(5), 714–720. https://doi.org/10.1016/j.cub.2017.01.020

Smith, R. E., Tournier, J. D., Calamante, F., & Connelly, A. (2012). Anatomically-constrained tractography: Improved diffusion MRI streamlines tractography through effective use of anatomical information. *NeuroImage*, *62*(3), 1924–1938. https://doi.org/10.1016/j.neuroimage.2012.06.005

Smith, R. E., Tournier, J. D., Calamante, F., & Connelly, A. (2015). SIFT2: Enabling dense quantitative assessment of brain white matter connectivity using streamlines tractography. *NeuroImage*, *119*, 338–351. https://doi.org/10.1016/j.neuroimage.2015.06.092

Smith, S. M., Jenkinson, M., Woolrich, M. W., Beckmann, C. F., Behrens, T. E. J., Johansen-Berg, H., Bannister, P. R., De Luca, M., Drobnjak, I., Flitney, D. E., Niazy, R. K., Saunders, J., Vickers, J., Zhang, Y., De Stefano, N., Brady, J. M., & Matthews, P. M. (2004). Advances in functional and structural MR image analysis and implementation as FSL. *NeuroImage*, *23*, S208–S219. https://doi.org/10.1016/j.neuroimage.2004.07.051

Soares, J. M., Marques, P., Alves, V., & Sousa, N. (2013). A hitchhiker's guide to diffusion tensor imaging. *Frontiers in Neuroscience*, *7*(7 MAR), 1–14. https://doi.org/10.3389/fnins.2013.00031

Sotiropoulos, S. N., Jbabdi, S., Xu, J., Andersson, J. L., Moeller, S., Auerbach, E. J., Glasser, M. F., Hernandez, M., Sapiro, G., Jenkinson, M., Feinberg, D. A., Yacoub, E., Lenglet, C., Van Essen, D. C., Ugurbil, K., & Behrens, T. E. J. (2013). Advances in diffusion MRI acquisition and processing in the Human Connectome Project. *NeuroImage*, *80*, 125–143. https://doi.org/10.1016/j.neuroimage.2013.05.057

Sowell, E. R., Peterson, B. S., Kan, E., Woods, R. P., Yoshii, J., Bansal, R., Xu, D., Zhu, H., Thompson, P. M., & Toga, A. W. (2007). Sex differences in cortical thickness mapped in 176 healthy individuals between 7 and 87 years of age. *Cerebral Cortex*, *17*(7), 1550–1560. https://doi.org/10.1093/cercor/bhl066

Stevens, F. L., Hurley, R. A., & Taber, K. H. (2011). Anterior cingulate cortex: Unique role in cognition and emotion. *Journal of Neuropsychiatry and Clinical Neurosciences*, *23*(2), 121–125. https://doi.org/10.1176/jnp.23.2.jnp121

Stiles, J., & Jernigan, T. L. (2010). The basics of brain development. *Neuropsychology Review*, *20*(4), 327–348. https://doi.org/10.1007/s11065-010-9148-4

Stroop, J. R. (1935). Studies of interference in serial verbal reactions. *Journal of Experimental Psychology*, *18*(6), 643–662. https://doi.org/10.1037/h0054651

Takeuchi, H., Taki, Y., Sassa, Y., Hashizume, H., Sekiguchi, A., Nagase, T., Nouchi, R., Fukushima, A., & Kawashima, R. (2012). Regional gray and white matter volume associated with stroop interference: Evidence from voxel-based morphometry. *NeuroImage*, *59*(3), 2899–2907. https://doi.org/10.1016/j.neuroimage.2011.09.064

Tamnes, C. K., Walhovd, K. B., Dale, A. M., Østby, Y., Grydeland, H., Richardson, G., Westlye, L. T., Roddey, J. C., Hagler, D. J., Due-Tønnessen, P., Holland, D., & Fjell, A. M. (2013). Brain development and aging: Overlapping and unique patterns of change. *NeuroImage*, *68*, 63–74. https://doi.org/10.1016/j.neuroimage.2012.11.039

Tettamanti, M., Moro, A., Messa, C., Moresco, R. M., Rizzo, G., Carpinelli, A., Matarrese, M., Fazio, F., & Perani, D. (2005). Basal ganglia and language: Phonology modulates dopaminergic release. *NeuroReport*, *16*(4), 397–401. https://doi.org/10.1097/00001756-200503150-00018

Tieges, Z., Snel, J., Kok, A., & Richard Ridderinkhof, K. (2009). Caffeine does not modulate inhibitory control. *Brain and Cognition*, *69*(2), 316–327. https://doi.org/10.1016/j.bandc.2008.08.001

Tissier, C., Linzarini, A., Allaire-Duquette, G., Mevel, K., Poirel, N., Dollfus, S., Etard, O., Orliac, F., Peyrin, C., Charron, S., Raznahan, A., Houdé, O., Borst, G., & Cachia, A. (2018). Sulcal polymorphisms of the IFC and ACC contribute to inhibitory control variability in children and adults. *ENeuro*, *5*(1). https://doi.org/10.1523/ENEURO.0197-17.2018

Toga, A. W., & Thompson, P. M. (2003). Mapping brain asymmetry. *Nature Reviews Neuroscience*, *4*(1), 37–48. https://doi.org/10.1038/nrn1009

Tohka, J., Zijdenbos, A., & Evans, A. (2004). Fast and robust parameter estimation for statistical partial volume models in brain MRI. *NeuroImage*, *23*(1), 84–97. https://doi.org/10.1016/j.neuroimage.2004.05.007

Toro, R., & Burnod, Y. (2005). A morphogenetic model for the development of cortical convolutions. *Cerebral Cortex*, *15*(12), 1900–1913. https://doi.org/10.1093/cercor/bhi068

Toro, R., Perron, M., Pike, B., Richer, L., Veillette, S., Pausova, Z., & Paus, T. (2008). Brain size and folding of the human cerebral cortex. *Cerebral Cortex*, *18*(10), 2352–2357. https://doi.org/10.1093/cercor/bhm261

Torre, G. A., & Eden, G. F. (2019). Relationships between gray matter volume and reading ability in typically developing children, adolescents, and young adults. *Developmental Cognitive Neuroscience*, *36*(August 2018), 100636. https://doi.org/10.1016/j.dcn.2019.100636

Torre, G. A., Matejko, A. A., & Eden, G. F. (2020). The relationship between brain structure and proficiency in reading and mathematics in children, adolescents, and

emerging adults. *Developmental Cognitive Neuroscience*, *45*. https://doi.org/10.1016/j.dcn.2020.100856

Tournier, J. D., Calamante, F., & Connelly, A. (2010). Improved probabilistic streamlines tractography by 2nd order integration over fibre orientation distributions. *Proceedings of the International Society for Magnetic Resonance in Medicine*, *1670*.

Tournier, J. D., Smith, R., Raffelt, D., Tabbara, R., Dhollander, T., Pietsch, M., Christiaens, D., Jeurissen, B., Yeh, C. H., & Connelly, A. (2019). MRtrix3: A fast, flexible and open software framework for medical image processing and visualisation. *NeuroImage*, *202*(January), 116137. https://doi.org/10.1016/j.neuroimage.2019.116137

Unsworth, N., & Spillers, G. J. (2010). Working memory capacity: Attention control, secondary memory, or both? A direct test of the dual-component model. *Journal of Memory and Language*, *62*(4), 392–406. https://doi.org/10.1016/j.jml.2010.02.001

Unsworth, N., Spillers, G. J., & Brewer, G. A. (2009). Examining the relations among working memory capacity, attention control, and fluid intelligence from a dual-component framework. *Psychological Test and Assessment Modeling*, *51*(4), 388.

van den Wildenberg, W. P. M., Wylie, S. A., Forstmann, B. U., Burle, B., Hasbroucq, T., & Ridderinkhof, K. R. (2010). To Head or to Heed? Beyond the Surface of Selective Action Inhibition: A Review. *Frontiers in Human Neuroscience*, *4*. https://doi.org/10.3389/fnhum.2010.00222

Van der Elst, W., Van Boxtel, M. P. J., Van Breukelen, G. J. P., & Jolles, J. (2006). The Stroop Color-Word Test. *Assessment*, *13*(1), 62–79. https://doi.org/10.1177/1073191105283427

Van Essen, D. C. (1997). A tension-based theory of morphogenesis and compact wiring in the central nervous system. *Nature*, *385*(6614), 313–318. https://doi.org/10.1038/385313a0

Van Essen, D. C., Donahue, C. J., Coalson, T. S., Kennedy, H., Hayashi, T., & Glasser, M. F. (2019). Cerebral cortical folding, parcellation, and connectivity in humans, nonhuman primates, and mice. *Proceedings of the National Academy of Sciences of the United States of America*, *116*(52), 26173–26180. https://doi.org/10.1073/pnas.1902299116

Van Essen, D. C., Smith, S. M., Barch, D. M., Behrens, T. E. J., Yacoub, E., & Ugurbil, K. (2013). The WU-Minn Human Connectome Project: An overview. *NeuroImage*, *80*, 62–79. https://doi.org/10.1016/j.neuroimage.2013.05.041

Vanston, J. E., & Strother, L. (2017). Sex differences in the human visual system. *Journal of Neuroscience Research*, *95*(1–2), 617–625. https://doi.org/10.1002/jnr.23895

Vogt, B. A., & Gabriel, M. (Eds.). (1993). *Neurobiology of Cingulate Cortex and Limbic Thalamus*. Birkhäuser Boston. https://doi.org/10.1007/978-1-4899-6704-6

Vogt, B. A., Nimchinsky, E. A., Vogt, L. J., & Hof, P. R. (1995). Human cingulate cortex: Surface features, flat maps, and cytoarchitecture. *Journal of Comparative*

Neurology, *359*(3), 490–506. https://doi.org/10.1002/cne.903590310

Vogt, B. A., Vogt, L., Farber, N. B., & Bush, G. (2005). Architecture and neurocytology of monkey cingulate gyrus. *Journal of Comparative Neurology*, *485*(3), 218–239. https://doi.org/10.1002/cne.20512

Voorhies, W. I., Miller, J. A., Yao, J. K., Bunge, S. A., & Weiner, K. S. (2021). Cognitive insights from tertiary sulci in prefrontal cortex. *Nature Communications*, *12*(1), 1–14. https://doi.org/10.1038/s41467-021-25162-w

Votinov, M., Goerlich, K. S., Puiu, A. A., Smith, E., Nickl-Jockschat, T., Derntl, B., & Habel, U. (2021). Brain structure changes associated with sexual orientation. *Scientific Reports*, *11*(1), 5078. https://doi.org/10.1038/s41598-021-84496-z

Vuoksimaa, E., Panizzon, M. S., Chen, C. H., Fiecas, M., Eyler, L. T., Fennema-Notestine, C., Hagler, D. J., Fischl, B., Franz, C. E., Jak, A., Lyons, M. J., Neale, M. C., Rinker, D. A., Thompson, W. K., Tsuang, M. T., Dale, A. M., & Kremen, W. S. (2015). The Genetic Association between Neocortical Volume and General Cognitive Ability Is Driven by Global Surface Area Rather Than Thickness. *Cerebral Cortex*, *25*(8), 2127–2137. https://doi.org/10.1093/cercor/bhu018

Weber, D., Skirbekk, V., Freund, I., & Herlitz, A. (2014). The changing face of cognitive gender differences in Europe. *Proceedings of the National Academy of Sciences of the United States of America*, *111*(32), 11673–11678. https://doi.org/10.1073/pnas.1319538111

Welker, W. (1990). *Why Does Cerebral Cortex Fissure and Fold?* (pp. 3–136). https://doi.org/10.1007/978-1-4615-3824-0_1

Westlye, L. T., Grydeland, H., Walhovd, K. B., & Fjell, A. M. (2011). Associations between regional cortical thickness and attentional networks as measured by the attention network test. *Cerebral Cortex*, *21*(2), 345–356. https://doi.org/10.1093/cercor/bhq101

Wierenga, L. M., Doucet, G. E., Dima, D., Agartz, I., Aghajani, M., Akudjedu, T. N., Albajes-Eizagirre, A., Alnæs, D., Alpert, K. I., Andreassen, O. A., Anticevic, A., Asherson, P., Banaschewski, T., Bargallo, N., Baumeister, S., Baur-Streubel, R., Bertolino, A., Bonvino, A., Boomsma, D. I., … Tamnes, C. K. (2020). Greater male than female variability in regional brain structure across the lifespan. *Human Brain Mapping*, *June 2020*, 470–499. https://doi.org/10.1002/hbm.25204

Wierenga, L. M., Langen, M., Oranje, B., & Durston, S. (2014). Unique developmental trajectories of cortical thickness and surface area. *NeuroImage*, *87*, 120–126. https://doi.org/10.1016/j.neuroimage.2013.11.010

Wierenga, L. M., Sexton, J. A., Laake, P., Giedd, J. N., & Tamnes, C. K. (2018). A key characteristic of sex differences in the developing brain: Greater variability in brain structure of boys than girls. *Cerebral Cortex*, *28*(8), 2741–2751. https://doi.org/10.1093/cercor/bhx154

Williams, C. M., Peyre, H., Toro, R., & Ramus, F. (2021a). Neuroanatomical norms in the UK Biobank: The impact of allometric scaling, sex, and age. *Human Brain Mapping*, *42*(14), 4623–4642. https://doi.org/10.1002/hbm.25572

Williams, C. M., Peyre, H., Toro, R., & Ramus, F. (2021b). Sex differences in the brain are not reduced to differences in body size. *Neuroscience and Biobehavioral Reviews*, *130*(September), 509–511. https://doi.org/10.1016/j.neubiorev.2021.09.015

Windes, J. D. (1968). Reaction time for numerical coding and naming of numerals. *Journal of Experimental Psychology*, *78*(2, Pt.1), 318–322. https://doi.org/10.1037/h0026289

Winkler, A. M., Kochunov, P., Blangero, J., Almasy, L., Zilles, K., Fox, P. T., Duggirala, R., & Glahn, D. C. (2010). Cortical thickness or grey matter volume? The importance of selecting the phenotype for imaging genetics studies. *NeuroImage*, *53*(3), 1135–1146. https://doi.org/10.1016/j.neuroimage.2009.12.028

Xu, G., Knutsen, A. K., Dikranian, K., Kroenke, C. D., Bayly, P. V., & Taber, L. A. (2010). Axons pull on the brain, but tension does not drive cortical folding. *Journal of Biomechanical Engineering*, *132*(7), 1–8. https://doi.org/10.1115/1.4001683

Xu, L., Groth, K. M., Pearlson, G., Schretlen, D. J., & Calhoun, V. D. (2009). Source-based morphometry: The use of independent component analysis to identify gray matter differences with application to schizophrenia. *Human Brain Mapping*, *30*(3), 711–724. https://doi.org/10.1002/hbm.20540

Yan, C., Gong, G., Wang, J., Wang, D., Liu, D., Zhu, C., Chen, Z. J., Evans, A., Zang, Y., & He, Y. (2011). Sex- and brain size-related small-world structural cortical networks in young adults: A DTI tractography study. *Cerebral Cortex*, *21*(2), 449–458. https://doi.org/10.1093/cercor/bhq111

Yan, H., Zuo, X.-N., Wang, D., Wang, J., Zhu, C., Milham, M. P., Zhang, D., & Zang, Y. (2009). Hemispheric asymmetry in cognitive division of anterior cingulate cortex: A resting-state functional connectivity study. *NeuroImage*, *47*(4), 1579–1589. https://doi.org/10.1016/j.neuroimage.2009.05.080

Yeatman, J. D., Dougherty, R. F., Ben-Shachar, M., & Wandell, B. A. (2012). Development of white matter and reading skills. *Proceedings of the National Academy of Sciences of the United States of America*, *109*(44). https://doi.org/10.1073/pnas.1206792109

Yeatman, J. D., Rauschecker, A. M., & Wandell, B. A. (2013). Anatomy of the visual word form area: Adjacent cortical circuits and long-range white matter connections. *Brain and Language*, *125*(2), 146–155. https://doi.org/10.1016/j.bandl.2012.04.010

Yeatman, J. D., Weiner, K. S., Pestilli, F., Rokem, A., Mezer, A., & Well, B. A. (2014). The vertical occipital fasciculus: A century of controversy resolved by in vivo measurements. *Proceedings of the National Academy of Sciences of the United States of America*, *111*(48), E5214–E5223. https://doi.org/10.1073/pnas.1418503111

Yotter, R. A., Nenadic, I., Ziegler, G., Thompson, P. M., & Gaser, C. (2011). Local cortical surface complexity maps from spherical harmonic reconstructions. *NeuroImage*, *56*(3), 961–973. https://doi.org/10.1016/j.neuroimage.2011.02.007

Ypma, R. J. F., Moseley, R. L., Holt, R. J., Rughooputh, N., Floris, D. L., Chura, L. R., Spencer, M. D., Baron-Cohen, S., Suckling, J., Bullmore, E. T., & Rubinov, M. (2016). Default Mode Hypoconnectivity Underlies a Sex-Related Autism Spectrum.

Biological Psychiatry: Cognitive Neuroscience and Neuroimaging, *1*(4), 364–371. https://doi.org/10.1016/j.bpsc.2016.04.006

Yücel, M., Stuart, G. W., Maruff, P., Velakoulis, D., Crowe, S. F., Savage, G., & Pantelis, C. (2001). Hemispheric and gender-related differences in the gross morphology of the anterior cingulate/paracingulate cortex in normal volunteers: An MRI morphometric study. *Cerebral Cortex*, *11*(1), 17–25. https://doi.org/10.1093/cercor/11.1.17

Yücel, M., Stuart, G. W., Maruff, P., Wood, S. J., Savage, G. R., Smith, D. J., Crowe, S. F., Copolov, D. L., Velakoulis, D., & Pantelis, C. (2002). Paracingulate morphologic differences in males with established schizophrenia: A magnetic resonance imaging morphometric study. *Biological Psychiatry*, *52*(1), 15–23. https://doi.org/10.1016/S0006-3223(02)01312-4

Zalesky, A., Fornito, A., & Bullmore, E. T. (2010). Network-based statistic: Identifying differences in brain networks. *NeuroImage*, *53*(4), 1197–1207. https://doi.org/10.1016/j.neuroimage.2010.06.041

Zhang, F. F., Peng, W., Sweeney, J. A., Jia, Z. Y., & Gong, Q. Y. (2018). Brain structure alterations in depression: Psychoradiological evidence. *CNS Neuroscience and Therapeutics*, *24*(11), 994–1003. https://doi.org/10.1111/cns.12835

Zhang, R., Geng, X., & Lee, T. M. C. (2017). Large-scale functional neural network correlates of response inhibition: an fMRI meta-analysis. *Brain Structure and Function*, *222*(9), 3973–3990. https://doi.org/10.1007/s00429-017-1443-x

7. Appendices

7.1 Experiment 2

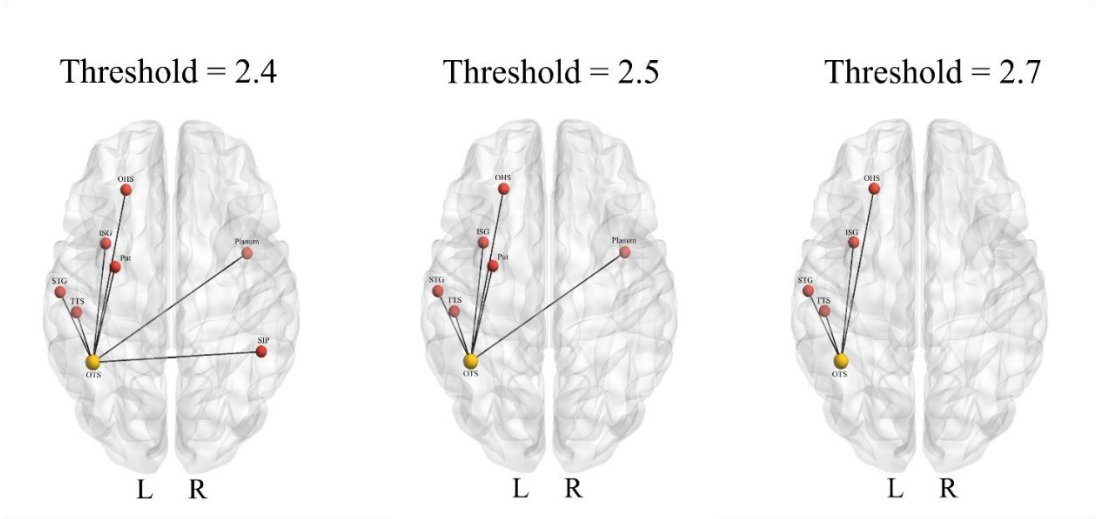

Appendices; Experiment 2; Figure S1. Reading-related networks observed at thresholds 2.4, 2.5 and 2.7 (p-FWE < 0.05). *Anatomical labels from the Destrieux Atlas (Destrieux et al., 2010) were adopted. OTS = occipitotemporal sulcus; STG = superior temporal gyrus; TTS = temporal transverse sulcus; Put = putamen; ISG = insular short gyrus; OHS = orbital H-shaped sulcus; L = left hemisphere; SIP = sulcus intermedius primus; Planum = planum polare; R = right hemisphere; L = left hemisphere; R = right hemisphere. The figure is adapted with permission from Del Mauro, Del Maschio et al. (2022).*

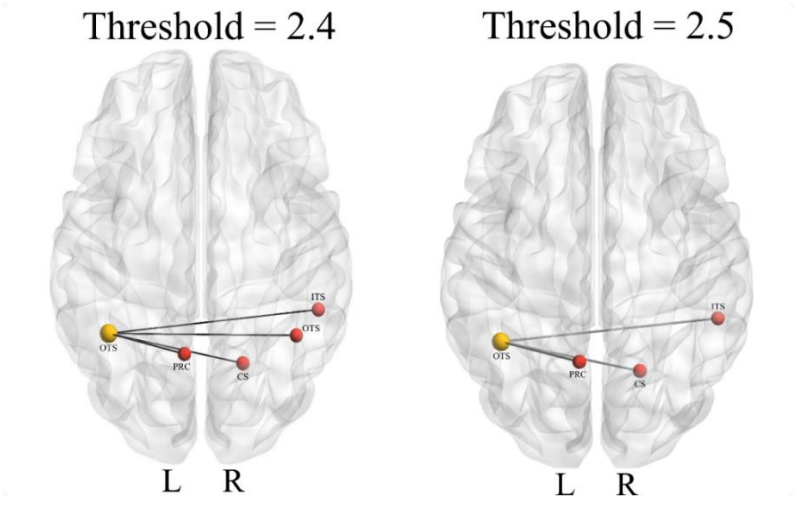

Appendices; Experiment 2; Figure S2. Network associated with posterior occipitotemporal sulcus (OTS) interruption at thresholds 2.4 and 2.5 (p-FWE < 0.05). *Anatomical labels from the Destrieux Atlas (Destrieux et al., 2010) were adopted. OTS = occipitotemporal sulcus; PRC = precuneus; CS = Calcarine sulcus; ITS = inferior temporal sulcus; L = left hemisphere; R = right hemisphere. The figure is adapted with permission from Del Mauro, Del Maschio et al. (2022).*

7.2 Experiment 3

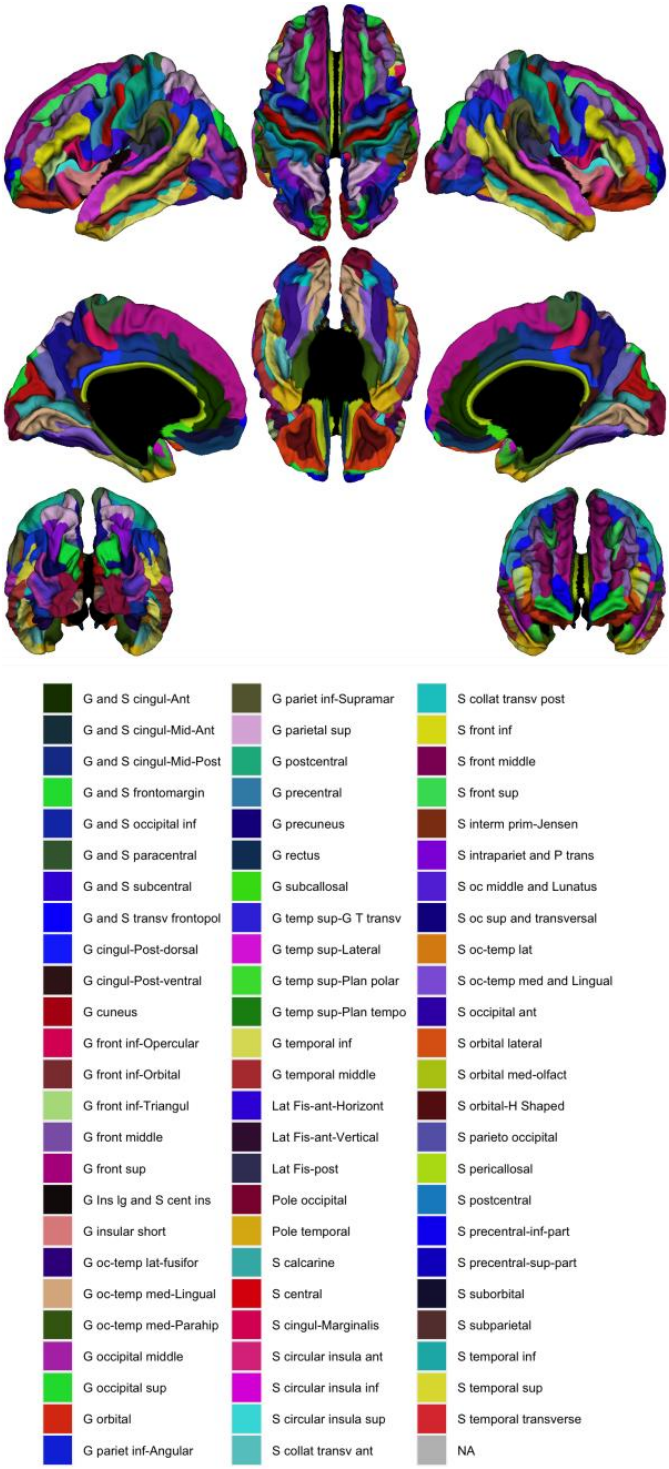

Appendices; Experiment 3; Figure S1. *Destrieux atlas (Destrieux et al., 2010). The figure is adapted with permission from Del Mauro, Del Maschio, Sulpizio, et al. (2022).*

Frontal components

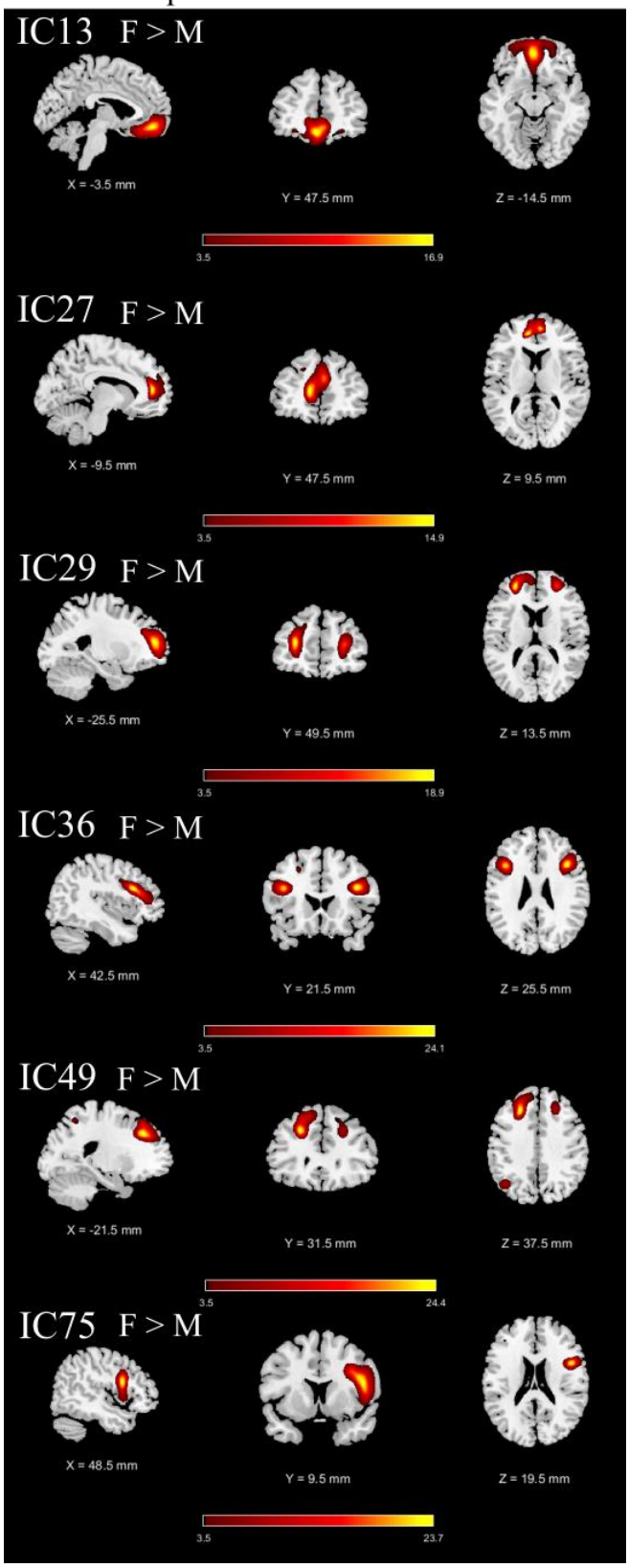

Appendices; Experiment 3; Figure S2. ICs grouped as frontal components. *All frontal components showed larger gray matter volume (GMV) in females. Colormap is based on Z-score thresholded at $|Z \geq 3.5|$. The figure is adapted with permission from Del Mauro, Del Maschio, Sulpizio, et al. (2022).*

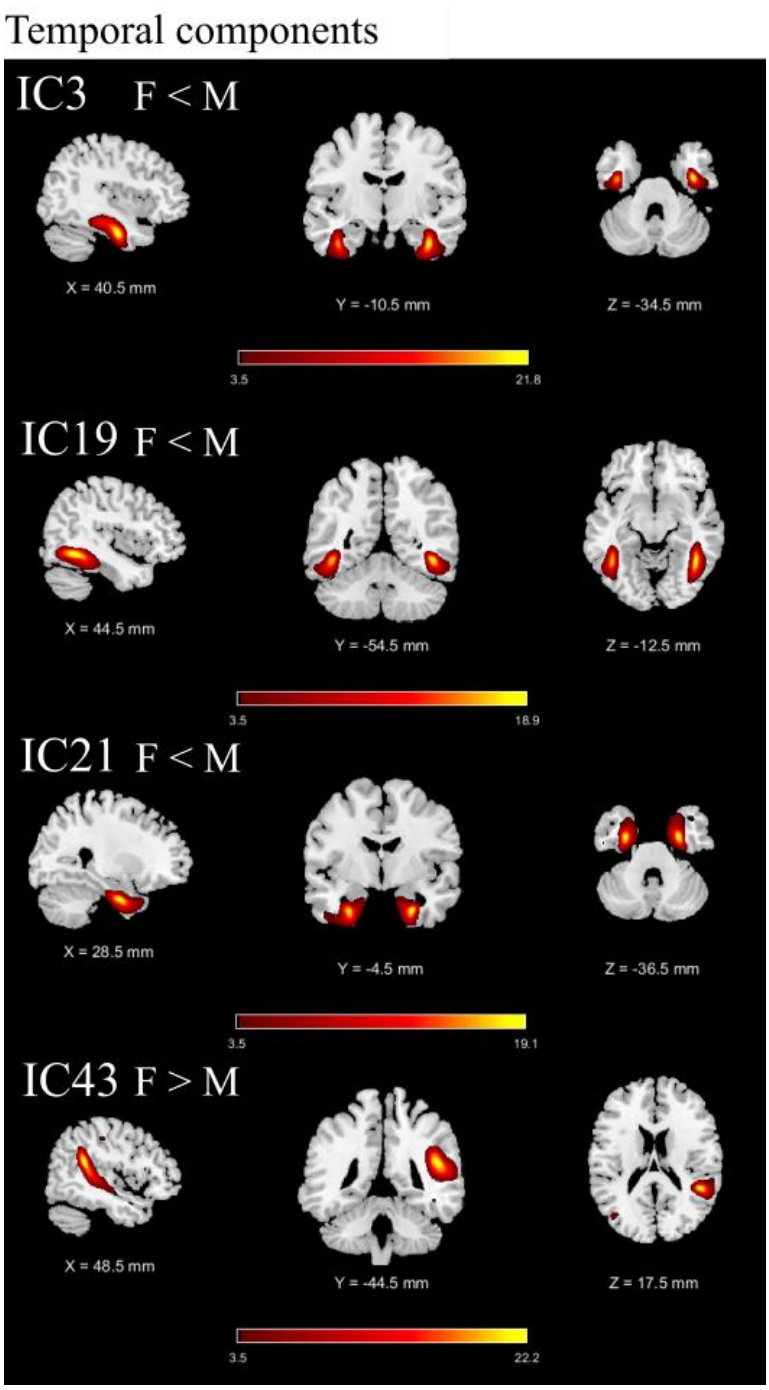

Appendices; Experiment 3; Figure S3. ICs grouped as temporal and parahippocampal components. *Males showed larger gray matter volume (GMV) in IC3, IC19 and IC21, while females showed larger GMV in the IC43. Colormap is based on Z-score thresholded at |Z ≥ 3.5|. The figure is adapted with permission from Del Mauro, Del Maschio, Sulpizio, et al. (2022).*

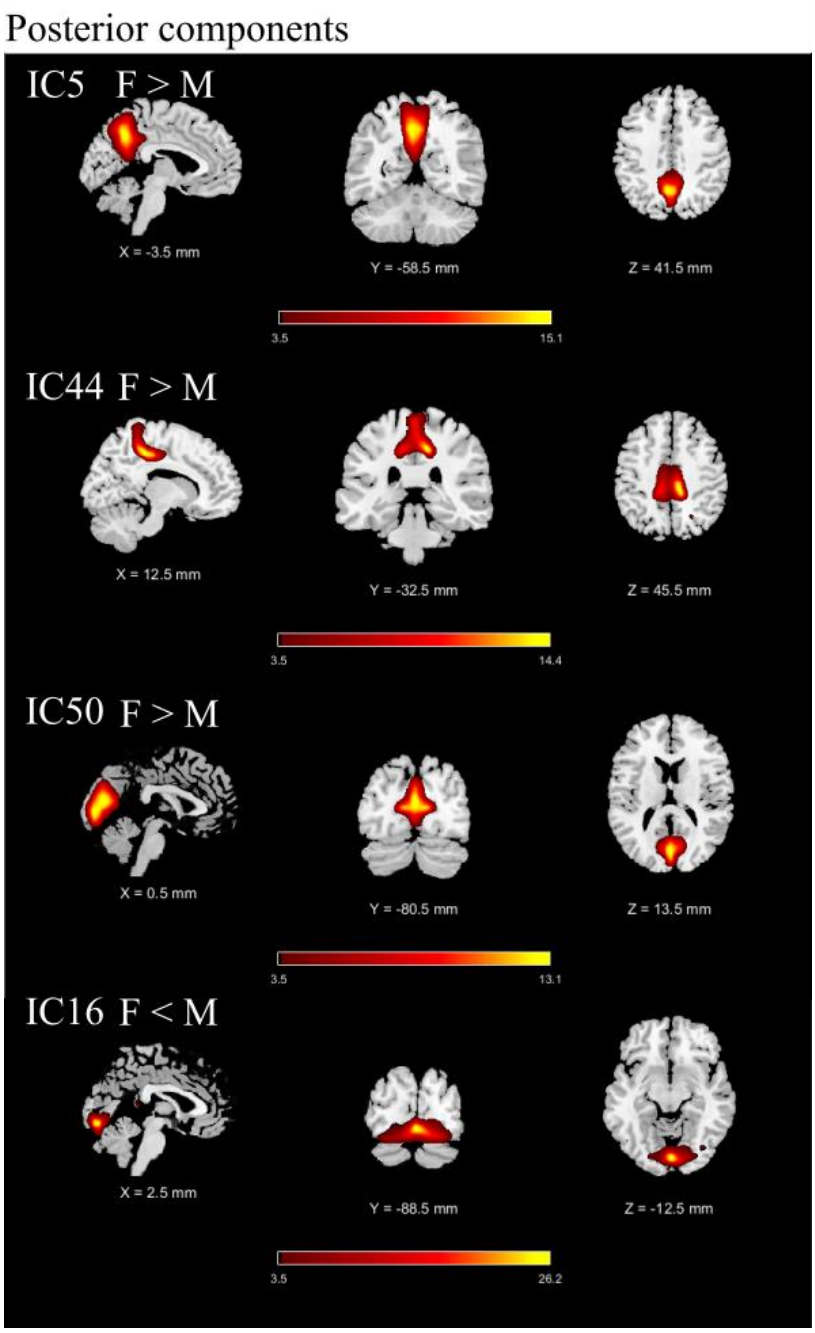

Appendices; Experiment 3; Figure S4. ICs grouped as posterior components. *Females showed larger gray matter volume (GMV) in IC5, IC44 and IC50, while males showed larger GMV in the IC16. Colormap is based on Z-score thresholded at $|Z \geq 3.5|$. The figure is adapted with permission from Del Mauro, Del Maschio, Sulpizio, et al. (2022).*

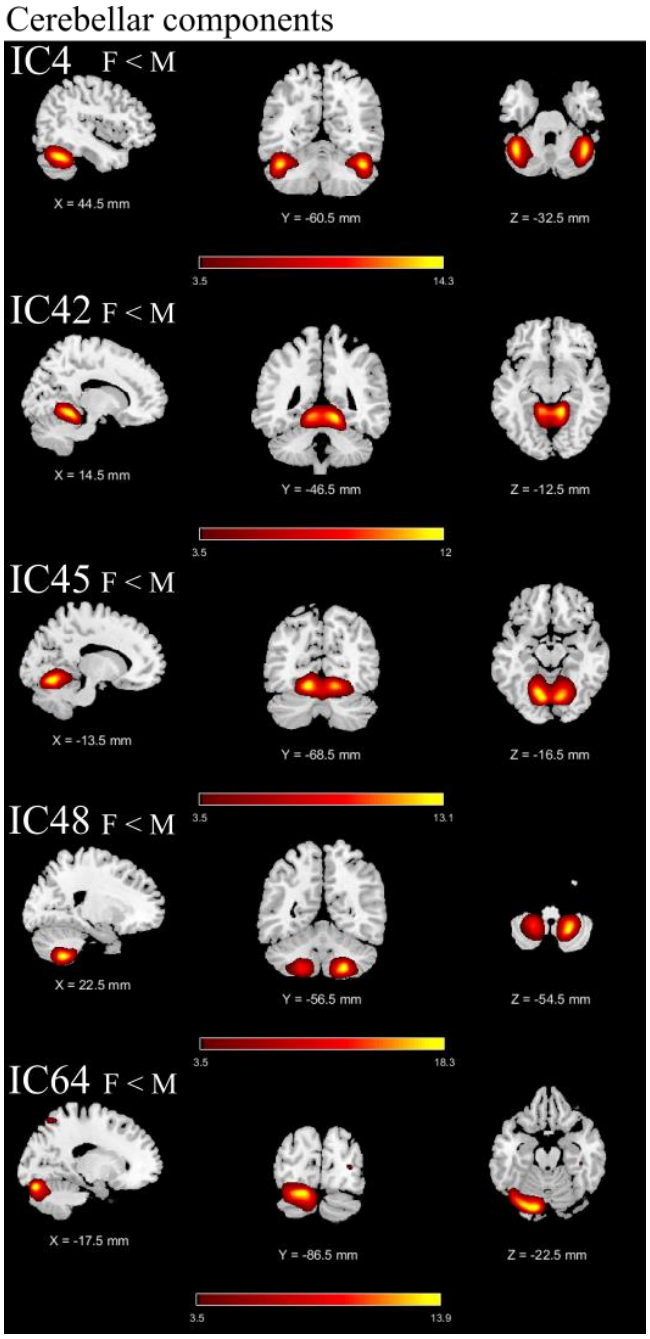

Appendices; Experiment 3; Figure S5. ICs grouped as cerebellar components. *All the componentss showed larger gray matter volume (GMV) in males. Colormap is based on Z-score thresholded at $|Z \geq 3.5|$. The figure is adapted with permission from Del Mauro, Del Maschio, Sulpizio, et al. (2022).*

ROIs	Hemisphere	p-FDR	T-value	Cohen's *d*
Long insular gyrus and central insular sulcus	L	0.01069	-3.2991	-0.2297198
Short insular gyri	L	<0.001	-6.3562	-0.442589
Superior parietal lobule (lateral part of P1)	L	<0.001	4.471	0.31132048
Straight gyrus (gyrus rectus)	L	0.02298	-3.0346	-0.2113024
Horizontal ramus of the anterior segment of the lateral sulcus (or fissure)	L	0.03479	-2.8457	-0.1981491
Occipital pole	L	0.00722	-3.4753	-0.2419888
Superior frontal sulcus	L	0.02807	2.9541	0.20569712
Intraparietal sulcus (interparietal sulcus) and transverse parietal sulci	L	0.0076	3.4377	0.2393707
Superior occipital sulcus and transverse occipital sulcus	L	<0.001	4.1959	0.29216497
Medial orbital sulcus (olfactory sulcus)	L	<0.001	-4.3834	-0.3052208
Transverse temporal sulcus	L	0.00323	3.7706	0.26255088
Subcentral gyrus (central operculum) and sulci	R	0.00657	-3.5267	-0.2455679
Long insular gyrus and central insular sulcus	R	<0.001	-4.5086	-0.3139386
Short insular gyri	R	<0.001	-5.8665	-0.4084906
Lateral occipito-temporal gyrus (fusiform gyrus, O4-T4)	R	0.03479	-2.8345	-0.1973692
Superior parietal lobule (lateral part of P1)	R	0.00339	3.7279	0.25957764
Postcentral gyrus	R	0.01717	3.1416	0.21875295
Occipital pole	R	<0.001	-4.4445	-0.3094753
Superior frontal sulcus	R	0.03886	2.7827	0.19376236
Lateral occipito-temporal sulcus	R	0.00923	-3.3616	-0.2340718
Medial orbital sulcus (olfactory sulcus)	R	0.03479	-2.8651	-0.1995

Appendices; Experiment 3; Table S1. Sex differences across regional values of gray matter volume corrected for total brain volume. *Only regions significantly different between sexes are reported. Regions of interest (ROIs), hemisphere, corrected p-values (p-FDR), t-values and effect sizes (Cohen's d) are reported. Notes that negative t-values and effect sizes indicate higher regional values in males.*

ROIs	Hemisphere	p-FDR	T-value	Cohen's *d*
Superior parietal lobule (lateral part of P1)	L	0.01896	3.3332	0.232094
Occipital pole	L	0.00712	-3.7457	-0.26082
Superior segment of the circular sulcus of the insula	L	0.01019	-3.5945	-0.25029
Intraparietal sulcus (interparietal sulcus) and transverse parietal sulci	L	0.04677	2.9604	0.206136
Superior occipital sulcus and transverse occipital sulcus	L	0.00173	4.4099	0.307066
Short insular gyri	R	0.00678	-3.8309	-0.26675
Superior parietal lobule (lateral part of P1)	R	0.02638	3.1838	0.221691
Occipital pole	R	0.00324	-4.1088	-0.2861
Superior segment of the circular sulcus of the insula	R	0.01642	-3.4164	-0.23789
Lateral occipito-temporal sulcus	R	0.02638	-3.1656	-0.22042

Appendices; Experiment 3; Table S2. Sex differences across regional values of surface area corrected for total surface area. *Only regions significantly different between sexes are reported. Regions of interest (ROIs), hemisphere, corrected p-values (p-FDR), t-values and effect sizes (Cohen's d) are reported. Notes that negative t-values and effect sizes indicate higher regional values in males.*

ROIs	Hemisphere	p-FDR	T-value	Cohen's *d*
Subcentral gyrus (central operculum) and sulci	L	0.02275	-2.6655	-0.1856016
Transverse frontopolar gyri and sulci	L	0.0026	3.4087	0.2373514
Anterior part of the cingulate gyrus and sulcus	L	0.01806	2.7699	0.19287108
Middle-anterior part of the cingulate gyrus and sulcus	L	<0.001	5.231	0.36424009
Middle–posterior part of the cingulate gyrus and sulcus	L	<0.001	4.3411	0.3022754
Middle frontal gyrus (F2)	L	0.02994	2.5642	0.17854797
Superior frontal gyrus (F1)	L	<0.001	5.8039	0.40413172
Long insular gyrus and central insular sulcus	L	<0.001	-6.3794	-0.4442044
Short insular gyri	L	<0.001	-5.4739	-0.3811535
Angular gyrus	L	<0.001	6.6595	0.46370806
Supramarginal gyrus	L	<0.001	5.0811	0.35380239
Superior parietal lobule (lateral part of P1)	L	<0.001	4.2204	0.29387094
Postcentral gyrus	L	<0.001	5.1212	0.3565946
Straight gyrus (gyrus rectus)	L	<0.001	-4.091	-0.2848607
Subcallosal area, subcallosal gyrus	L	<0.001	-4.3831	-0.3051999
Polar plane of the superior temporal gyrus	L	<0.001	-6.7833	-0.4723284
Inferior temporal gyrus (T3)	L	0.02261	-2.6811	-0.1866878
Temporal pole	L	<0.001	4.8987	0.34110169
Calcarine sulcus	L	0.01223	-2.9166	-0.203086
Marginal branch (or part) of the cingulate sulcus	L	<0.001	4.269	0.29725501
Inferior segment of the circular sulcus of the insula	L	<0.001	-7.1572	-0.4983634
Inferior frontal sulcus	L	0.02275	-2.6702	-0.1859289
Superior frontal sulcus	L	0.03021	2.5477	0.17739906
Sulcus intermedius primus (of Jensen)	L	0.03005	2.5561	0.17798396
Intraparietal sulcus (interparietal sulcus) and transverse parietal sulci	L	0.00685	3.1016	0.2159677
Superior occipital sulcus and transverse occipital sulcus	L	0.03595	2.4541	0.17088159
Anterior occipital sulcus and preoccipital notch (temporo-occipital incisure)	L	0.0435	2.378	0.16558267
Medial orbital sulcus (olfactory sulcus)	L	<0.001	-5.7581	-0.4009426
Postcentral sulcus	L	<0.001	5.2947	0.36867559
Subparietal sulcus	L	<0.001	3.8631	0.26899176
Transverse temporal sulcus	L	<0.001	5.9895	0.41705525
Inferior occipital gyrus (O3) and sulcus	R	0.0025	-3.4267	-0.2386048
Transverse frontopolar gyri and sulci	R	<0.001	4.1246	0.28720028
Anterior part of the cingulate gyrus and sulcus	R	0.03049	2.5303	0.17618748
Posterior–dorsal part of the cingulate gyrus	R	<0.001	-3.7496	-0.2610886
Posterior–ventral part of the cingulate gyrus (isthmus of the cingulate gyrus)	R	<0.001	-6.7161	-0.4676492
Middle frontal gyrus (F2)	R	0.0178	2.7816	0.19368576
Superior frontal gyrus (F1)	R	<0.001	3.9438	0.27461098
Long insular gyrus and central insular sulcus	R	<0.001	-4.3438	-0.3024634
Short insular gyri	R	<0.001	-6.1494	-0.4281893
Lateral occipito-temporal gyrus (fusiform gyrus, O4-T4)	R	<0.001	-6.007	-0.4182738
Angular gyrus	R	0.00536	3.1811	0.22150337
Superior parietal lobule (lateral part of P1)	R	0.00191	3.5066	0.24416828

Postcentral gyrus	R	<0.001	4.6563	0.32422312
Subcallosal area, subcallosal gyrus	R	0.00142	-3.5933	-0.2502053
Lateral aspect of the superior temporal gyrus	R	0.00348	-3.3199	-0.2311682
Polar plane of the superior temporal gyrus	R	<0.001	-9.3509	-0.6511131
Inferior temporal gyrus (T3)	R	<0.001	-4.3815	-0.3050885
Middle temporal gyrus (T2)	R	0.00104	-3.6821	-0.2563885
Temporal pole	R	<0.001	3.8241	0.26627615
Calcarine sulcus	R	<0.001	-4.9405	-0.3440123
Inferior segment of the circular sulcus of the insula	R	<0.001	-9.6973	-0.6752333
Superior segment of the circular sulcus of the insula	R	0.00375	-3.2917	-0.2292046
Posterior transverse collateral sulcus	R	0.03049	-2.5254	-0.1758463
Intraparietal sulcus (interparietal sulcus) and transverse parietal sulci	R	<0.001	5.3997	0.37598685
Orbital sulci (H-shaped sulci)	R	0.03049	-2.5272	-0.1759716
Postcentral sulcus	R	0.01699	2.804	0.1952455
Inferior part of the precentral sulcus	R	0.03595	-2.4541	-0.1708816
Inferior temporal sulcus	R	0.02094	-2.7137	-0.1889578
Superior temporal sulcus	R	<0.001	-4.7952	-0.3338949

Appendices; Experiment 3; Table S3. Sex differences across regional values of cortical thickness corrected for average cortical thickness. *Only regions significantly different between sexes are reported. Regions of interest (ROIs), hemisphere, corrected p-values (p-FDR), t-values and effect sizes (Cohen's d) are reported. Note that negative t-values and effect sizes indicate higher regional values in males.*

ROIs	Hemisphere	p-FDR	T-value	Cohen's *d*
Superior parietal lobule (lateral part of P1)	L	0.05297	-1.965	-0.13683
Superior parietal lobule	L	0.1143	-1.5945	-0.11103
Vertical ramus of the anterior segment of the lateral sulcus (or fissure)	L	0.05216	-1.9747	-0.1375
Intraparietal sulcus (interparietal sulcus) and transverse parietal sulci	L	0.24137	1.1806	0.082206
Superior occipital sulcus and transverse occipital sulcus	L	0.09264	-1.7	-0.11837
Anterior occipital sulcus and preoccipital notch (temporo-occipital incisure)	L	0.05608	-1.9373	-0.1349
Transverse temporal sulcus	L	0.53313	-0.629	-0.0438
Superior parietal lobule (lateral part of P1)	R	0.15109	-1.4479	-0.10082
Inferior frontal sulcus	R	0.06026	-1.9028	-0.13249
Intraparietal sulcus (interparietal sulcus) and transverse parietal sulci	R	0.69722	0.3892	0.0271
Temporal transverse sulcus	R	0.08667	-1.7348	-0.1208

Appendices; Experiment 3; Table S4. Regional values of fractal dimension (FD) (corrected for FD of the cortical ribbon) where no significant sex difference was detected. *Only regions not significantly different between sexes are reported. Regions of interest (ROIs), hemisphere, corrected p-values (p-FDR), t-values and effect sizes (Cohen's d) are reported.*

ICs	p-FDR	T-value	Cohen's *d*
IC1	0.00438	3.1785	0.22132233
IC3	<0.001	-5.8084	-0.4044451
IC4	<0.001	-6.6603	-0.4637638
IC5	0.01242	2.7738	0.19314264
IC13	0.01142	2.8139	0.19593485
IC14	<0.001	4.9934	0.34769575
IC16	<0.001	-13.3582	-0.9301457
IC17	<0.001	-4.8424	-0.3371815
IC18	<0.001	3.8022	0.26475123
IC19	0.00748	-2.9745	-0.2071176
IC21	<0.001	-8.5977	-0.598667
IC27	0.0493	2.2719	0.15819481
IC29	<0.001	4.2191	0.29378042
IC31	0.00133	3.542	0.24663322
IC36	<0.001	6.3793	0.44419744
IC42	<0.001	-5.0017	-0.3482737
IC44	0.00132	3.5598	0.24787266
IC45	0.00534	-3.0918	-0.2152853
IC47	0.00882	2.9099	0.20261943
IC48	<0.001	-4.4557	-0.3102551
IC49	0.00137	3.5188	0.24501778
IC50	0.00534	3.0913	0.2152505
IC51	<0.001	5.6585	0.39400737
IC64	<0.001	-3.7702	-0.262523
IC73	<0.001	5.4354	0.37847268
IC75	<0.001	4.2775	0.29784687
IC43	<0.001	3.9697	0.27641443

Appendices; Experiment 3; Table S5. Sex differences across independent components (ICs) estimated with the source-based morphometry. *Only significant results are reported. For each component, we reported the corrected p-value (p-FDR), the t-values and the effect size (Cohen's d). Negative t-values and effect sizes indicate higher regional values in males.*